

The Calabi-Yau Landscape: from Geometry, to Physics, to Machine-Learning

Yang-Hui He

Contents

1	Prologus Terræ Sanctæ	8
1.1	A Geometrical Tradition	12
1.1.1	Preliminary Example & 1, 2, ?	14
1.2	$10 = 4 + 2 \times 3$: a Physical Motivation	16
1.2.1	Triadophilia	20
1.3	Topological Rudiments	23
1.3.1	The Hodge Diamond	24
2	The Compact Calabi-Yau Landscape	27
2.1	The Quintic	28
2.1.1	Topological Quantities: Exact Sequences	31
2.1.2	Topological Quantities: Computer Algebra	34
2.2	CICY: Complete Intersection Calabi-Yau	38
2.2.1	Topological Quantities: Statistics	44
2.3	Other Datasets	46
2.3.1	Hypersurfaces in Weighted \mathbb{CP}^4	47
2.3.2	Elliptic Fibrations	49

2.4	Ne Plus Ultra: The Kreuzer-Skarke Dataset	51
2.4.1	Reflexive Polytopes	52
2.4.2	CY Hypersurfaces: Gradus ad Parnassum	54
2.4.3	1, 16, 4319, 473800776	57
2.5	Cartography of the Compact Landscape	65
2.6	Epilogue: Recent Developments	66
3	The Non-Compact Calabi-Yau Landscape	69
3.1	Another $10 = 4 + 2 \times 3$	70
3.1.1	Quiver Representations & a Geometer's AdS/CFT	71
3.1.2	The Archetypal Example	75
3.2	Orbifolds and Quotient Singularities	78
3.2.1	McKay Correspondence	81
3.2.2	Beyond ADE	84
3.3	Toric Calabi-Yau Varieties	85
3.3.1	Cone over \mathbb{P}^2	87
3.3.2	The Conifold	91
3.3.3	Bipartite Graphs and Brane Tilings	95
3.4	Cartography of the Affine Landscape	98
3.4.1	Gorenstein Singularities	100
3.4.2	The non-Compact Landscape	101
4	Machine-Learning the Landscape	103
4.1	The Typical Problem	104

4.2	WWJD	107
4.3	Rudiments of Machine-Learning	110
4.3.1	MLP: Forward Propagating Neural Networks	112
4.3.2	Convolutional Neural Networks	115
4.3.3	Support Vector Machines	117
4.4	Machine-Learning Algebraic Geometry	123
4.4.1	Warm-up: Hypersurface in Weighted \mathbb{P}^4	124
4.4.2	Learning CICYs	134
4.4.3	Outlook	138
4.5	Epilogue	141
A	Complex Geometry: Rudiments	143
A.1	Covariantly Constant Spinor	147
A.2	A Lightning Refresher on Toric Varieties	149
A.3	Dramatis Personae	152
B	Gröbner Bases	156
B.0.1	An Elimination Problem	159
B.0.2	Hilbert Series	160
C	Brane Tilings	166

*Catherinæ, Iacobo, & Elizabethæ,
Parentibusque suis,
pro amore Catharinae, Sanctae Alexandriae,
lacrimarum Mariae semper Virginis,
et ad Maiorem Dei Gloriam
hoc opusculum dedicat auctor . . .*

Preface

“La Géométrie, qui ne doit qu’obéir à la Physique quand elle se réunit avec elle, lui commande quelquefois.”

– Jean d’Alembert, *Essai d’une nouvelle théorie de la résistance des fluides*

Algebraic and differential geometry have been the *point d’appui* between pure mathematics and fundamental physics in the twentieth century. The two pillars of modern physics: (1) general relativity of the theory of gravitation and (2) the gauge theory of the Standard Model of elementary particles, are the physical realization of, respectively, (1) metrics on Riemannian manifolds and (2) connections of bundles with Lie structure. This fruitful dialogue persisted through the parallel development of these two strands of natural philosophy and was made evermore pertinent within the context of string theory, conceived to unify gravity with quantum field theory, and thereby providing an answer to Einsteins famous dream of a Theory of Everything (ToE). Whether string theory - with its cornerstones of supersymmetry and extra space-time dimensions yet to be verified by some ingenious experiment - is truly “the” theory of Nature remains to be seen. What is indisputable is that the theory has been a Muse to pure mathematics: from enumerative geometry to Moonshine, from quantum invariants to mock modular forms, etc., the discipline has provided novel, and rather unique, methods of attack on tackling a myriad of mathematical problems.

Central to string theory is the study of Calabi-Yau manifolds, serving as

a beacon to such important investigations as compactification, mirror symmetry, moduli space and duality. Since their incipience in a conjecture of E. Calabi in 1954-7 in an esteemed tradition in geometry of relating curvature to topology, to the celebrated proof by S.-T. Yau in 1977-8, to the prescription thereof as a large class of vacua in string theory by Candelas-Horowitz-Strominger-Witten in 1986, Calabi-Yau manifolds have been an inspiring protagonist in modern mathematics and theoretical physics.

There have, of course, been quite a few books already on the subject. These range from the excellent account of the master himself in *The Shape of Inner Space: String Theory and the Geometry of the Universe's Hidden Dimensions*, by S.-T. Yau and S. Nadis [1], to the now classic *The Elegant Universe*, by B. Green [2], both aimed at the general audience; from the vintage compendium *Calabi-Yau Manifolds, a Bestiary for Physicists*, by T. Hübsch [3], to the modern lecture notes *A survey of Calabi-Yau manifolds* by S.-T. Yau [4], *Calabi-Yau Manifolds and Related Geometries* by M. Gross, D. Huybrechts, and D. Joyce [5], as well as *Calabi-Yau Varieties: Arithmetic, Geometry and Physics*, by R. Laza, M. Schütt, and N. Yui (Eds. [6]), aimed at the specialist.

Why a New Book: Why, then, the astute reader asks, another book on Calabi-Yau manifolds?

The primary reason is that there has been a revolution over the last score of years in Science, perhaps not a paradigm shift, but certainly a transformation in style and methodology: the twenty-first century now firmly resides within the age of big data and artificial intelligence. It is therefore inevitable that mathematical physics and pure mathematics should too profit from this burgeoning enterprise. Whilst it is well-established that string theory and Calabi-Yau manifolds have been at the interface between theoretical physics and pure mathematics from the 1980s, it is less known that since around the turn of the millennium, they have also served as a bench-mark to various problems in computational mathematics as well as a passionate advocate for

data-mining.

Specifically, the author, as well as many other groups in string theory, enjoyed long collaborations with experts in large-scale computational projects, e.g., Macaulay2, Singular, Bertini in algebraic geometry, GAP in group theory, MAGMA or PARI/GP in number theory, and indeed the umbrella scheme of SageMath. Furthermore, even before the establishment of such online databases such as

1. “the database of L-functions, modular forms and related objects”
<http://www.lmfdb.org/>
2. “the Graded Ring Database of algebraic varieties”
<http://www.grdb.co.uk/>
3. “the Knot atlas” <http://katlas.org/>, etc.,

which have become standard in the mathematics literature over the last two decades or so, the now-famous 473 million hypersurfaces in toric varieties from reflexive 4-polytopes and the resulting Calabi-Yau database was born from Kreuzer-Skarke in the mid-1990s. This impressive resource still remains one of the largest datasets in mathematics:

<http://hep.itp.tuwien.ac.at/~kreuzer/CY/>

Contemporaneous to these, there have emerged an increasing number of online Calabi-Yau databases, of varying specialization and often of augmented sophistication in user interface, such as the “Toric Calabi-Yau Database”

<http://www.rossealtman.com/> ,

the “Heterotic Compactification Database”

<http://www-thphys.physics.ox.ac.uk/projects/CalabiYau/> ,

and the “Calabi-Yau Manifold Explorer”

<https://benjaminjurke.com/academia-and-research/calabi-yau-explorer/>

,
set up by various international collaboration of which the author has been a part, as well as “The Calabi-Yau Operator Database” for Picard-Fuchs PDEs

<http://cydb.mathematik.uni-mainz.de/> ,

elliptically fibred Calabi-Yau manifolds

<http://ctp.lns.mit.edu/wati/data.html> , etc.

In addition, the reader is encouraged to read the enlightening transcripts of the ICM 2018 panel discussion on machine-aided proofs and databases in mathematics [10].

Why This Book: It is therefore evident that a new book on Calabi-Yau manifolds, and more widely, on algebraic geometry, is very much in demand. Such a book should emphasize that the subject is not only at the intersection between mathematics and physics, but resides, in fact, at the cusp of pure and applied mathematics, theoretical physics, computer science and data science. This book should briefly introduce the mathematical background and the physical motivation, brief because the material can be found in many textbooks. It should then delve into the heart of the matter, addressing

1. how does one explicitly construct a Calabi-Yau manifold;
2. how do these constructions lead to problems in classification, ranging from the combinatorics of lattice polytopes to the representation of quivers and finite graphs;
3. what databases have thus far been established and
4. how to use a combination of analytic techniques and available software to compute requisite quantities, such as Hodge numbers and bundle cohomology

Throughout, algorithms and computerization will serve as the skein which threads the material, with an appreciation of their complexity and the indefatigability with which the community has utilized them to compile databases, in order to extract new mathematics and new physics. In this sense, the book will focus not on the *theory* but the *practice* of Calabi-Yau manifolds.

The Calabi-Yau Landscape and Beyond: There have been many practitioners in mapping the landscape of Calabi-Yau manifolds throughout the years, exploring diverse features of interest to physicists and mathematicians alike, such as the founders S.-T. Yau in the mathematics and P. Candelas in the physics, as well as M. Stillman and D. Grayson in the computational geometry. To the fruitful collaboration with and sagacious guidance by these experts over the years the author is most grateful.

More recently, in 2017-8, a daring paradigm was proposed in [229,230]. A natural question was posed: confronted with the increasingly available data on various geometric properties of Calabi-Yau varieties which took many tour de force efforts to calculate and compile, can machine-learning be applied to Calabi-Yau data, and to data in pure mathematics in general? Indeed,

Can artificial intelligence “learn” algebraic geometry?

That is, can machine-learning arrive at correct answers such as cohomology or topological invariant, *without* understanding the nuances of the key techniques of the trade, such as Groebner bases, resolutions or long exact sequences? This was shown to be mysteriously possible in many cases to astounding accuracy. There had subsequently been some activity in the field, in applying big-data techniques to various problems in string theory by a host of independent groups the Zeistgeist of data science has thus breathed its nurturing spirit into the field of mathematical physics.

Target Audience: This book has grown out of a timely series of invited colloquia, seminars and lectures (one long version of the lecture slides, of which this book is a pedagogical expansion, is available at qgm.au.dk/fileadmin/www.qgm.au.dk/Events/2018/CYlandscape.pdf), delivered by the author in the 2017-8 academic year, at the National Centre for Science and Technology, Taiwan; Northeastern University, Boston; Ludwig-Maximilians-Universität, Munich; Imperial College, London; L’Institut Confucius, Geneva; University of Warwick, UK; Nankai and Tianjin Univer-

sities, China; University of Plymouth, UK; Universities of Bruxelles and Leuven, Belgium; University of Nottingham, UK; Albert Einstein Institute, Potsdam; Niels Bohr Institute, Copenhagen; University of the Witwatersrand, Johannesburg; Trinity College, Dublin; Brown University, Providence; Harvard University, Boston and University of Pennsylvania, Philadelphia. To the kind hospitality of the various hosts he is most grateful. The audience is intended to be primarily beginning graduate students in mathematics, as well as those in mathematical and theoretical physics, all with a propensity towards computers. We will take a data-driven perspective, sprinkled with history, anecdotes, and actual code.

In a sense, the list of available books mentioned earlier is aimed either at a general audience or to a more senior graduate student. The middle-ground of beginning PhD students, master students, or even advanced undergraduate students is left wanting. Students with some familiarity of Reid's undergraduate algebraic geometry [12] but not yet fully prepared for Hartshorne [13] and Griffiths-Harris [14], or with some acquaintance of Artin's introductory algebra [15] but not yet fully feathered for Fulton-Harris [16], may find it difficult to approach the subject matter of Calabi-Yau manifolds. For them this writing is designed.

In a way, the purpose of this book is to use Calabi-Yau databases as a playground, and explore aspects of computational algebraic geometry and data science, in the spirit of the excellent texts of Cox-Little-O'Shea [7] and Schenck [8]. Perhaps, due to the author's constant enjoyment as an outsider, the book is intended to be some mathematics for physicists, some physics for mathematicians, and some data science for both. Throughout our promenade in the landscape, there will be a continued preference of intuition over rigour, computation over formalism, and experimentation over sophistry. It is the author's hope that we shall embark on a memorable adventure in the land of mathematics, physics and data-science, with Calabi-Yau manifolds leading as our Beatrice, and Interdisciplinarity guiding as our Virgil, and we, like Dante, diligently remarking upon our journey.

Acknowledgements

To the invaluable guidance and help of my mentors, official and unofficial, I owe eternal gratitude. Each has been a guiding light at various stages of my career: Professor Amihay Hanany, Professor Burt Ovrut, Professor Philip Candelas, Professor Dame Jessica Rawson, Professor Andre Lukas, Professor Alex Scott, Professor Shing-Tung Yau, Professor Mo-Lin Ge, and Professor Minhyong Kim. To them I raise my cup of thanksgiving.

To the host of collaborators whose friendship I have enjoyed over the years, I owe a million happy thoughts. Their camaraderie has always offered a beacon of hope even within the darkest moments of confusion. To them I raise my glass of brotherly love.

To my wife, Dr. Elizabeth Hunter He, *rosa Hibernia dliectissima mea*, without whose patience and support this book would not have come into being. To my children, Katherine Kai-Lin and James Kai-Hong, without whose distractions this book would also not have come into being. To my parents, without whose love and nurturing nothing much of mine would have ever come into being.

1

Prologus Terræ Sanctæ

“Cæterum ad veridicam, sicut iam polliciti sumus, Terræ Sanctæ descriptionem, stylum vertamus.”

– Burchardus de Monte Sion, *Prologus Terræ Sanctæ*

That Zeitgeist should exist in the realm of scientific enquiry is perhaps more surprising than its purported influence in the growth of civilizations. Whilst the latter could be conceived of as the emergence of vague concoction of cross-cultural ideas, the former requires precise concepts and objects to almost simultaneously appear, oftentimes independently and even mysteriously, within different disciplines of research. In mathematics, what initially surface as “Correspondences” in seemingly disparate subfields necessitates a timely arrival of hitherto unthinkable technique for the final construction of a proof. An archetypal example of this is *Moonshine*, a list of daring conjectures by McKay-Thompson-Conway-Norton in the late 1980s relating finite groups to modular forms, which until then lived in utterly different worlds. It so happened that Borchers was learning quantum field theory (QFT) with conformal symmetry - yet another world - around this time, when he noted that the structure of its vertex operator algebra furnished the requisite representation and achieved his Fields medal winning proof of 1992. The right

set of ideas was indeed “in the air”.

The involvement of physics was perhaps as surprising as the initial correspondence. But herein lies the crux of our tale. The past half-century has witnessed the cross-fertilization between mathematics and theoretical physics in a manner worthy of that illustrious tradition since Newton: Riemannian geometry and general relativity, operator theory and quantum mechanics, fiber bundles and gauge theory of elementary particles, etc. An impressive list of theories, such as the likes of mirror symmetry, supersymmetric indices, and Moonshine, have been the brain-children of this fruitful union. It indeed seems that QFTs with additional symmetry, specifically, conformal symmetry and supersymmetry, is the right set of ideas.

The ultimate manifestation of QFTs with such rich symmetries is, with doubt, string theory. Marrying the conformal symmetries of the world-sheet with the supersymmetry of incorporated fermions, string theory materialized in the 1970-80s as an attempt to unify gravity as described by general relativity with quantum theory as described by the gauge theory of the Standard Model (SM) into a Theory of Everything, the holy grail of fundamental physics. The theory still remains the best candidate for a hope of reconciling the macroscopic world of stars and galaxies with the microscopic world of elementary particles of the SM, which would in turn demystify singularities such as black-holes or the Big Bang.

To date, there is no experimental evidence for string theory, none at all for its cornerstones of supersymmetry and extra space-time dimensions, nor is it obvious that definitive signatures of either would be discovered in the near future: we must patiently await some ingenious experiment in some marvellous indirect observation. Why, then, string theory? While we refer the reader to the excellent response in J. Conlon’s eponymous book [11], as mathematicians and mathematical physicists our affinity to the theory is already more than justified. As mentioned above, the theory has not only made revolutionary contributions to theoretical physics in the guise of holography, QFT dualities and quantum entanglement, but furthermore,

in an unexpected manner, it has been serving as a *constant Muse to pure mathematics*.

Time and again, its general framework has provided unexpected insights and results to geometry, representation theory and even number theory. Hence, regardless of whether the theory will eventually become the unified theory of everything, its pursuit, now, in the past decades, and in foreseeable future, is just and fitting. String theory is thus the rightful heir of that noble lineage of the interaction between geometry, algebra and physics which took a firm footing in the twentieth century, it is certainly not a *fin-de-siècle* fancy, but has rather transitioned us, as a perspicacious mentor, into the mathematics and physics of the twenty-first century. Central to this development is the study of **Calabi-Yau varieties**, whose curvature flatness endows them with beautiful mathematical structure and physical utility, rendering them the perfect illustration of this interaction.

As we now ground ourselves into the incipience of the twenty-first century, it behoves us to contemplate as to whether a particular spirit permeates our Time. The answer is immediate: this is the Age of Data.

From the sequencing of the Human genome, to the sifting of particle jets in the LHC, to the search for exo-planets, the beginning of this century has amassed, utilized and analysed data on an unprecedented scale, due to the explosive growth and availability of computing power and artificial intelligence (AI). Whilst it is well known that problems string theory has long been a Physical Beatrice to the Pure Mathematical Dante, it is perhaps less appreciated that over the past three decades they too have repeatedly provided benchmarks to computational mathematics, especially in computational algebraic geometry and combinatorial geometry.

The story, as we will shall see, goes back to the late 1980s, reaching its first climax in the mid-1990s: interestingly, the now classic complete intersection Calabi-Yau (CICY) [45] and Kreuzer-Skarke (KS) [61] datasets place “big data” in pure mathematics and mathematical physics to a time ordinarily thought to predate the practice of data-mining. More recently, a steadily

expanding group of researchers in mathematical physics, have been advocating to the physics community (q.v. [9]) the power of and the importance of interacting with **Macaulay2** [32], **Singular** [33], **Bertini** [34] in algebraic geometry, **GAP** [35] in group theory, **MAGMA** [37] in number theory etc., as well as the overarching **Sagemath** [38]. Indeed, the first sessions in theoretical high-energy physics [40] in the biannual “Society for Industrial and Applied Mathematics” (SIAM) meetings on applied algebraic geometry have emerged.

The protagonist of our chronicle is therefore engendered from the union of mathematics, physics and data science and it is this trinity that will be the theme of this book. Over the years, various fruitful collaborations between theoretical physicists, pure and applied mathematicians, and now data scientists and computer scientists, have been constructing and compiling databases of objects which may *ab initio* seem to be only of abstract mathematical interest but instead links so many diverse areas of research: Calabi-Yau manifolds constitute the exemplar of this paradigm. Thus, as much as our ethereal *Zeitgeist* being *Data*, it too should be *Interdisciplinarity*.

By now, there is a landscape of data and a plethora of analytic techniques as well as computer algorithms, freely available, but lacking a comprehensive roadmap. This is our **Calabi-Yau Landscape**. There are still countless goldmines buried in this landscape, with new mathematical conjectures laying hidden (e.g, the vast majority of the manifolds obtainable from the KS dataset by triangulations have been untouched [64]) and new physics to be uncovered (e.g. the unexpected emergence of Calabi-Yau structure in the scattering of ordinary ϕ^4 QFTs [65, 66]).

Europe’s obsession with Jerusalem in the Middle Ages lead to the publication of one of the very first printed maps, based on Burchardus de Monte Sion’s thirteenth century “Prologue of the Holy Land” [25]. We have thus named our prologue in homage to this early cartographical work, drawing upon the analogy that we too will be mapping out the landscape of an im-

portant terrain.

1.1 A Geometrical Tradition

Our story begins ¹ with the mid-1950s, when E. Calabi made his famous conjecture [29]

CONJECTURE 1 (Calabi Conjecture) *Let (M, g, ω) be a compact Kähler manifold and R a $(1, 1)$ -form such that $[R] = [c_1(M)]$. Then $\exists!$ Kähler metric \tilde{g} and Kähler form $\tilde{\omega}$ such that $[\omega] = [\tilde{\omega}] \in H^2(M; \mathbb{R})$ and that $R = \text{Ric}(\tilde{\omega})$, the Ricci form of $\tilde{\omega}$.*

This is quite a mouthful! We make a few remarks to put this conjecture into context and which will help us digest it. First, this statement is in the long tradition since Gauß–Bonnet in relating analysis (e.g., curvature) to topology (e.g., Chern classes). For two-dimensional real manifolds S , typified by the sphere, the integral of the curvature of S is famously related to its Euler characteristic χ . When S is compact and orientable, χ completely determines the topology.

The situation in higher dimensions is expectedly much more complicated; nevertheless, the extra structure of being Kähler helps us. Indeed, the Chern classes $c_k(M) = c_k(T_M) \in H^{2k}(M)$, for Kähler manifolds, have an important property: the Ricci $(1, 1)$ -form, the Kähler $(1, 1)$ -form and $c_1(M)$, as real 2-forms, all reside in $H^2(M; \mathbb{R})$. The content of the conjecture is that the Chern class determines, in a unique way, the behaviour of the curvature. In fact, uniqueness was already shown by Calabi and it is the existence of $(\tilde{g}, \tilde{\omega})$ that remained the challenge.

Second, the case when $R = 0$ (Ricci-flatness) is obviously important, here,

¹ We leave a brief recapitulation of the rudiments and notation of Kähler geometry to Appendix A.

it means that for Kähler M , unique existence of Ricci-flat Kähler metric is equivalent to the vanishing of $c_1(M)$. The case of [Kähler-Einstein](#), i.e., when $R = \lambda g$, where the Ricci form is proportional to the metric form for some $\lambda \in \mathbb{R}$ best illustrates the situation. Here, there is a natural trichotomy: $\lambda > 0$ (ample), $\lambda = 0$ (Ricci-flat) and $\lambda < 0$ (anti-ample, or general type).

Third, from a computational perspective, to appreciate the power of the statement, suppose we wished to go hardcore and tried to find an explicit metric in some local coordinate. Even with the help of extra properties such as Kähler, the Ricci-flat equations are a set of complicated non-linear PDEs in the components of the metric for which there is little chance of a hope for analytic solution. We are now at liberty to only check an algebraic/topological quantity, the first Chern class, many examples of which we shall compute throughout the book, would govern the Ricci curvature. In particular, its vanishing would guarantee the uniqueness and existence of a Ricci-flat metric.

The existence part of the Calabi Conjecture was finally settled by S.-T. Yau [30], some twenty years later:

THEOREM 1 (Yau) *The Calabi Conjecture holds.*

In particular, the case of $R = 0$ is now called [Calabi-Yau](#) manifolds in honour of this achievement, which uses ingenious existence methods for the solution of a Monge-Ampère PDE and for which Yau received the Fields Medal in 1982.

It should be pointed out the proof is an existence proof and to date *no explicit Ricci-flat Kähler metric has been found on any compact Calabi-Yau manifold* (beyond the trivial case of products of tori) and this remains an important open problem. Importantly, before proceeding, the reader is pointed to the survey [4], which gives a fantastic bird's-eye-view of the historical developments and well most of the active areas of research related to Calabi-Yau manifolds.

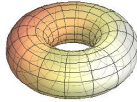
					...
$g(\Sigma) = 0$	$g(\Sigma) = 1$	$g(\Sigma) > 1$			
$\chi(\Sigma) = 2$	$\chi(\Sigma) = 0$	$\chi(\Sigma) < 0$			
Spherical	Ricci-Flat: CY_1	Hyperbolic			
+ curvature	0 curvature	- curvature			

Figure 1.1: The trichotomy of Riemann surfaces Σ of genus $g(\Sigma)$, in terms of its Euler number $\chi(\Sigma) = 2 - 2g(\Sigma)$.

1.1.1 Preliminary Example & 1, 2, ? ...

We will give many explicit examples later in the book, but for now, in order to reify the above concepts, let us present a preliminary though extremely example of a Calabi-Yau manifold. It is well-known that all compact smooth orientable surfaces (we also only consider the case without boundary/punctures) are, in fact, complex varieties of dimension one. In other words, 2-manifolds can be complexified to 1-folds: these are the Riemann surfaces Σ considered as algebraic curves. Note that, we henceforth adopt the standard though perhaps confusing appellation that

- an *n -manifold* refers to a manifold of real dimension n ;
- an *n -fold* refers to one of complex dimension n .

Furthermore, we will often use the acronym CY_n to mean a Calabi-Yau n -fold.

Back to Riemann surfaces of real dimension 2. Here, all 2-forms are trivially closed. Whence, the complex structure naturally supplants a Kähler structure: thus Riemann surfaces are not only complex but are moreover Kähler and our foregoing discussions apply.

As mentioned above, it is also a classic result that the topological type of Σ is determined by a single quantity, the **Euler Characteristic** (or Euler number)

$$\chi(\Sigma) = 2 - 2g(\Sigma) \quad (1.1)$$

where $g(\Sigma)$ is the genus. Here, the trichotomy is familiar, as shown in Fig. 1.1:

- $\chi(\Sigma) > 0$: spherical geometry $g(\Sigma) = 0$ where the metric is of (constant) positive curvature;
- $\chi(\Sigma) = 0$: flat/torus geometry $g(\Sigma) = 1$ where the metric is Ricci flat;
- $\chi(\Sigma) < 0$: hyperbolic geometry $g(\Sigma) > 1$ where the metric is of negative curvature.

Of course, the relation between the curvature R and the Euler number is the celebrated theorem of Gauß-Bonnet

$$\chi(\Sigma) = \frac{1}{2\pi} \int_{\Sigma} R . \quad (1.2)$$

Indeed, the torus $T^2 \simeq (S^1)^2$ case of $g(\Sigma) = 1$ is the only compact, smooth, Ricci-flat, Kähler manifold of complex dimension one. That is,

PROPOSITION 1 *A (compact, smooth) Calabi-Yau 1-fold is the torus T^2 as a Riemann surface/complex curve.*

We are therefore reassured that in dimension 1, a Calabi-Yau manifold is none other than one of the most familiar objects in mathematics. Indeed, T^2 is \mathbb{C}/L , the quotient of the complex plane by a lattice (as we remember from our first lesson in topology that identifying the opposite sides of a sheet of A4 paper gives a doughnut), and thus a metric on T^2 can be inherited from the flat metric on the plane. Algebraically, a torus can be realized as an [elliptic curve](#), the central object to geometry and number theory; there is thus a

programme in understanding the arithmetic, in addition to the geometry, of Calabi-Yau manifolds [6, 130].

In complex dimension 2, the 4-torus $T^4 \simeq (S^1)^4$ is analogously Calabi-Yau. There is another, called the [K3-surface](#) which deserves an entire treatise to itself [131–133]. However, this seemingly innocent sequence of numbers 1, 2, ... of Calabi-Yau manifolds in complex dimension 1, 2, ... does *not* persist. In fact, the next number in this sequence - which is perhaps the most pertinent to physics as we shall see next - for number of inequivalent Calabi-Yau 3-folds, is already *unknown*. What we do know is that there is a vast landscape thereof and much of this book will be a status report on how much we do know of this landscape.

1.2 $10 = 4 + 2 \times 3$: a Physical Motivation

While the aforementioned advances in geometry were being made, theoretical physicists were working on the ultimate Theory of Everything. By the late 1970s, a theory of strings, born from an initial attempt to explain the mass-spin correlation of the zoo of elementary particles in the 1960s, showed great promise in unifying gravity with quantum field theory. As this book is neither on string theory nor really on algebraic geometry, but rather on the algorithms and data which emerge, the reader is referred to the canon [24], or to [26] for technical and historical accounts.

As far as Calabi-Yau manifolds are concerned, the physics side of the story began in 1985, with the paper which began what is now called “[string phenomenology](#)” [110], a field aimed at constructing the Standard Model as a low-energy limit of string theory (the gravity side is called “string cosmology” and the conjunction of the two should, in principle, encompass all that is within the universe). The paper immediately followed the discovery of the [heterotic string](#) [111], which, being a unified theory of gravity and a QFT

with a Lie algebra as large as $E_8 \times E_8$ or $SO(32)$, caused much excitement².

The primary reason for this optimism is that the Standard Model gauge group $G_{SM} = SU(3) \times SU(2) \times U(1) \subset E_8$ (recall that the $SU(3)$ factor for QCD governing the dynamics of baryons and the $SU(2) \times U(1)$, that of QED, governing the leptons). It has been an old question in particle physics as to why the Standard Model gauge group is of the structure of non-semisimple Lie group but is rather such a seemingly arbitrary product of three unitary groups.

The fact that G_{SM} is not a (semi-)simple Lie group has troubled many physicists since the early days: it would be more pleasant to place the baryons and leptons in the same footing by allowing them to be in the same representation of a larger simple gauge group. This is the motivation for the sequence in (1.3) below: starting from $SU(5)$, theories whose gauge groups are simple are called **grand unified theories** (GUTs), the most popular historically had been $SU(5)$, $SO(10)$ and E_6 , long before string theory came onto the scene in theoretical physics. Various attempts have been made in harnessing the following inclusion of Lie groups

$$SU(3) \times SU(2) \times U(1) \subset SU(5) \subset SO(10) \subset E_6 \subset E_7 \subset E_8, \quad (1.3)$$

with all the various semisimple groups to the right of G_{SM} furnishing different candidate GUT theories. Thus, a unified theory with a natural E_8 gauge group was most welcome³. Oftentimes, we add one more $U(1)$ factor to G_{SM} , denoted as $U(1)_{B-L}$, to record the difference between baryon and lepton number, in which case

$$G'_{SM} = SU(3) \times SU(2) \times U(1) \times U(1)_{B-L} \quad (1.4)$$

² By fusing the bosonic string (whose critical dimension is 26) with the superstring (whose critical dimension is 10) in the process of “heterosis” by assigning them to be respectively left and right moving modes of the string, the fact that $26 - 10 = 16$ gives 16 internal degrees of freedom to furnish a gauge symmetry. Beautifully, in 16 dimensions there are only two even self-dual integral lattices in which quantized momenta could take value, viz., the root lattices of $E_8 \times E_8$ and of $D_{16} = \mathfrak{so}(32)$.

³According to Witten, in the sense of string phenomenology, “heterotic compactification is still the best hope for the real world.”

and the above sequence of embeddings skips $SU(5)$.

The downside, of course, is that (standard, critical, supersymmetric) string theory lives in $\mathbb{R}^{1,9}$ and compared to our $\mathbb{R}^{1,3}$ there must be 6 extra dimensions. This remains a major challenge to the theory even today. There are two philosophies in addressing $10 = 4 + 6$, to (1) take the extra dimension to be small in the spirit of Kaluza-Klein or to (2) take them to be large in the spirit of holography. The former is called **compactification** and the latter **brane-world** and conveniently correspond mathematically to compact and non-compact Calabi-Yau varieties, as we shall see in the first two chapters of this book.

In brief, [110] gave the conditions for which the heterotic string, when compactified would give a supersymmetric gauge theory in $\mathbb{R}^{1,3}$ with potentially realistic particle spectrum. Here, compactification means that the 10-dimensional background is taken to be of the form $\mathbb{R}^{1,3} \times M_6$ with $\mathbb{R}^{1,3}$ our familiar space-time and M_6 some small (Planck-scale) curled up 6-manifold, endowed with a vector bundle V at the Planck scale too small to be currently observed directly. Specifically, with more generality, the set of conditions, known as the *Strominger System* [113], for the low energy low-dimensional theory on $\mathbb{R}^{1,3}$ to be a supersymmetric gauge theory are

1. M_6 is complex;
2. The Hermitian metric g on M_6 and h on V satisfy
 - (a) $\partial\bar{\partial}g = i\text{Tr}F\wedge F - i\text{Tr}R\wedge R$ where F is the curvature (field strength) 2-form for h and R the (Hull) curvature 2-form for g ;
 - (b) $d^\dagger g = i(\partial - \bar{\partial})\ln\|\Omega\|$, where Ω is a holomorphic 3-form on M_6 which exists ⁴;
3. F satisfies the Hermitian Yang-Mills equations

$$\omega^{a\bar{b}}F_{a\bar{b}} = 0, \quad F_{ab} = F_{\bar{a}\bar{b}} = 0. \quad (1.5)$$

⁴ Recently, Li-Yau [114] showed that this is equivalent to ω being balanced, i.e., $d(\|\Omega\|g^2) = 0$.

A sequence of arguments (cf. Appendix A.1) then leads to the fact that the simplest solution to the above conditions is that

PROPOSITION 2 *M_6 is Kähler, complex dimension 3, and of $SU(3)$ holonomy.*

Furthermore, one can take the vector bundle V to be simply the tangent bundle T_M . We can now refer to Berger's famous holonomy classification [31] as to what such a manifold is.

THEOREM 2 (Berger) *For M a Riemannian manifold of real dimension d which locally is not a product space nor a symmetric space, then special holonomy and manifold type obey:*

<i>Holonomy $\mathcal{H} \subset$</i>	<i>Manifold Type</i>
$SO(d)$	<i>Orientable</i>
$U(d/2)$	<i>Kähler</i>
$SU(d/2)$	<i>Calabi-Yau</i>
$Sp(d/4)$	<i>Hyper-Kähler</i>
$Sp(d/4) \times Sp(1)$	<i>Quaternionic-Kähler</i>

Moreover, for $d = 7, 8$, there are two more possibilities, viz., G_2 and $Spin(7)$. These two, together with the $SU(d/2)$ and $Sp(d/4)$ cases, are Ricci flat.

Thus, our internal 6-manifold M is, in fact, a Calabi-Yau 3-fold⁵ and our two strands of thought, in the §1.1 and in the present, naturally meet. This is

⁵ The reader might wonder how curious it is that two utterly different developments, one in mathematics, and another in physics, should both lead to Rome. Philip Candelas recounts some of the history. The paper [110] started life as two distinct manuscripts, one by Witten, and the other, by Candelas-Horowitz-Strominger, the latter began during a hike to Gibraltar reservoir, near Santa Barbara, in the fall of 1985. Both independently came to the conclusion that supersymmetry required a covariantly constant spinor and thus vanishing Ricci curvature for the internal manifold M . It was most timely that Horowitz had been a postdoctoral researcher of Yau, and Strominger also coincided with Yau when both were at the IAS, thus a phone-call to Yau settled the issue about the relation to $SU(3)$ holonomy and hence Calabi-Yau. Thus the various pieces fell, rather quickly, into place, the two manuscripts were combined, and the rest, was history.

another golden example of a magical aspect of string theory: it consistently infringes, almost always unexpectedly rather than forcibly, upon the most profound mathematics of paramount concern, and then quickly proceeds to contribute to it.

1.2.1 Triadophilia

As seen from the above, string phenomenology aims to obtain the particle content and interactions of the standard model as a low-energy limit. In terms of the representation of G'_{SM} in (1.4), denoted as $(\mathbf{a}, \mathbf{b})_{(c,d)}$ where \mathbf{a} is a representation of $SU(3)$, \mathbf{b} , that of $SU(2)$, and (a, b) are the charges of the two Abelian $U(1)$ groups, the Standard Model elementary particles (all are fermions except the scalar Higgs) are as follows

$SU(3) \times SU(2) \times U(1) \times U(1)_{B-L}$	Multiplicity	Particle
$(\mathbf{3}, \mathbf{2})_{1,1}$	3	left-handed quark
$(\mathbf{1}, \mathbf{1})_{6,3}$	3	left-handed anti-lepton
$(\bar{\mathbf{3}}, \mathbf{1})_{-4,-1}$	3	left-handed anti-up
$(\bar{\mathbf{3}}, \mathbf{1})_{2,-1}$	3	left-handed anti-down
$(\mathbf{1}, \mathbf{2})_{-3,-3}$	3	left-handed lepton
$(\mathbf{1}, \mathbf{1})_{0,3}$	3	left-handed anti-neutrino
$(\mathbf{1}, \mathbf{2})_{3,0}$	1	up Higgs
$(\mathbf{1}, \mathbf{2})_{-3,0}$	1	down Higgs

(1.6)

In addition to these are vector bosons: (I) the connection associated to the group $SU(3)$, called the gluons, of which there are 8, corresponding to the dimension of $SU(3)$, and (II) the connection associated to $SU(2) \times U(1)$, called W^\pm , Z , and the photon; a total of 4. We point out that in this book the Standard Model - and indeed likewise for all ensuing gauge theories - we shall actually mean the (minimal) supersymmetric extension thereof, dubbed the **MSSM**, and to each of the fermions above there is a bosonic partner and vice versa.

Of note in the table is the number 3, signifying that the particles replicate themselves in three families, or **generations**, except for the recently discovered Higgs boson, of which is only a single doublet under $SU(2)$. That there should be 3 and only 3 generations, with vastly disparate masses, is an experimental fact with confidence [115] level $\sigma = 5.3$ and has *no satisfactory theoretical explanation to date*. The possible symmetry amongst them, called flavour symmetry, is independent of the gauge symmetry of $G_{SM'}$.

Upon compactification of the E_8 heterotic string on a Calabi-Yau 3-fold M_6 , a low-energy supersymmetric QFT is attained. Thus, our paradigm is simply

$$\text{Geometry of } M_6 \longleftrightarrow \text{physics of } \mathbb{R}^{1,3}.$$

What a marvellous realization of Kepler's old adage "Ubi materia, ibi geometria"!

Now, the tangent bundle T_M is of $SU(3)$ holonomy, thus E_8 is broken to E_6 since $SU(3)$ is the commutant of E_6 within E_8 . In particular, the fundamental 248 representation of E_8 branches as:

$$\begin{aligned} E_8 &\rightarrow SU(3) \times E_6 \\ 248 &\rightarrow (1, 78) \oplus (3, 27) \oplus (\bar{3}, \bar{27}) \oplus (8, 1) . \end{aligned} \quad (1.7)$$

It is possible to package all of the SM particles in (1.6) into the 27 representation of E_6 , in a SUSY E_6 -GUT theory. From (1.7), this is associated with the fundamental 3 of $SU(3)$. The 27 representation is thus associated to $H^1(T_M)$ and the conjugate $\bar{27}$, to $H^1(T_M^\vee)$. Similarly, the 1 representation of E_6 is associated with the 8 of $SU(3)$, and thus to $H^1(T_M \otimes T_M^\vee)$. Thus, we have that

$$\begin{aligned} \text{generations of particles} &\sim H^1(T_M) , \\ \text{anti-generations of particles} &\sim H^1(T_M^\vee) . \end{aligned}$$

In general, even when taking an arbitrary bundle V instead of just T_M , the

lesson is that

Particle content in $\mathbb{R}^{1,3} \longleftrightarrow$ cohomology groups of V, V^\vee
and of their exterior/tensor powers

The interactions, i.e., cubic Yukawa couplings in the Lagrangian, constituted by these particles (fermion-fermion-Higgs) are tri-linear maps taking the cohomology groups to \mathbb{C} ; this works out perfectly for a Calabi-Yau 3-fold: for example,

$$H^1(M, V) \times H^1(M, V) \times H^1(M, V) \rightarrow H^3(M, \mathcal{O}_M) \simeq \mathbb{C} . \quad (1.8)$$

An immediate *constraint* is, as mentioned above, that there be 3 net generations, meaning that

$$|h^1(X, T_M) - h^1(X, T_M^\vee)| = 3 . \quad (1.9)$$

Thus, the endeavour of finding Calabi-Yau 3-folds with the property (1.9) began in 1986. We will see in the following section that the difference on the left-hand-side is half of the Euler number χ .

Thus, one of the first problems posed by physicists to what Candelas calls “card-carrying”⁶ algebraic geometers was made specific:

QUESTION 1 *Are there smooth, compact, Calabi-Yau 3-folds, with Euler number $\chi = \pm 6$?*

This geometrical “love for threeness”, much in the same spirit as triskaidekaphobia, has been dubbed by Candelas et al. as **Triadophilia** [116]. More recently, independent of string theory or any unified theories, why there

⁶ I have always interpreted - as I have always perceived him to be a gentleman in the classic sense - to mean “visiting-card” carrying, as in a passage from, say, Jane Austen. However, when it finally occurred to me to check with him after misquoting him over the years, he assured me that he actually meant “Party-membership-card” carrying, as in a passage from, say, Solzhenitsyn. In any event, whatever the card, one who carries it must be quite serious about it indeed.

might be geometrical reasons for three generations to be built into the very geometry of the Standard Model has been explored [117].

1.3 Topological Rudiments

From the previous two sections, we have seen two parallel strands of development, in mathematics and in theoretical physics, converging on the subject of Calabi-Yau manifolds, a vast subject on which this book can only touch upon a specialized though useful portion; for such marvellous topics as mirror symmetry, enumerative geometry, etc., the reader is referred to the classics [27, 28].

For now, we nevertheless have a working definition of a (smooth, compact) Calabi-Yau n -fold, it is a manifold M of complex dimension n , which furthermore obeys one of the following *equivalent* conditions:

- Kähler with $c_1(T_M) = 0$;
- Kähler (M, g, ω) with vanishing Ricci curvature $R(g, \omega) = 0$;
- Kähler metric with global holonomy $\subset SU(n)$;
- Kähler and admitting nowhere vanishing global holomorphic n -form $\Omega^{(n,0)}$;
- Admits a covariantly constant spinor;
- M is a projective manifold with (1) canonical bundle (sheaf), the top wedge power of the cotangent bundle (sheaf),

$$K_M := \bigwedge^n T_M^\vee$$

being trivial, i.e., $K_M \simeq \mathcal{O}_M$ and (2) $H^i(M, K_M) = 0$ for all $0 < i < n$.

We remark that the global form $\Omega^{(n,0)}$ prescribes a volume-form $V = \Omega \wedge \bar{\Omega}$. When $n = 3$, it can be written in terms of the Gamma matrices γ and the covariant constant spinor η (cf. Appendix A) as $\Omega^{(3,0)} = \frac{1}{3!} \Omega_{mnp} dz^m \wedge dz^n \wedge dz^p$ with $\Omega_{mnp} := \eta_-^T \gamma^{[m} \gamma^n \gamma^{p]} \eta_-$.

It is clear that in the above, the last definition is the most general. So long as M is a projective variety it is not even required that it be smooth and K_M could be a sheaf obeying the said conditions. Throughout this book, because the emphasis is on the algebraic, liberal usage of the first and last definitions will be made, and we will see how they translate to precise algebraic conditions from which we will make explicit construction of examples.

1.3.1 The Hodge Diamond

We now present the most key topological quantities of a Calabi-Yau 3-fold. From the Hodge decomposition (q.v. Eq. (A.1) in Appendix A), the Betti numbers of a Kähler n -fold M splits as

$$b_k = \sum_{\substack{p,q=0 \\ p+q=k}}^n h^{p,q}(M) , \quad k = 0, \dots, n . \quad (1.10)$$

Now, complex conjugation (since M has at least complex structure) implies that $h^{p,q} = h^{q,p}$. Moreover, Poincaré duality implies that $h^{p,q} = h^{n-p,n-q}$. Therefore, the $(n+1)^2$ Hodge numbers $h^{p,q}$ automatically reduces to only $((n+1)(n+2)/2 - (n-1))/2 + (n-1)$. The clearest way to present this information is via a so-called **Hodge Diamond** (a rhombus, really).

For $n = 3$, for example, the diamond looks like

$$\begin{array}{ccccccc}
 & & & & h^{0,0} & & \\
 & & & & h^{0,1} & & h^{0,1} \\
 & & & h^{0,2} & & h^{1,1} & & h^{0,2} \\
 h^{0,3} & & & h^{2,1} & & h^{2,1} & & h^{0,3} \quad . \\
 & & h^{0,2} & & h^{1,1} & & h^{0,2} \\
 & & h^{0,1} & & h^{0,1} & & \\
 & & & & h^{0,0} & &
 \end{array} \quad (1.11)$$

Further simplifications to the diamond can be made. Because there is a unique non-vanishing holomorphic n -form, $h^{n,0} = h^{0,n} = 1$. Next, we can contract any $(p, 0)$ -form with $\bar{\Omega}$ to give a (p, n) -form, and a subsequent Poincaré duality gives a $(n - p, 0)$ -form. This thus implies that $h^{p,0} = h^{n-p,0}$.

Next, we consider some special impositions. In the case of M being compact and connected, it is standard that $b_0 = 1$. Therefore, the top and bottom tip $h^{0,0} = 1$. Furthermore, if M is simply-connected, i.e., the first fundamental group $\pi_1(M) = 0$, then $H_1(M)$, being the Abelianization of $\pi_1(M)$, also vanishes. This means that $h^{1,0} = h^{0,1} = 0$.

Putting the above together, the Hodge diamond of a compact, connected, simply connected Calabi-Yau 3-fold becomes:

$$\begin{array}{ccccccc}
 & & & & & & b^0 & & 1 \\
 & & & & & & b^1 & & 0 \\
 & & & 0 & & h^{1,1} & & 0 & \\
 & & 0 & & h^{1,1} & & 0 & & \\
 1 & & h^{2,1} & & h^{2,1} & & 1 & \longrightarrow & b^2 & & h^{1,1} \\
 & & 0 & & h^{1,1} & & 0 & & b^3 & & 2 + 2h^{2,1} \\
 & & 0 & & 0 & & & & b^4 & & h^{1,1} \\
 & & & & 1 & & & & b^5 & & 0 \\
 & & & & & & & & b^6 & & 1
 \end{array} \quad (1.12)$$

In other words, the Calabi-Yau 3-folds of our primary concern are actually governed by only 2 degrees of freedom

1. The [Kähler parametres](#), of which there are $h^{1,1}(M)$;
2. The [complex structure parametres](#), of which there are $h^{2,1}(M)$.

More precisely, by Hodge decomposition $H^{p,q}(M) = H^q(M, \bigwedge^p T_M^\vee)$ (cf. (A.1)), we can express our two key Dolbeault cohomology groups as those valued in the tangent bundle T_M and its dual, T_M^\vee , the cotangent bundle:

$$H^{1,1}(M) = H^1(M, T_X^\vee), \quad H^{2,1}(M) = H^{1,2}(M) = H^2(X, T_X^\vee) \simeq H^1(X, T_X), \quad (1.13)$$

where in the last step we have used [Serre Duality](#), that for a vector bundle V on a compact smooth Kähler manifold M of complex dimension n , we have

$$H^i(M, V) \simeq H^{n-i}(M, V^\vee \otimes K_M), \quad (1.14)$$

and since M is Calabi-Yau, the canonical bundle $K_M \simeq \mathcal{O}_M$. This pair of non-negative⁷ integers $(h^{1,1}, h^{2,1})$, the [Hodge pair](#), will play a crucial rôle in the ensuing.

It is well known that the Euler number of a compact smooth manifold can be expressed as an alternating sum of Betti numbers:

$$\chi(M) = \sum_{i=0}^{\dim_{\mathbb{R}}(M)} (-1)^i b^i. \quad (1.15)$$

Thus, combining with (1.10) and for our shape of the Hodge diamond, we arrive at

$$\begin{aligned} \chi(M) &= 1 - 0 + h^{1,1} - (2 + 2h^{2,1}) + h^{1,1} - 0 + 1 \\ &= 2(h^{1,1} - h^{2,1}) \end{aligned} \quad (1.16)$$

for our Calabi-Yau 3-fold.

⁷ In almost all cases, they are both positive integers. The case of $h^{2,1} = 0$ is called *rigid* because here the manifold would afford no complex deformations. The Hodge number $h^{1,1}$, on the other hand, is at least 1 because M is at least Kähler.

2

The Compact Calabi-Yau Landscape

“In the end, the search for a single, all-encompassing theory of nature amounts, in essence, to the search for the symmetry of the universe.”

– Shing-Tung Yau

By now we hope the reader would be intrigued by the richness of Calabi-Yau manifolds and thus motivated, would be impatient for explicit examples with which to befriend. Acquainting ourselves with a “bestiary” (in the spirit of [3]) of Calabi-Yau manifolds will indeed constitute much of the ensuing. As the approach of this book is algebraic, we will construct all our manifolds as **Algebraic Varieties**.

The neophyte might be alarmed at the seeming sophistication of our choice, since it has become customary for the beginning student to learn the rudiments of differential geometry before algebraic geometry, and thereby be familiar with charts and transition functions, *before* polynomial rings and ideals. This is perhaps ironic, since from a practical, and certainly com-

putational, point of view, algebraic varieties are simply vanishing locii of multi-variate polynomials, well known to school mathematics after an entrée to Cartesian geometry. Luckily, powerful theorems such as that of Chow [14] allow us to realize (complex analytic) manifolds as algebraic varieties and vice versa.

Since we are only considering complex manifolds, all our examples will be constituted by the intersection of polynomials in complex variables. Immediately, our Calabi-Yau 1-folds as algebraic torii described in Proposition 1 finds its incarnation: we recall from any second term course in complex analysis that the zero-locus of a cubic polynomial in two complex variables, say $(x, y) \in \mathbb{C}^2$, is a torus. Thus, an Calabi-Yau 1-fold as an elliptic curve is a cubic in \mathbb{C}^2 ; this is an affine variety in $\mathbb{C}[x, y]$.

While in the next chapter focus will be made on affine varieties, for the present chapter we will exclusively consider **projective varieties**. This is for the sake of compactness, as it is well-known that a projective space is attained by adding the “point-at-infinity” to an affine space. Hence, affine complex coordinates $(x, y) \in \mathbb{C}^2$ is promoted to projective coordinates $(x, y, z) \in \mathbb{C}^3$ with the extra identification that $(x, y, z) \sim \lambda(x, y, z)$ for any non-zero $\lambda \in \mathbb{C}^\times$. In other words, the elliptic curve is a cubic in \mathbb{CP}^2 with homogeneous coordinates $[x : y : z]$. We will adopt the convention in complex algebraic geometry that \mathbb{P}^n is understood to be \mathbb{CP}^n :

$$\mathbb{P}_{[z_1:z_2:\dots:z_n]}^n := \mathbb{C}_{(x_0,x_1,\dots,x_n)}^{n+1} / \sim ; \quad (x_0, x_1, \dots, x_n) \sim \lambda(x_0, x_1, \dots, x_n), \quad \lambda \in \mathbb{C}^\times . \quad (2.1)$$

We will almost exclusively work with polynomials embedded in (2.1) as well as some of its natural generalizations.

2.1 The Quintic

In the above, we constructed CY_1 as a cubic ($d = 3$) in \mathbb{P}^2 ($n = 2$), algebraically furnishing a torus into an elliptic curve. Two simple numerologies

should be noted:

- $1 = 2 - 1$: the dimension of the CY is 1 less than that of the ambient space since it is defined by a single polynomial; this is an example of a **hypersurface**.
- $3 = 2 + 1$: the degree of the polynomial exceeds the dimension of the ambient projective space by 1, and is thus equal to the number of homogeneous coordinates; this we will see to be precisely the Calabi-Yau condition.

We wish to construct a Calabi-Yau $(n - 1)$ -fold M realized as a hypersurface in \mathbb{P}^n , i.e., a single homogeneous polynomial of degree d in $n + 1$ projective coordinates. The formal way of doing this is to first write down the Euler short exact sequence [13]

$$0 \rightarrow T_M \rightarrow T_{\mathbb{P}^n}|_M \rightarrow N_{M/\mathbb{P}^n} \rightarrow 0 . \quad (2.2)$$

The sequence essentially states that the tangent bundle of the ambient space $A = \mathbb{P}^n$, when restricted to the hypersurface M , breaks up into the tangent bundle T_M of M and the normal bundle N_{M/\mathbb{P}^n} as M embeds into \mathbb{P}^n . However, T_A does not quite *split* into the direct (Whittney) sum of the two, but is a non-trivial *extension* of the two. One consequence of (2.2) is the Adjunction [13] formula $K_M = \left(K_{\mathbb{P}^n} \otimes N_{M/\mathbb{P}^n}^\vee \right)|_M$ for the canonical bundle K_M . Now, because M is defined by a single polynomial of degree d , this normal bundle is simply $\mathcal{O}_{\mathbb{P}^n}(d)$.

We now appeal to the axioms of the (total) Chern class (cf. Definition 18 in Appendix A). First, normalization axiom $c(\mathcal{O}_{\mathbb{P}^n}(1)) = 1 + H$ gives us the total Chern class of the tangent bundle ¹:

$$c(T_{\mathbb{P}^n}|_M) = (1 + H)^{n+1} , \quad (2.3)$$

¹ This can itself be derived from the sequence of bundles on projective space:
 $0 \rightarrow \mathcal{O}_{\mathbb{P}^n} \rightarrow \mathcal{O}_{\mathbb{P}^n}(1)^{\oplus(n+1)} \rightarrow T_{\mathbb{P}^n} \rightarrow 0 .$

where H is the hyperplane (divisor) class of $\mathbb{P}^{n-1} \hookrightarrow \mathbb{P}^n$. Next, the normal bundle, being $\mathcal{O}_{\mathbb{P}^n}(d)$, is a line bundle of degree d and has only two contributions to the total Chern class

$$c(\mathcal{O}_{\mathbb{P}^n}(d)) = c_0(\mathcal{O}_{\mathbb{P}^n}(d)) + c_1(\mathcal{O}_{\mathbb{P}^n}(d)) = 1 + d H . \quad (2.4)$$

The short exact sequence (2.2) (cf. (A.4)) implies that

$$c(T_M)c(N_{M/\mathbb{P}^n}) = c(T_{\mathbb{P}^n}|_M) , \quad (2.5)$$

whence, recalling that $c_k(T_M) \in H^{2k}(M; \mathbb{R})$, we arrive at the expression for our desired Chern class for M :

$$\begin{aligned} c(T_M) &= (1 + H)^{n+1}(1 + d H)^{-1} \\ &= (1 + (n + 1) H + \binom{n + 1}{2} H^2 + \dots)(1 - d H + d^2 H^2 - \dots) \\ &= 1 + (n + 1 - d)H + \left(\binom{n + 1}{2} + d^2 - d(n + 1) \right) H^2 + \dots \end{aligned} \quad (2.6)$$

In the above, the order H^k term is $c_k(T_M)$ so we expand only to order H^{n-1} since M is of complex dimension $n - 1$ and cannot afford any Chern classes above this dimension.

Immediately, we see that $c_1(T_M) = (n + 1 - d)H$. Using the vanishing c_1 condition in the definition of Calabi-Yau manifolds from §1.3 (because \mathbb{P}^n is Kähler, its holomorphic subvarieties as defined by polynomials in the projective coordinates are automatically Kähler), we arrive at our suspected result:

PROPOSITION 3 *A homogeneous degree $d = n + 1$ polynomial (in the $n + 1$ projective coordinates) as a hypersurface in \mathbb{P}^n defines a Calabi-Yau $(n - 1)$ -fold.*

In particular, we encounter our first Calabi-Yau 3-fold: the degree 5 polynomial in \mathbb{P}^4 , viz., the **Quintic**, Q .

In fact, we have done more. In (2.6), setting $n = 4, d = 5$, we have all the Chern classes for Q :

$$c(T_Q) = 1 + 10H^2 - 40H^3 . \quad (2.7)$$

The top Chern class, here c_3 , is the **Euler class**. Its integral over M should give the Euler number:

$$\chi(Q) = -40 \int_Q H^3 = -40 \cdot 5 = -200 , \quad (2.8)$$

where the integral of H^3 over M is a consequence of Bézout's theorem: H^3 , the intersection of 3 hyperplanes, is the class of 5 points. Another way to think of this is to pull back the integral from M to one on the ambient space A . For $\omega \in H^{n,n}(M)$ and $\mu \in H^{k,k}(A)$ where M is co-dimension k in A so that the normal bundle is rank k , we have $\int_M \omega = \int_A \mu \wedge \omega$. For our present case $\mu = d H$.

2.1.1 Topological Quantities: Exact Sequences

We now have our favourite Calabi-Yau 3-fold, the Quintic, of Euler number -200 . From (1.16), we immediately see that

$$h^{1,1} - h^{2,1} = -100 . \quad (2.9)$$

Obtaining each individual Hodge number, on the other hand, is an entirely different kettle of fish. This perfectly illustrates the principle of index theorems: the alternating sum is given by some topological quantity whilst individual terms require more sophisticated and often computationally involved methods. Within our context, the specific index theorem is a version of Atiyah-Singer [14], stating that

THEOREM 3 (Atiyah-Singer, Hirzebruch-Riemann-Roch) *For a holomorphic vector bundle V on a smooth compact complex manifold M of com-*

plex dimension n , the alternating sum (index) in bundle-valued cohomology is given by

$$\text{ind}(V) = \sum_{i=0}^n (-1)^i \text{rk} H^i(M, V) = \int_M \text{Ch}(V) \wedge \text{Td}(T_M) ,$$

where $\text{Ch}(V)$ is the Chern character for V and $\text{Td}(T_M)$ is the Todd class for the tangent bundle of M .

If we took the simple case of $V = T_M$, and use (A.7) and (A.8) from the appendix, we would obtain the Euler number as a special case of the index theorem ² so that for 3-folds,

$$\chi(M) = \chi(T_M) = \int_M c_3(T_M) . \quad (2.10)$$

Luckily, we do not need to do much in this very case to obtain the individual terms. First, there is only one Kähler class, that inherited from the ambient \mathbb{P}^4 – indeed, $H^2(\mathbb{P}^n; \mathbb{Z}) \simeq \mathbb{Z}$ for any n , corresponding to the hyperplane class, so that $h^{1,1}(\mathbb{P}^n) = 1$ upon Hodge decomposition. Hence,

$$h^{1,1}(Q) = 1 . \quad (2.11)$$

In general, however, it must be emphasized that ambient classes *do not* descend 1-1 to projective varieties and other measures need to be taken, as we shall see.

² In detail, we proceed as follows. Take $V = T_M$, of rank $r = n = \dim_{\mathbb{C}} M$, we have

$$\begin{aligned} \int_M c_n(T_M) &= \sum_{i=0}^r (-1)^i \text{Ch}(\wedge^i T_M^{\vee}) \text{Td}(T_M) && \text{Borel-Serre, (A.9)} \\ &= \sum_{i=0}^n (-1)^i \chi(M, \wedge^i T_M^{\vee}) && \text{Hirzebruch-Riemann-Roch, Theorem 3} \\ &= \sum_{p,q=0}^n (-1)^{p+q} \text{rk} H^q(M, \wedge^p T_M^{\vee}) && \text{definition of } \chi \text{ as index} \\ &= \sum_{i=0}^n (-1)^i h^i(M, \mathbb{C}) = \chi(M) && \text{Hodge Decomposition A.1 .} \end{aligned}$$

Alternatively, we can try to obtain $h^{2,1}$. As mentioned in §1.3.1, these correspond to complex structure. What this means is the following. A generic quintic in $\mathbb{P}^4_{[z_0:\dots:z_4]}$ can be written as a sum over all possible degree 5 monomials in the 5 projective variables z_i ; each monomial has a complex coefficient. Perhaps the most familiar form of Q is

$$Q := \sum_{i=0}^4 z_i^5 - \psi \prod_{i=0}^4 z_i, \quad \psi \in \mathbb{C}, \quad (2.12)$$

consisting of the sum of the 5-th powers, usually called the [Fermat form](#), together with a deformation by the product, with ψ as an explicit complex parametre. The question of complex structure is then to ascertain how many such coefficients, up to variable redefinitions, there are. Again, what we shall do below is a back-of-the-envelope calculation, which *does not* work in general. Nevertheless, its simplicity is illustrative.

First, how many possible degree 5 monomials can be written in 5 variables? This is a standard combinatorial problem and one can quickly convince oneself that the number of degree d monomials in k variables is the so-called multiset coefficient $\binom{n+d-1}{d}$. Next, we need to subtract the reparametrizations coming from linear transformations, i.e., from $PSL(5; \mathbb{Z})$, of which there are $5^2 - 1$. Finally, we are at liberty to rescale the polynomial by an overall constant. Therefore, in all, there are

$$h^{2,1}(Q) = \binom{5+5-1}{5} - (5^2 - 1) - 1 = 126 - 24 - 1 = 101 \quad (2.13)$$

complex deformation parametres. We have therefore rather fortuitously obtained the correct values of the Hodge pair $(1, 101)$ for the quintic and we can check that indeed their difference is -100, as is required by the Euler number in (2.9).

The proper way to perform this above computation is, as might be expected, by sequence chasing. We once more appeal to the Euler sequence (2.2), which induces a long exact sequence in cohomology (the sexy way of saying this is that the cohomological functor H^\bullet is covariant on short exact

sequences):

$$\begin{array}{ccccccc}
0 & \rightarrow & H^0(Q, T_Q) & \rightarrow & H^0(Q, T_{\mathbb{P}^4}|_Q) & \rightarrow & H^0(Q, N_{Q/\mathbb{P}^4}) & \rightarrow \\
& & \boxed{H^1(Q, T_Q)} & \xrightarrow{d} & H^1(Q, T_{\mathbb{P}^4}|_Q) & \rightarrow & H^1(Q, N_{Q/\mathbb{P}^4}) & \rightarrow \\
& & H^2(Q, T_Q) & \rightarrow & \dots & & &
\end{array} \quad (2.14)$$

In the above, we have boxed the term which we will wish to compute, viz., $H^{2,1}(Q) \simeq H^1(Q, T_Q)$. The first term $H^0(Q, T_Q) = H^{1,3}(Q)$ vanishes because Q is Calabi-Yau. The boundary map d actually has 0 rank (q.v. [3] and Eq (6.1) of [48]) and we thus have a short exact sequence $0 \rightarrow H^0(Q, T_{\mathbb{P}^4}|_Q) \rightarrow H^0(Q, N_{Q/\mathbb{P}^4}) \rightarrow H^{2,1}(X) \rightarrow 0$ so that

$$h^{2,1}(X) = h^0(X, N_Q) - h^0(X, T_{\mathbb{P}^4}|_Q) . \quad (2.15)$$

Thus, we have reduced the problem to counting global holomorphic sections. Each of the two terms can be obtained by Leray tableaux [14] (cf. summary in Appendix C.2 of [50] for the present case).

2.1.2 Topological Quantities: Computer Algebra

If a single manifold as simple as the quintic requires so extensive set of techniques, one can only imagine how involved the generic computation in algebraic geometry is. The beginning student may not appreciate how *difficult* dealing with systems of polynomials (a concept introduced at primary school) really is: the system is highly non-linear, especially when the degrees are high. Whilst non-linearity typically invokes the thought of transcendental functions, the field of non-linear algebra is an entire enterprise by itself.

We are fortunate that we live within the age of computers, where at least anything algorithmic such as exact or Leray sequences need not be performed by hand. The discipline of **computational algebraic geometry** is vast and it is not our place to give an introduction thereto here. The keen reader is referred to the fantastic textbook [8] for a pedagogical treatment (cf. also

Appendix A.3 of [49] for a tutorial in the present context of computing bundle cohomology). Nevertheless, the key idea to the matter, viz, the **Gröbner Basis**, is so vital we shall take an immediate foray in Appendix B.

If the reader only wishes for a black-box, much as one wishes to evaluate a complicated integral on **Mathematica** without the desire for the detailed steps, then perhaps the most intuitive software out there is **Macaulay2** [32] a glimpse of whose powers we will now see. The advantages of **Macaulay2** are manifold:

- it is free (downloadable from <http://www2.macaulay2.com/Macaulay2/> and every student of algebraic geometry is encouraged to do so);
- it is included in latest distributions of linux/MacOS/Win10 Ubuntu;
- it has been incorporated into SageMath [38] (cf. <http://doc.sagemath.org/html/en/reference/interfaces/sage/interfaces/macaulay2.html> for calling **Macaulay2** from within **SageMath**);
- the aforementioned book [8] uses it as a companion in instruction; and
- for a quick online experiment without the need to download, one could simply access it “in the cloud” at web.macaulay2.com.

Let us now redo the above Hodge computations for the Quintic in **Macaulay2**. All commands in **Macaulay2** are case-sensitive and there is a habit that the first letter is in lower case and in the case of multiple words concatenated into one, the second starts with a capital. First, we define the polynomial ring R in which we work, consisting of 5 complex variables z_i . The coefficient field ³ is here taken to be $\mathbb{Z}/1979\mathbb{Z}$ (or any other large-ish

³ One must not confuse the coefficient ring/field with the ground ring/field: the former is where the coefficients take value and can be varied quite liberally in all our computations, the latter is where the variables take value, which for us will always be \mathbb{C} .

prime of one's choice); this is the case with most packages in algebraic geometry as the coefficients can grow very quickly in manipulations such as Gröbner bases so we take them modulo some prime. One could always try a few different primes in case the variety becomes singular over particular primes of bad reduction. Thence, we define

```
R = ZZ/1979[z_0, z_1, z_2, z_3, z_4] ;
```

A shorthand for writing this is $R = \mathbb{Z}/1979[z_0 \dots z_4]$. Next, we define a specific quintic polynomial ($\psi = 2$ in (2.12))

```
polyQ = z_0^5 + z_1^5 + z_2^5 + z_3^5 + z_4^5 + 2*z_0*z_1*z_2*z_3*z_4 ;
```

A shorthand for this is `poly = (sum for i from 0 to 4 list x_i^5) + 2 * (product for i from 0 to 4 list z_i)` ;

we remark that we have chosen a particular homogeneous degree 5 polynomial for convenience. Final topological quantities should neither depend on the choice of prime for the coefficient ring nor on the particular form of the polynomial (we remember from Cartesian geometry that ellipses are simply deformed circles).

We now enter the important step of defining the algebraic variety

```
quintic = Proj( R/ideal(polyQ) ) ;
```

Here, we define $polyQ$ as an ideal of the ring R and form the quotient ring $R/\langle polyQ \rangle$ first ⁴. From this quotient ring we form the Proj, which is the projective version of Spec, the maximal spectrum of a ring, to which affine varieties correspond. Roughly, Proj turns quotient rings to projective algebraic

⁴ Indeed, unlike Mathematica, whose primary user is the theoretical physicist, to whom notational flexibility is more important than rigour, all the software mentioned in the preface, and Macaulay2 in particular, are written for the mathematician, where clarity and strictness cannot be relaxed.

varieties, furnishing the explicit map in the ring-variety correspondence [7]. In the case of multiple defining polynomials, say f_1, f_2, \dots , we can simply use `ideal({f_1, f_2, ... })`, which is the most general situation.

Thus, we have `quintic` as a projective variety. We can check its dimension using `dim quintic`, which returns 3, as required. Now, we can check that this quintic is smooth with the built-in command `singularLocus(quintic)`, which returns `Proj(R/1)`, meaning that the smooth locus corresponds to an ideal defined by 1, which of course is not possible since ideals correspond to the vanishing set of polynomials. In other words, there is no singular loci and our quintic is smooth. By convention, the dimension of `Proj(R/1)` is recorded as $-\infty$, as can be checked by the `dim` command. This is indeed in congruence with our conclusions from (B.3) from the Appendix, where $\psi = 2$ is a smooth point in complex structure moduli space.

Now, we move into the heart of the matter by establishing the cotangent bundle (the `prune` command simplifies by “pruning” a sheaf):

```
cotan = prune( cotangentSheaf(quintic) );
```

One can check that this is a rank 3 bundle simply with `rank(cotan)`. Moreover, one can find the canonical bundle as (the exterior power is the wedge product \wedge^3)

```
KQ = prune( exteriorPower(3, cotan) );
```

At this point, we appreciate that whilst the software is extremely convenient, even the state-of-art computers are beginning to struggle a bit: all commands so far take milliseconds to execute on a simple laptop, the exterior power, however, will take quite some time and memory and one might even need to set the prime 1979 to something smaller to enable memory allocation to store the coefficients generated in due course.

We should obtain the result `00 Quintic^1` for `KQ`, meaning that $K_Q = \mathcal{O}_Q$, the trivial structure sheaf (in computational algebraic geometry, sheafs/bundles are denoted by modules via the [sheaf-module correspondence](#)), whereby computationally proving that Q is indeed a Calabi-Yau 3-fold.

Finally, we can use Hodge decomposition (A.1) to compute the requisite topological invariants:

```
H11Q = HH^1 ( cotan );
H21Q = HH^1 ( exteriorPower( 2, cotan ) );
```

In the above, `HH` is the sheaf-cohomology operator, and we readily obtain the results `(ZZ/1979)^1` and `(ZZ/1979)^101` as free-modules respectively for `H11Q` and `H21Q` (one can use the `rank` command to obtain the numbers 1 and 101 respectively).

We conclude this section with a few lessons: (1) algebraic geometry is algorithmic. Finding geometric quantities ultimately reduces to manipulating systems of polynomials, be they reduction or finding (co)kernels of matrices with polynomial components; (2) software such as `Macaulay2` have very conveniently implemented the cruces such as finding Gröbner bases or syzygies, and for simple cases are our indispensable aide; (3) Sadly, computing Gröbner bases is a doubly-exponential running time process, for example, an estimate on the complexity of the Buchberger algorithm has an upper-bound on the degrees of the elements as $\sim (d^2/2 + d)^{2^{n-1}}$ where d is the maximal total degree of the input polynomials and n is the number of variables [41].

2.2 CICY: Complete Intersection Calabi-Yau

While we had enjoyed our promenade in the land of exact sequences and of computational geometry, the quintic - the wealth of beautiful mathematics and physics we had only a tiny glimpse - was less than desirable as far as

(1.9) is concerned: the Euler number (2.9) of -200 is far from ± 6 , it is not even divisible by 3.

An immediate generalization presents itself: instead of a single *hypersurface*, what about a set of polynomials in \mathbb{P}^n ; after all, any projective variety can be so realized. This is clearly too much. The first generalization of a hypersurface is a **complete intersection**, where the codimension of the variety is equal to the number of polynomials. This is a case of the “best possible” intersection where each defining polynomial slices out one dimension. It should be emphasized that complete intersection is obvious very rare and generically k polynomials intersection in \mathbb{P}^n will definitely *not* give a variety of dimension $n - k$.

Cyclic Manifolds How many complete intersection Calabi-Yau 3-folds can be written inside \mathbb{P}^n . Again, this is a simple combinatorial problem: partition $n + 1 = \sum_{i=1}^k n_i$ (the generalization of Proposition 3), together with $n - 3 = k$ (complete intersection condition). There are easily seen to be 5 solutions in total, of which $n = 4, k = 1, n_1 = 5$ is the quintic. By similar considerations as in §2.1, we can compute their Hodge numbers. They all have $h^{1,1} = 1$, as descended from the ambient \mathbb{P}^n . These are consequently called **cyclic** because $H^2(M; \mathbb{Z}) \simeq \mathbb{Z}$, the infinite cyclic group. Adopting the notation $[n|n_1, n_2, \dots, n_k]$ to mean the complete intersection of homogeneous polynomials f_1 of degree n_1 , f_2 of degree n_2 , etc., the 5 solutions are

$$[4|5], [5|2, 4], [5|3, 3], [6|3, 2, 2] \text{ and } [7|2, 2, 2, 2]. \quad (2.16)$$

In fact, the first column is redundant as it is one less than the sum of the rest. By adjunction formula/Euler sequence as before, we can also compute the second Chern class (the first is, of course, 0, and the third integrates to the Euler number) as a multiple of the class H^2 for the hyperplane class $H \subset \mathbb{P}^n$ (for Q , we recall from (2.7), this is 10). By Bézout, we can also find the volume normalization (triple intersection) $d(M) = \int_M H^3$ (for Q , we

recall from (2.8) that this is 5). We summarize the data for all five in Table 2.1.

Intersection	A	Configuration	$\chi(M)$	$h^{1,1}(M)$	$h^{2,1}(M)$	$d(M)$	$c_2(T_M)$
Quintic	\mathbb{P}^4	[4 5]	-200	1	101	5	10
Quadric & quartic	\mathbb{P}^5	[5 2 4]	-176	1	89	8	7
Two cubics	\mathbb{P}^5	[5 3 3]	-144	1	73	9	6
Cubic & 2 quadrics	\mathbb{P}^6	[6 3 2 2]	-144	1	73	12	5
Four quadrics	\mathbb{P}^7	[7 2 2 2 2]	-128	1	65	16	4

Table 2.1: The 5 cyclic Calabi-Yau 3-folds as complete intersections in an ambient space which is a single \mathbb{P}^n . The configuration, Hodge numbers, Euler number are given, together with the second Chern class $c_2(T_M)$, as the coefficient of H^2 for the hyperplane $H \in \mathbb{P}^n$, as well as the volume $d(M) = \int_M H^3$.

Our bestiary of Calabi-Yau 3-folds has now increased from 1 to 5. Again, none has $\chi = \pm 6$, though 2 have Euler number divisible by 6. Can we proceed further? What about generalizing the ambient space to a product of projective spaces instead of a single one? This was considered by [45–48] in the second lustrum of the 1980s. As with the partition problem of (2.16), this amounts to writing the configuration

$$M = \left[\begin{array}{c|cccc} n_1 & q_1^1 & q_1^2 & \cdots & q_1^K \\ n_2 & q_2^1 & q_2^2 & \cdots & q_2^K \\ \vdots & \vdots & \vdots & \ddots & \vdots \\ n_m & q_m^1 & q_m^2 & \cdots & q_m^K \end{array} \right]_{m \times K}, \quad \begin{array}{l} \sum_{r=1}^m n_r = K + 3 \\ \sum_{j=1}^K q_i^j = n_i + 1 \quad \forall i = 1, \dots, m \end{array} \quad (2.17)$$

as a set of K polynomials of multi-degree $q_j^i \in \mathbb{Z}_{\geq 0}$ in the ambient space $A = \mathbb{P}^{n_1} \times \dots \times \mathbb{P}^{n_m}$. The complete intersection condition $\dim(A) - \dim(M) = 3$ translates to $\sum_{r=1}^m n_r = K + 3$, and the $c_1(T_M) = 0$ condition, to $\sum_{j=1}^K q_r^j = n_r + 1$ for each $r = 1, \dots, m$. Again, the left-most column is redundant and may be omitted without ambiguity. The Calabi-Yau 3-fold corresponding to such a configuration as (2.17) is called with the affectionate acronym “CICY”, for Completely Intersection CY_3 .

CICY Classifying CICY matrices, checking redundancies and equivalence, is already a highly non-trivial task, and in some sense constituted one of the very first emergence of (then) big-data to pure mathematics and theoretical physics. Candelas and Lutken recount the fascinating tale of how this was achieved on the then CERN super-computer, involving dot-matrix printers and magnetic tapes, or Schimmrigk, on staring at VAX machines in Austin over long nights.

The result has persisted in two amusing forms, in the corner of Philip's office as a rather large pile of perforated print-out and in Andy's, on a magnetic tape, should the reader even belong to the generation to know what these mean. Luckily, the data has been resurrected [50] and is now accessible at

<http://www-thphys.physics.ox.ac.uk/projects/CalabiYau/cicylist/> in text and Mathematica [39] format (indeed, the webpage of André Lukas has a very useful collection of CICY and other related matter [51]). All requisite data, viz., the Hodge pair, the second Chern class and the triple intersection $d(M)$, have also been computed by [3, 45–48]. Hence, though we reside firmly within the Age of Data and AI and nowadays even the most abstract branches of mathematics have enjoyed information explosion, data mining in algebraic geometry and theoretical physics dates to as early as the late 1980s. One is perhaps reminded of a popular internet meme that technically Moses was the first person to download from the Cloud onto a tablet.

The presentation of the topological data in addition to the Hodge pair require the following. One first fixes a basis $\{J^r\}_{r=1,\dots,h^{1,1}}$ of $H^2(M, \mathbb{Z})$ so that the Kähler cone is $\mathcal{K} = \{t_r J^r | t_r \in \mathbb{R}_{>0}\}$. For the cyclic case, there is only one $J = H$. In general, J will not descend 1-1 from the m hyperplane classes of the ambient product of projective spaces, and when they do, the CICY is called *favourable*. The triple intersection form in this basis is written as

$$d_{rst} := \int_M J^r \wedge J^s \wedge J^t, \quad (2.18)$$

which can be computed by pulling back integration from the ambient product

of projective space where integration is standard, viz.,

$$\int_M \bullet = \int_A \mu \wedge \bullet, \quad \mu := \bigwedge_{j=1}^K \left(\sum_{r=1}^m q_r^j J_r \right). \quad (2.19)$$

The form d_{rst} is a *completely symmetric tensor* with respect to the three indices (note that J^r is a real 2-form so that commuting them across \wedge generates 2 minus signs that cancel).

The total Chern class of a Kähler 3-fold can be written as

$$c(T_M) = \sum_r [c_1(T_M)]_r J^r + \sum_{r,s} [c_2(T_M)]_{rs} J^r J^s + \sum_{r,s,t} [c_3(T_M)]_{rst} J^r J^s J^t. \quad (2.20)$$

For us, $c_1 = 0$ and moreover (2.10) reads

$$\chi(M) = \sum_{r,s,t} d_{rst} [c_3(T_M)]_{rst}, \quad (2.21)$$

leaving us with c_2 as an independent set of quantities to be determined.

Compact CY₃ Data: We remark that the above data is in some sense complete because of an important result of Wall [53]

THEOREM 4 (Wall) *The homotopy type of a compact Kähler 3-fold is completely determined by (1) the Hodge numbers $h^{p,q}$; (2) the triple intersection number d_{rst} ; and (3) the first Pontrjagin class $p_1(T_M) = c_1(T_M)^2 - 2c_2(T_M)$.*

Therefore, for all the Calabi-Yau databases out there, it suffices to record the Hodge numbers, the intersection 3-tensor d and c_2 (often written as a vector in the dual basis to J^r by contracting with d , i.e., as $[c_2(T_M)]_r := \sum_{s,t} [c_2(T_M)]_{rst} d_{rst}$). This was indeed the data shown, for example, for the 5 cyclics in Table 2.1. In this sense, our Calabi-Yau 3-fold data is a list of

integers

$$\boxed{\{(h^{1,1}, h^{2,1}) ; [c_2]_r ; d_{rst}\}}, \quad r, s, t = 1, \dots, h^{1,1} . \quad (2.22)$$

Theorem 4 should also be contrasted with the complex dimension 1 case: there, as we recall, a single integer (the genus or the Euler number) completely characterizes the topological type of a Riemann surface. In complex dimension 3, we essentially need three sets of integers. In complex dimension 2, the situation is actually quite complicated and is intimately related to the celebrated Poincaré Conjecture for 4-manifolds. At least for simply-connected cases, a classical result of Milnor [54] states that the intersection form in middle cohomology suffices to classify the topology.

While we are on the subject of generalities, an important result should be borne⁵ in mind (q.v. e.g., [55]):

PROPOSITION 4 *All compact smooth 3-folds can be smoothly embedded into \mathbb{P}^7 .*

In other words, *in principle*, to classify all Calabi-Yau 3-folds, we only need to systematically write all possible polynomials, degree by degree, hypersurface by hypersurface (indeed, we are by no means restricted to complete intersection - of which there is only one, as we saw in Table 2.1 - there can be any number of defining polynomials). As deceptively simple as this may seem, it is evidently far too difficult a task upon further reflection!

⁵ I am grateful to Mark Gross for reminding me of this. The argument uses the fact that the secant variety to a smooth 3-fold M is at most of complex dimension $2 \cdot 3 + 1 = 7$. Embed this into \mathbb{P}^r . If $r > 7$, then there is a point $p \in \mathbb{P}^r$ not on M , so that there is a projection π_p from p to a hyperplane H , giving us $\pi_p : M \leftrightarrow H \simeq \mathbb{P}^{r-1}$. We can inductively proceed until $r = 7$.

2.2.1 Topological Quantities: Statistics

Let us return to CICYs. The configuration matrix (2.17), as might be expected, readily gives almost all the data in (2.22). One can show [3] that, with $\mu := \bigwedge_{j=1}^K \left(\sum_{r=1}^m q_r^j J_r \right)$ and with normalization $\int_{\mathbb{P}^{n_r}} J^s = \delta_{rs}$ upon integrating the ambient A as a product of projective spaces:

$$\begin{aligned}
c_1^r(T_M) &= 0 \\
c_2^{rs}(T_M) &= \frac{1}{2} \left[-\delta^{rs}(n_r + 1) + \sum_{j=1}^K q_j^r q_j^s \right] \\
c_3^{rst}(T_M) &= \frac{1}{3} \left[\delta^{rst}(n_r + 1) - \sum_{j=1}^K q_j^r q_j^s q_j^t \right] \\
d_{rst} &= \int_A \mu \wedge J^r \wedge J^s \wedge J^t \\
\chi &= \sum_{r,s,t} d_{rst} c_3^{rst} = \text{Coefficient}(c_3^{rst} J_r J_s J_t \mu, \prod_{r=1}^m J_r^{n_r}). \quad (2.23)
\end{aligned}$$

We said ‘almost’, because as always, it is a difficult task to find the individual Hodge numbers for which there is no short-cut, nor explicit formulae as above.

Nevertheless, the full Hodge list was computed in [48] and all the inequivalent configurations, classified in [45–47]. We summarize some key results as follows

- There are **7890** matrices (dropping the first redundant column in (2.17)) from 1×1 (the Quintic, denoted as $[5]_{-200}^{1,101}$) to a maximum of 12 rows, or a maximum of 15 columns;
- All entries $q_j^r \in [0, 5]$;
- The transpose of any CICY matrix is also a CICY;
- The 5 cyclics in Table 2.1 are the only ones with a single row, and their transposes give 4 more.

- There are 266 distinct Hodge pairs $(h^{1,1}, h^{2,1}) = (1, 65), \dots, (19, 19)$;
- There are 70 distinct Euler numbers $\chi \in [-200, 0]$ (all non-positive and none has $|\chi| = 6$).

Recently, it was shown [56] by explicit computer-check using [35] that 195 have freely-acting symmetries (whereby admitting smooth quotients) with 37 different finite groups, from the simplest $\mathbb{Z}/2\mathbb{Z}$, to $(\mathbb{Z}/8\mathbb{Z}) \rtimes H_8$, of order 64.

Other famous CICYs include the Tian-Yau manifold $TY = \begin{bmatrix} 1 & 3 & 0 \\ 1 & 0 & 3 \end{bmatrix}_{-18}^{14,23}$ as well as its transpose, the Schön manifold $S = \begin{bmatrix} 1 & 1 \\ 3 & 0 \\ 0 & 3 \end{bmatrix}_0^{19,19}$, both of which

have been central in string phenomenology. It was found by Yau in the early days that TY had a freely-acting $\mathbb{Z}/3\mathbb{Z}$ symmetry, so that its quotient (which is not a CICY) $[TY/(\mathbb{Z}/3\mathbb{Z})]_{-6}^{6,9}$ has $\chi = -6$. At this time, this quotient was *the* answer to triadophilia. Whilst it had problems with too much extra matter and a less-than-ideal E_6 GUT group, it was taken seriously as string theory's potential solution to the universe [57].

The manifold S is also interesting, it already existed in the mathematics literature [58] as a prime example of elliptic fibration (to which we shall turn later) and a paragon of a self-mirror ($h^{1,1} = h^{2,1}$) manifold. On S , one could find a $(\mathbb{Z}/3\mathbb{Z})^2$ discrete symmetry so that the quotient is a very beautiful (again, non-CICY) self-mirror manifold of Hodge pair $(3, 3)$. In [116], a discussion of these two manifolds, their related cousins as well as quotients, is presented in pedagogical detail.

It is expedient to present the distribution of the Hodge numbers over the CICY dataset. In Figure 2.1 we show the frequency plot/histogram for $h^{1,1}$ (somewhat Gaussian), $h^{2,1}$ (somewhat Poisson) and χ respectively on the left. On the right of the said figure, we plot the distinct values of the Hodge pair (there are only 266 points since there is much multiplicity). As is customary we plot twice the difference, i.e., the Euler number on the abscissa and the

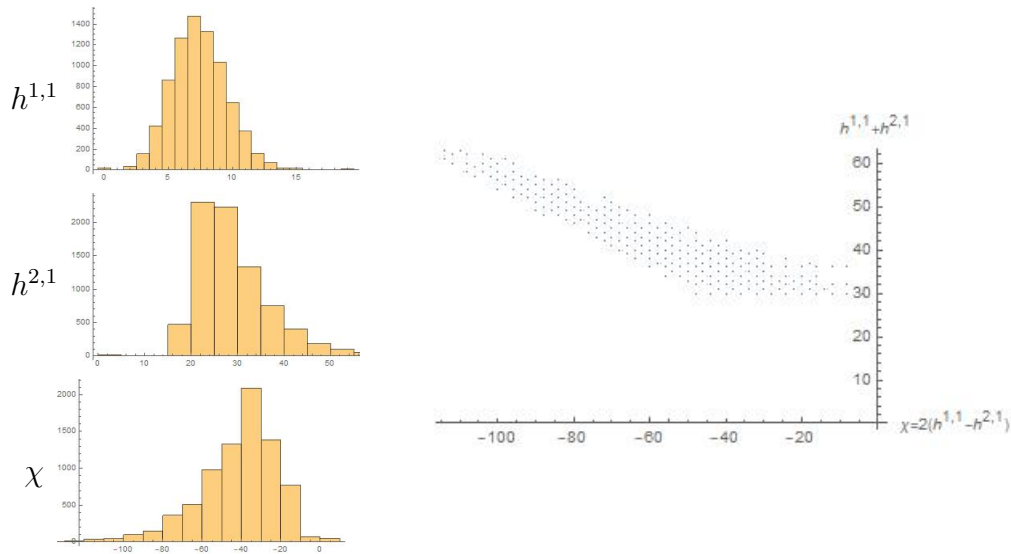


Figure 2.1: The distribution of the Hodge numbers and the Euler numbers for Calabi-Yau 3-folds; a plot of the distinct Hodge pairs, organized as $h^{1,1} + h^{2,1}$ versus Euler number $\chi = 2(h^{1,1} - h^{2,1})$.

sum, on the ordinate. This way, mirror symmetry will be very apparent as a flip along the vertical: a mirror pair of Calabi-Yau 3-folds will be two points symmetric about the y-axis. Moreover, the line $y = |x|$ serves as a natural lower perimeter.

Note the peculiarity of the dataset, that all Euler numbers are non-positive. This is perfect case where one should be constantly vigilant when confronting data (by the standards of the 1990s, rather “big” data), 8 thousand points might have led some to falsely speculate that Calabi-Yau Euler numbers cannot be positive and mirror symmetry would not exist!

2.3 Other Datasets

Prompted by simultaneous developments in physics and mathematics, the early 1990s saw further Calabi-Yau datasets, the prominent ones of which we

now present.

2.3.1 Hypersurfaces in Weighted $\mathbb{C}\mathbb{P}^4$

Perhaps puzzled by the skewness in the CICY χ distribution, Philip Candelas - who, being one of the forefathers of mirror symmetry, was surely aware of this asymmetry - looked to beyond CICYs with his friends. This led to a series of works shortly after the CICYs in the early 1990s [69, 70]. Now, CICYs generalized the quintic by extending a single \mathbb{P}^4 to a product of \mathbb{P}^n 's, another natural extension is to consider weights. Consider the ambient space A as *weighted* projective \mathbb{P}^4

$$A = W\mathbb{P}^4_{[w_0:w_1:w_2:w_3:w_4]} := (\mathbb{C}^5 - \{0\}) / \sim, \quad \text{where} \\ (x_0, x_1, x_2, x_3, x_4) \sim (\lambda^{w_0} x_0, \lambda^{w_1} x_1, \lambda^{w_2} x_2, \lambda^{w_3} x_3, \lambda^{w_4} x_4). \quad (2.24)$$

Indeed, when all $w_i = 1$, this is simply \mathbb{P}^4 . As one might expect, a homogeneous polynomial of degree $\sum_{i=0}^4 w_i$ embedded in A as a hypersurface is Calabi-Yau.

There is a serious complication however: $W\mathbb{P}^4$ is in general singular and resolution is needed in addition to choosing a generic enough hypersurface which avoids any singularities. All this was performed in [69] and we will not delve too much into the details here as we shall later introduce a dataset into which these $W\mathbb{P}^4$ hypersurfaces are subsumed. Nevertheless, this dataset is very convenient in presentation - a single 5-vector of positive integers and, as we see below, is very illustrative in many regards.

In all, [69] found 7555 inequivalent Calabi-Yau 3-folds as 5-vectors, giving us 2780 distinct Hodge pairs and with

$$\chi \in [-960, 960]; \quad h^{1,1}, h^{2,1} \in [1, 491]. \quad (2.25)$$

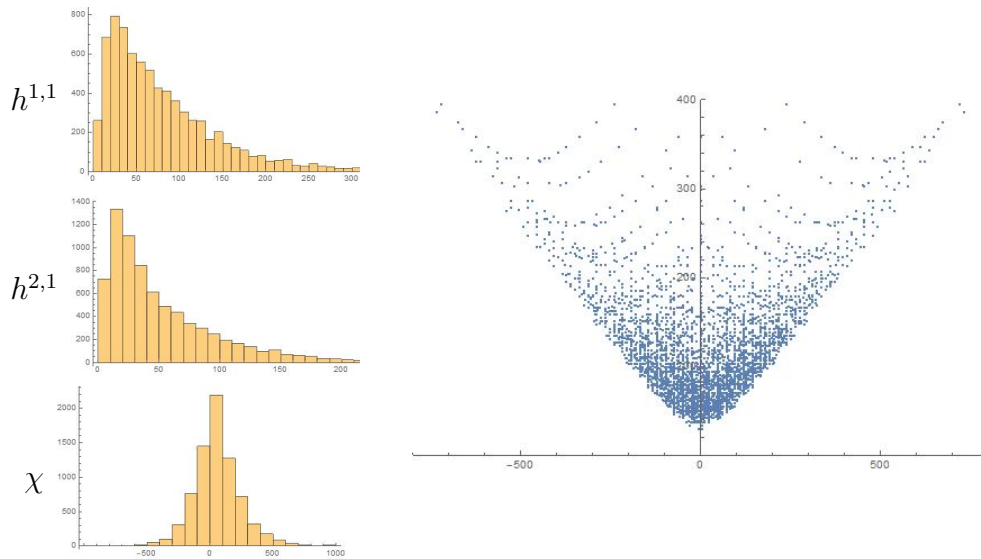


Figure 2.2: The distribution of the Hodge numbers and the Euler numbers for hypersurfaces in $W\mathbb{P}^4$; a plot of the distinct Hodge pairs, organized as $h^{1,1} + h^{2,1}$ versus $\chi = 2(h^{1,1} - h^{2,1})$.

The value 960 is interesting ⁶: it is in fact the largest in magnitude for χ of any Calabi-Yau 3-fold known to date, despite all the plethora of constructions over the decades. In Figure 2.2, we show the histograms for $h^{1,1}$, $h^{2,1}$ (somewhat Poisson) and χ (somewhat Gaussian), as well as a plot of the distinct Hodge numbers. Now, the Euler number has both positive and negative values, with most concentration on the vertical: the left-right symmetry is mirror symmetry, with apparently self-mirror manifolds dominating in number. The full list of distinct Hodge pairs can be downloaded from

<http://hep.itp.tuwien.ac.at/~kreuzer/pub/misc/wp4.spec.gz>

as part of the legacy database of

<http://hep.itp.tuwien.ac.at/~kreuzer/CY/>

⁶ I have bet a bottle of port, as it is a postprandial tradition fortified by drink in some Oxbridge colleges, against Andrew Dancer of Jesus, Oxford, in his College betting book - the volume into which we signed starting from when Napoleon marched into Prussia - that the 960 could never be exceeded. In retrospect, it was realized that the terms of the bet - neither of us being legally trained - were not entirely unambiguous: should some $|\chi| > 960$ 3-fold ever be found after our lifetimes, who would be there to collect or offer the prize?

upon which we shall expound in depth later in the chapter.

2.3.2 Elliptic Fibrations

The 1990s saw a surge of interest in elliptic fibrations, in the mathematics because of the minimal model programme [71–73], and systematic construction of bundles over threefolds [74, 75] (generalizing Atiyah’s classical result on vector bundles over the elliptic curve [76]), and in the physics because of the emergence of so-called F-theory, which is an elliptic-fibration over type IIb string theory [78, 79].

The idea of an elliptic fibration is straight-forward. Recall that an elliptic curve - an algebraic realization of CY_1 - is a cubic in \mathbb{P}^2 . This can be brought to Weierstraß form

$$zy^2 = 4x^3 - g_2xz^2 - g_3z^3, \quad (2.26)$$

where x, y, z are projective coordinates on \mathbb{P}^2 and g_2, g_3 are complex parameters⁷ which in terms of the modular parametre τ are the celebrated Eisenstein series.

Now, fibration simply means that we promote g_2 and g_3 to specific functions (sections) of chosen coordinates of a base B . Being a 3-fold and with fibres elliptic curves ($\dim_{\mathbb{C}} = 1$), it means that the base B must be a complex surface ($\dim_{\mathbb{C}} = 2$). Thus one only needs to modify our variables so that they become sections of appropriate bundles over B . Specifically, it turns out taking the anti-canonical line bundle $L := K_B^{-1} = (\wedge^2 T_B^{\vee})^{-1}$ of B , it suffices to take (x, y, z, g_2, g_3) as global sections of $(L^{\oplus 2}, L^{\oplus 3}, L^{\oplus 0} = \mathcal{O}_B, L^{\oplus 4}, L^{\oplus 6})$ respectively (one can check that the equation become homogeneous degree 6 in terms of the sections of L).

The situation is simplest, for instance, when the base is \mathbb{P}^2 , say with homogeneous coordinates r, s, t . We can directly write the variables as ho-

⁷ The version with which we are perhaps more familiar from our undergraduate days is when $z = 1$, so that we are dealing with the non-compact version embedded in $\mathbb{C}[x, y]$.

mogeneous polynomials of the specified degrees in terms of (r, s, t) and we are back to writing the Calabi-Yau 3-fold as a hypersurface. The general case is more involved as one needs to find the right projective coordinates to embed K_B^{-1} so that the 3-fold can be written as a projective variety.

There is a common belief that most Calabi-Yau 3-folds are elliptically fibered (numbers such as 80%, if not more, have been in the air) and it is still very much an active area of research to identify which CY_3 is in fact an elliptic fibration. For CICYs, this was done in [80] and for the largest set of toric hypersurfaces (which we shall shortly address), systematic studies were carried out in [81], especially for the extremal values. Some explorations in the landscape of elliptic Calabi-Yau 3-folds have been nicely summarized on Wati Taylor's webpage at <http://ctp.lns.mit.edu/wati/data.html>.

Whilst there is, to our knowledge, no complete database of elliptic fibration yet, there is a classification [77] of the possible bases B as well as a computation of Hodge numbers [82]. In brief, the Chern classes of the 3-fold can be written in terms of those of the base as [75]

$$\begin{aligned} c_1(X) &= 0, \\ c_2(X) &= c_2(B) + 11c_1(B)^2 + 12\sigma c_1(B), \\ c_3(X) &= -60c_1(B)^2. \end{aligned} \tag{2.27}$$

The base itself can only be of 4 types:

1. del Pezzo surface $dP_{r=1,\dots,9}$, i.e., \mathbb{P}^2 blown up at r points;
2. Hirzebruch surface $\mathbb{F}_{r=0,\dots,12}$, i.e., \mathbb{P}^1 -bundle over \mathbb{P}^1 ;
3. Enriques surface E , i.e., a particular involution of K3 surface;
4. Blowups of \mathbb{F}_r ;

The del Pezzo and Hirzebruch surfaces are so central both to complex geometry and to today's theoretical physics that we shall devote an appendix

introducing some of their properties in A.3.

2.4 Ne Plus Ultra: The Kreuzer-Skarke Dataset

The mid to late 1990s saw the creation of what still is, by several orders of magnitude, the largest database in Calabi-Yau 3-folds (about 10^{10} , as we shall soon see), or, for that matter, the largest dataset in pure mathematics⁸. The idea is as before: how does one generalize \mathbb{P}^4 ? We have seen weighting and taking products as ambient spaces, a natural next generalization is to take A a toric variety.

Space-time certainly does not permit an introduction to this vast subject of toric varieties, and the reader is referred to the classic of [18], the modern tome of [19], or such preludes as the pertinent chapter in [27] and the brief introduction of [21, 22], as well as the tutorial in the appendix of [94] in our present context. We also leave the readers to Appendix A.2 to fresh their memory on some notations.

Suffice it to say here that whilst a (weighted) projective space of complex dimension n is \mathbb{C}^{n-1} (minus the origin), modulo the equivalence relation of the form (2.24), a toric variety of complex dimension n is \mathbb{C}^{n+k} (minus a point set furnished by the so-called Stanley-Reisner ideal), modulo a set of k equivalence relations (encoded by a charge matrix). All this data can be conveniently repackaged into lattice cones and polytopes in \mathbb{R}^n , and in particular the concept of reflexive polytopes, on the fundamentals of which we now take a lightning review.

⁸ Comparable dataset include the GAP project [35] and related atlas [36] on finite groups (about 10^7), the graded rings project [42] of algebraic varieties, especially Fano 3-folds (about 10^8), the knots [43] database (about 10^6) and the L-functions and modular forms database [44] (about 10^6).

2.4.1 Reflexive Polytopes

We begin by recalling

DEFINITION 1 A *Convex Lattice Polytope* Δ has 2 equivalent definitions:

1. (The Vertex Representation) Convex hull of set S of k lattice points $p_i \in \mathbb{Z}^n \subset \mathbb{R}^n$

$$\text{Conv}(S) = \left\{ \sum_{i=1}^k \alpha_i p_i \quad : \quad \alpha_i \geq 0, \sum_{i=1}^k \alpha_i = 1 \right\}$$

2. (The Half-hyperplane Representation): Intersection of integer inequalities $H \cdot \underline{x} \geq \underline{b}$, where $\underline{b} \in \mathbb{Z}^n$ and $\underline{x} \in \mathbb{R}^n$ and H is some $k \times n$ integer matrix.

Often we use Δ_n to emphasize the dimension n , and we also drop the adjective “convex” as it is understood to be so.

On Δ , the extremal points are called vertices, extremal lines, edges, and then 2-faces, 3-faces, etc, and the $(n - 1)$ -faces of codimension 1 are called facets. In low dimension, we are very familiar with Δ_n : $n = 2$ give lattice polygons (i.e., polygons whose vertices are given by a pair of integer Cartesian coordinates), $n = 3$ give lattice polyhedra, etc.

Next, in the land of lattice convex bodies, the concept of duality is central:

DEFINITION 2 Given a lattice polytope Δ , the *Polar Dual* is the polytope

$$\Delta^\circ := \{ \underline{v} \in \mathbb{R}^n \mid \underline{m} \cdot \underline{v} \geq -1 \quad \forall \underline{m} \in \Delta \} .$$

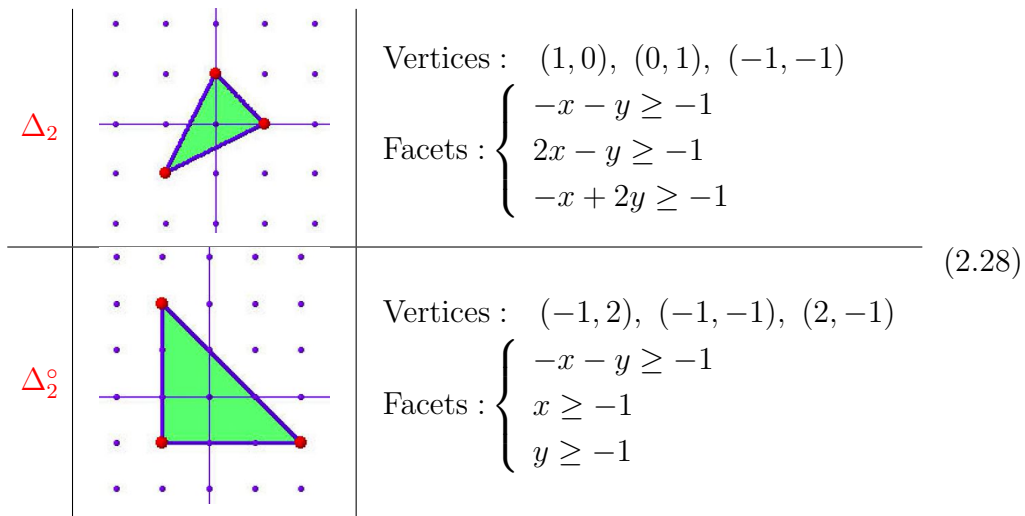
Indeed, this is a duality in the sense that $(\Delta^\circ)^\circ = \Delta$. Note that as defined, Δ° is not necessarily a lattice polytope since upon solving the inequality in

the definition, the vertices of Δ° are not guaranteed to be integer, but will be rational in general. However, in the special case that the polar dual is a lattice polytope, we have that

DEFINITION 3 *If Δ° is also a (convex) lattice polytope, then Δ (and also Δ° by duality) is called *reflexive*.*

In the even more special case that $\Delta = \Delta^\circ$, they are called self-dual or self-reflexive.

To illustrate the above definitions, we give the following pair of examples, which we might have seen from school days. Here, Δ_2 and its polar dual Δ_2° , both lattice polygons, are given in vertex and half-plane representations. One can check the duality between them and the fact that both enjoy integer vertices.



One important observation we make is the origin is the central point. This is, in fact, a general statement (cf. [85] for a popular account):

THEOREM 5 *Δ is a reflexive polytope $\Leftrightarrow \Delta$ has a single interior lattice (which can be shifted to be the origin) \Leftrightarrow the facets of Δ are distance 1 hyperplanes from this interior point.*

Having refreshed our minds on reflexive polytopes, the key fact we now use is that they allow us to construct compact toric varieties. This is done so via the so-called **Face Fan** $\Sigma(\Delta) \equiv \{\sigma = \text{pos}(F) \mid F \in \text{Faces}(\Delta)\}$ where $\text{pos}(F) \equiv \{\sum_i \lambda_i v_i \mid v_i \in F, \lambda_i \geq 0\}$. In other words, as we have a single interior point, we can subtend cones therefrom, joining the various vertices. Once we have the fan, we can obtain a compact toric variety $X(\Sigma)$. For our Δ_2 example above, we see the standard fan for \mathbb{P}^2 :

$$\Delta_2 = \begin{array}{c} \cdot \cdot \cdot \\ \cdot \cdot \cdot \\ \cdot \cdot \cdot \\ \cdot \cdot \cdot \\ \cdot \cdot \cdot \end{array} \Rightarrow \Sigma(\Delta_2) = \begin{array}{c} u_1 \\ \cdot \cdot \cdot \\ \sigma_0 \sigma_2 \\ \cdot \cdot \cdot \\ \sigma_1 \\ \cdot \cdot \cdot \\ u_2 \end{array} \Rightarrow X(\Sigma(\Delta_2)) = \mathbb{P}^2. \tag{2.29}$$

This is a nice way to think of \mathbb{P}^2 , as encoded by the lattice triangle with vertices $\{(1, 0), (0, 1), (-1, -1)\}$.

In general, a reflexive polytope Δ_n will define a compact (complex) n -fold, which is, however, not guaranteed to be smooth. They are called Gorenstein Fano, in that the anti-canonical sheaf is ample [86]. Indeed, as with toric varieties [19], $X(\Delta)$ is smooth iff the generators of all the cones $\sigma \subset \Sigma$ are part of a \mathbb{Z} -basis (i.e., $\det(\text{gens}(\sigma)) = \pm 1$). In such a smooth case, Δ is called **regular**.

2.4.2 CY Hypersurfaces: Gradus ad Parnassum

Once we have a reflexive polytope Δ_n and its associated compact toric variety $X(\Delta_n)$, a beautiful construction gives us

THEOREM 6 (Batyrev-Borisov [88]) *The anti-canonical divisor in $X(\Delta_n)$*

gives a smooth Calabi-Yau $(n - 1)$ -fold as a hypersurface:

$$0 = \sum_{\underline{m} \in \Delta} C_{\underline{m}} \prod_{\rho=1}^k x_{\rho}^{\langle \underline{m}, \underline{v}_{\rho} \rangle + 1},$$

where \underline{m} (over which the sum is performed) are all the lattice points inside and on Δ while \underline{v}_{ρ} are the vertices of Δ° . The coefficients $C_{\underline{m}}$ are complex numbers specifying, as for projective varieties, the complex structure.

In other words, if we have a reflexive Δ_4 , then we can easily obtain a hypersurface therein according to the recipe above, which is CY_3 .

The simplest Fano (toric) 4-fold is \mathbb{P}^4 (all \mathbb{P}^n are Fano because they have positive curvature), it corresponds to a Δ_4 much like how \mathbb{P}^2 is a toric variety in (2.29). Here, the vertices of the polytope and its polar dual are easily checked to be

$$\begin{aligned} \underline{m}_1 &= (-1, -1, -1, -1), & \underline{v}_1 &= (1, 0, 0, 0), \\ \underline{m}_2 &= (4, -1, -1, -1), & \underline{v}_2 &= (0, 1, 0, 0), \\ \Delta : \underline{m}_3 &= (-1, 4, -1, -1), & \Delta^{\circ} : \underline{v}_3 &= (0, 0, 1, 0), \\ \underline{m}_4 &= (-1, -1, 4, -1), & \underline{v}_4 &= (0, 0, 0, 1), \\ \underline{m}_5 &= (-1, -1, -1, 4), & \underline{v}_5 &= (-1, -1, -1, -1). \end{aligned} \tag{2.30}$$

We can find algorithmically (shortly we will see how this is done on the computer) all the lattice points in Δ of which there are 126 (reminiscent of (2.13)), giving us 126 monomials of degree 5 upon taking the dot product in the exponent. We have thus retrieved our favourite quintic 3-fold Q .

A SageMath Digression: It is expedient to take a slight digression on the details of the above computation, as a means to familiarize the reader with SageMath [38] (luckily the software Polymake [93], like Macaulay2 and Singular, have been incorporated). Indeed, the Python-style environment of SageMath and its over-arching vision has rendered it an almost indispensable tool to many contemporary researchers of mathematics and the student

versed therein would be very much at an advantage. Other than downloading the freely available software from <http://www.sagemath.org/>, an extremely convenient way to run SageMath is to do so “via the cloud”, which also allows collaborations, at <https://cocalc.com/>.

We begin with defining the polytope for \mathbb{P}^4 . For convenience, we define the dual Δ° from \underline{v} in (2.30):

```
P4dual = LatticePolytope([[1,0,0,0],[0,1,0,0],[0,0,1,0],
                          [0,0,0,1],[-1,-1,-1,-1]]);
P4 = P4dual.polar();
```

One now checks that the vertices of Δ are indeed as given by \underline{m} in (2.30):

```
P4.vertices()
```

All lattice points on and inside Δ can now be readily found

```
pts = P4.points()
```

This returns a long list of 4-vectors, and `len(pts)` checks that indeed there are 126 of them. Moreover, we can also check polar duality, that $(\Delta^\circ)^\circ = \Delta$ by `LatticePolytope(pts).polar().vertices()`, giving us back the vertices \mathbf{v} of Δ° .

Increasing Sophistication: Returning to our question of Calabi-Yau 3-folds, one would instantly ask whether there are any more than our old friend Q in \mathbb{P}^4 . Let us re-examine the 5 cyclic 3-folds in (2.16), their transposes,

being CICYs, are also CICY, and thus Calabi-Yau, though the ambient space A is more involved:

$$[4|5]_{-200}^{1,101}, \quad \left[\begin{array}{c|c} 1 & 2 \\ \hline 3 & 4 \end{array} \right]_{-168}^{2,86}, \quad \left[\begin{array}{c|c} 2 & 3 \\ \hline 2 & 3 \end{array} \right]_{-162}^{2,83}, \quad \left[\begin{array}{c|c} 2 & 3 \\ \hline 1 & 2 \\ \hline 1 & 2 \end{array} \right]_{-144}^{3,75}, \quad \left[\begin{array}{c|c} 1 & 2 \\ \hline 1 & 2 \\ \hline 1 & 2 \\ \hline 1 & 2 \end{array} \right]_{-128}^{4,68}$$

(2.31)

These are all hypersurfaces in (smooth, toric) Fano 4-folds, with the ambient space being, respectively, \mathbb{P}^4 , $\mathbb{P}^1 \times \mathbb{P}^3$, $\mathbb{P}^2 \times \mathbb{P}^2$, $\mathbb{P}^2 \times \mathbb{P}^1 \times \mathbb{P}^1$ and $(\mathbb{P}^1)^4$, the polytope data for which can also be readily written down. In a way, proceeding from these 5, to the weighted projective hypersurfaces, to the hypersurfaces in Gorenstein Fano toric 4-folds, constitute a sequential generalization and a slow climb in sophistication, a *gradus ad Parnassum*, as it were.

2.4.3 1, 16, 4319, 473800776 . . .

How many reflexive polyhedra Δ_n are there one might ask. That is, how many Δ_n are there in each dimension, up to $GL(n; \mathbb{Z})$ equivalence, an equivalence up to which toric varieties are defined. For $n = 1$, there is clearly just 1, the point. For $n = 2$, this is already non-trivial and it turns out there are exactly 16, a classical result dating at least to the early C20th (cf. [89] for an interesting account). For reference, we present these 16 in Figure 2.3. The nomenclature may seem mysterious, and to that we shall return in the next chapter.

The diagram is organized so that the number of vertices increases from 3 to 6 from left to right and that of the the area (total number of lattice points) increases from 4 to 10 from bottom to top. Polar duality is reflection along the middle horizontal, on which there are 4 self-reflexive ones. We have already seen the pair (1 - 16) in (2.28). Notable cases are toric del Pezzo surfaces $dP_{0,1,2,3}$ and the zeroth Hirzebruch surface \mathbb{F}_0 (cf. Appendix A.3), these are the 5 smooth Fano varieties of dimension 2. Hypersurfaces of the

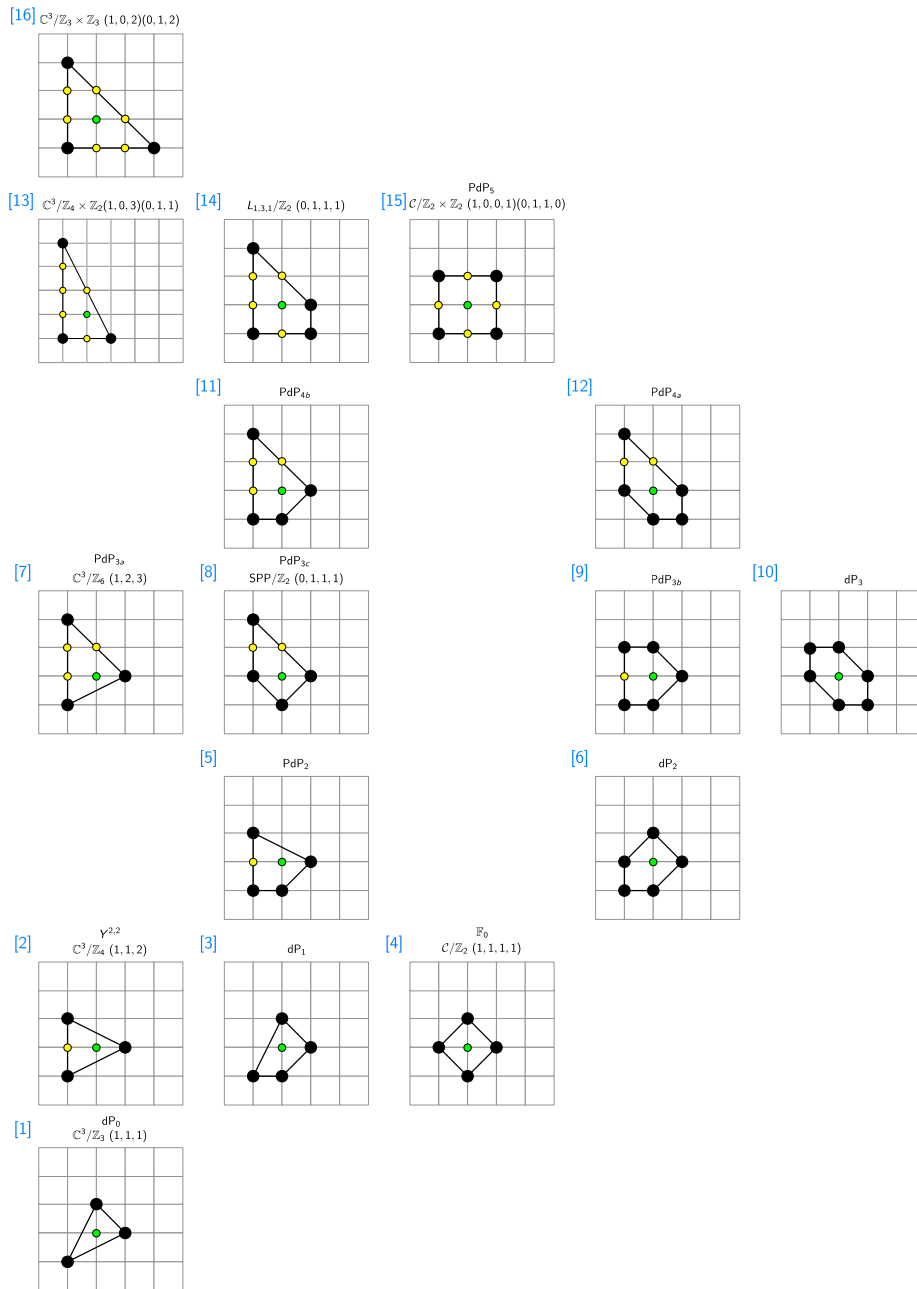


Figure 2.3: The 16 reflexive polygons Δ_2 . The single interior point (origin) is marked green, the vertices, black, and lattice points on the facets but are not vertices, in yellow. Figure taken from [186, 197].

form in Theorem 6 would give CY_1 , or 16 special elliptic curves.

At $n = 3$, this was already unknown to the mathematics community until our present story. Inspired by [88], M. Kreuzer and H. Skarke [KS] undertook the tremendous task to use the computing technology of the mid 1990s to address the $n = 4$ case (which would give a class of desired Calabi-Yau 3-folds) [60, 63], and in passing, solved the $n = 3$ case as a stepping stone [62]. To confront so formidable a problem by a brute-force computer search (for which the package PALP [67], one of the first softwares for combinatorial geometry, was developed ⁹) indeed required the courage of physicists more than the sublimity of mathematicians.

KS found that there are 4319 Δ_3 upto $GL(3; \mathbb{Z})$, of which 18 are regular (and correspond to smooth toric Fano 3-folds). Hypersurfaces of the form in Theorem 6 would give CY_2 , or 4319 algebraic K3 surfaces. The *ne plus ultra* was the tour-de-force computation for $n = 4$, taking more than half a year on two dual Pentium III/600MHz PCs and between 10 and 30 processors on a 64 processor SGI Origin 2000 (if the younger members of the readership even know what these are) [63], giving us 473,800,652 Δ_4 up to $GL(4; \mathbb{Z})$, of which 124 are regular.

This is “big data” even by today’s standards, let alone at the turn of the century. Thus, our bestiary of Calabi-Yau 3-folds, grew steadily to about 10^4 between the late 1980s to the mid 1990s, and suddenly exploded to 10^{10} (the actual number exceeds even this by many orders of magnitude as we shall see shortly) by the end of last decade of C20th.

In summary, we have two fascinating sequences:

dimension	1	2	3	4	...
# Reflexive Polytopes	1	16	4319	473,800,776	...
# Regular/Smooth	1	5	18	124	...

(2.32)

⁹ A recent update and useful manual have been provided in [90].

We have no idea what the next number is for the top row and for the bottom row, which is significantly fewer, at least a handful more have been found by exhaustive search [92], viz., $\{1, 5, 18, 124, 866, 7622, 72256, 749892, 8229721 \dots\}$. It seems possible that there might be a generating function for this, though so far there is no progress on this front. The reader is also referred to an excellent recent account of polytope classification and databases in [93]. In any event, the relevant data is available from KS's Calabi-Yau page <http://hep.itp.tuwien.ac.at/~kreuzer/CY/> (the some 473 million requires about 5 Gb of storage, which is not so astronomical for today's laptop) as well as the polytope database <https://polymake.org/polytopes/paffenholz/www/fano.html>.

Thus the status stands, partially impeded by the most untimely death of Max Kreuzer ¹⁰ until recently when Harald Skarke carried the torch and produced the remarkable estimate on the next number [96], a staggering $2^{26-4} \simeq 1.15 \times 10^{18}$ of which 185, 269, 499, 015 are explicitly found.

Topological Data: In dimension 3, we saw in (2.22) that the CY data is specified by the Hodge numbers, the 2nd Chern class and the intersection numbers. There is a beautiful formula [91] which gave the Hodge numbers in terms of the polytope data

$$\begin{aligned} h^{1,1}(X) &= \ell(\Delta^\circ) - \sum_{\text{codim}\theta^\circ=1} \ell^*(\theta^\circ) + \sum_{\text{codim}\theta^\circ=2} \ell^*(\theta^\circ)\ell^*(\theta) - 5; \\ h^{1,2}(X) &= \ell(\Delta) - \sum_{\text{codim}\theta=1} \ell^*(\theta) + \sum_{\text{codim}\theta=2} \ell^*(\theta)\ell^*(\theta^\circ) - 5. \end{aligned} \quad (2.33)$$

¹⁰ I have a profound respect for Max. It was not long after his visit to Oxford in 2009 - a very productive and convivial period from which I still vividly remember his distinctive and infectious laughter - that Philip, Andre and I received the shocking email that his doctors gave him only a few months. During the last weeks on his deathbed as cancer rapidly took hold of him, Max emailed us regularly and our many discussions continued as normal. His several posthumous papers on the ArXiv are testimonies to his dedication to science. I am honoured and humbled that he, one of the great pioneers of Calabi-Yau data, should write his last journal paper with us [95]. *In pace requiescat.*

In the above, Δ is the defining polytope for the Calabi-Yau hypersurface, Δ° , its dual; θ and θ° are the faces of specified codimension of these polytopes respectively. Moreover, $\ell(\cdot)$ is the number of integer points of a polytope while $\ell^*(\cdot)$ is the number of interior integer points. From the symmetry between the two expressions, we see immediately that

COROLLARY 1 *Polar duality $\Delta \leftrightarrow \Delta^\circ$ for the ambient toric variety is mirror symmetry for the CY_3 hypersurface.*

However, in order to compute the second Chern class and the intersection numbers, we again need to establish the sequence-chasing as in §2.14, requiring that, in particular, the ambient space be smooth. As we saw in (2.32), the number of regular polytopes (smooth varieties) are very rare and almost all the Δ require desingularization, which on the level of the polytope corresponds to “maximal triangulations” [60,67] (q.v., [64] for a tutorial on how this is done using PALP, and how to extract the Chern classes and intersection numbers). It should thus be emphasized that the actual CY hypersurfaces are much, much more than 473,800,776: even though the Hodge pair does not depend on triangulation, the Chern class c_2 and the intersection form d_{rst} do, so the topological type of the CY_3 crucially depend on different triangulations.

Unfortunately, triangulating polytopes is an exponentially expensive process. For small $h^{1,1}$ (up to 6), the full triangulations can be done on the computer while for large $h^{1,1}$ (between 240 and 491), methods were also devised to do so (q.v. Table 1 of [98] for the number of polytopes organized by $h^{1,1}$). To give an idea of the growth rate, the results from [64] on the low Kähler parametres are

$h^{1,1}$	1	2	3	4	5	6	...
# of Polytopes	5	36	244	1197	4990	17101	...
# of Triangulations	5	48	526	5348	57050	590085	...
# of CY	5	39	306	2014	13635	85682	...

(2.34)

where after triangulation, the number of unique Calabi-Yau hypersurfaces (having distinct data in the sense of (2.22)) is also checked. Note that the 5 $h^{1,1}$ cases are the 5 transposes of the cyclics as CICYs, the ambient spaces for which are of course smooth and require no triangulation.

The motivated readers, especially when led by a curiosity induced by insomnia to befriend some Calabi-Yau 3-folds - is highly encouraged to play with the interactive webpages (cf. accompanying papers [64, 251]) of Benjamin Jurke

<https://benjaminjurke.com/academia-and-research/calabi-yau-explorer/>
and Ross Altman

<http://www.rossealtman.com/> .

Furthermore, the reader will be happy to learn that the 16 and the 4319 are built into SageMath [38] using the command `ReflexivePolytope(d,n)` where d is the dimension and n is the n -th Δ . The 473, 800, 652, however, are currently too large to be built-in, but can be downloaded from

<http://hep.itp.tuwien.ac.at/~kreuzer/CY/>

in PALP format. We mention that in the KS dataset, the simplest case of \mathbb{P}^4 is given in a different but $SL(4; \mathbb{Z})$ equivalent form, with Δ° given as

```
4 5  M:126 5 N:6 5 H:1,101 [-200]
    1  1  1  1  -4
    0  5  0  0  -5
    0  0  5  0  -5
    0  0  0  5  -5
```

Here, the first row records that the ensuing matrix for Δ° will be 4×5 , that there are 126 lattice points and 5 vertices for Δ , 6 lattice points and 5 vertices for Δ° (the one more being the origin in the interior). Consequently the Hodge numbers are (1, 101) and $\chi = -200$ for the CY hypersurface.

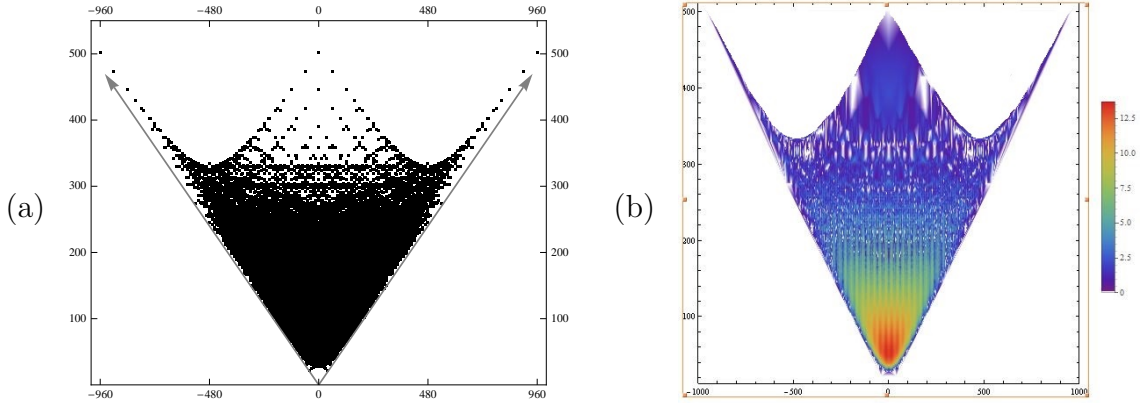


Figure 2.4: (a) A plot of the 30,108 distinct Hodge pairs for the Kreuzer-Skarke dataset of Calabi-Yau hypersurfaces in Gorenstein Fano toric 4-folds; (b) the same but with multiplicity over the log-density of the 473,800,652 over these distinct values.

A Georgia O’Keefe Plot: The KS dataset produced 30,108 distinct Hodge pairs, $\chi \in [-960, 960]$ (note that since the Hodge numbers are triangulation independent, even getting the full list of CY hypersurfaces someday when there is computing power to do all triangulations will not change this). The extremal values of ± 960 , as mentioned in the footnote of §2.3.1, are actually two hypersurfaces in weighted \mathbb{P}^4 , corresponding to the mirror pair of (11, 491) (for weights $w_i = [1 : 1 : 12 : 28 : 42]$) and (491, 11) (for weights $w_i = [21 : 41 : 249 : 581 : 851]$). As always, we can plot $h^{1,1} + h^{2,1}$ versus χ , as was done in [63].

This has become of the most iconic plots in string theory, as it is, *inter alia*, the best experimental evidence for mirror symmetry: every point has its mirror image along the vertical. We reproduce this plot in part (a) of Figure 2.4 (source: Philip Candelas’ office). My only contribution - undoubtedly inspired by my 4-year-old daughter - was to colour it in [99]: in part (b) of the said figure, a heat plot of the log-density (i.e., log of the multiplicity of how many different polytopes per point of Hodge pair: we have 473,800,652 Δ_4 but only 30,108 distinct values using (2.33)) is presented. It is also curious to note that (27, 27) is the most occupied point:

with a multiplicity of 910113. The distribution of the Hodge numbers follows pseudo-Voigt/Planickian curves and is the subject of [100].

There are numerous features of this plot, most of which are still unexplained. Other than the extremals of ± 960 , why is there a boundary on top (the two bounding straight-lines of funnel shape is just by definition of the plot, that the Hodge numbers are non-negative), why do they appear as parabolae? The papers of [98, 101] identify these as elliptic fibrations while [102] find intriguing E_n (del Pezzo) structure.

Independent of the KS dataset, no Calabi-Yau from *any* construction to date has ever produced a Hodge pair above those two puzzling parabolae though there is no theoretical reason why this is so. On the other hand, at the bottom tip, there is also a paucity of manifolds, and this is also true for CY databases in general. This zoo of manifolds of small Hodge numbers ¹¹, is also much investigated [103, 104, 116].

Of course, in addition to all the datasets mentioned above, the CICYs, the elliptic fibrations, the KS, etc, there have been many other constructions, such as using Grassmannians or flag varieties as ambient space [84] or various quotients, etc; and a good compendium is in Table 9 of [103]. Since these have not produced large or available databases online, nor are comparable in number to the KS set, we shall not address them here.

Finally, we mention that shortly before Max Kreuzer's passing, he produced partial results for some 10^{10} double-hypersurfaces in toric Fano varieties coming from reflexive polyhedra in dimension 5. Amazingly, none of their Hodge pairs reside outside the bounds of Figure 2.4.

¹¹ This tip of the plot, where Hodge number are small, is what Philip [116] calls a “des res”, or a “desired residence”, in reference to newspaper advertisements back in the day before social media.

2.5 Cartography of the Compact Landscape

Thus we have taken a promenade in the landscape of Calabi-Yau 3-folds, a contiguous development spanning a decade, from the late 1980s till the turn of the millenium. With the discovery of D-branes [105], M-theory on G_2 manifold [106], F-theory on 4-folds [77, 78, 107], and, of course, the holographic correspondence [108] all approximately within the final lustrum of the century, coupled with the computational limits of the time, the fervour of constructing datasets of compact smooth Calabi-Yau 3-folds by theoretical physicists was relatively cooled. Meanwhile, pure mathematicians interested in Calabi-Yau manifolds had too great a wealth of ideas ranging from enumerative geometry to homological mirror symmetry to preoccupy themselves with the mundanity of data-mining.

We saw above, and will shortly see and shall see again in Chapter 4 how there has been renewed interest in the various datasets. For now, we summarize the landscape of compact smooth Calabi-Yau 3-folds in the Venn diagram in Figure 2.5. The three major datasets are shown with size of the bubbles not to scale. The crosses are supposed to signify various other constructions mentioned above. Our most familiar friends, the quintic Q and the Schoen S , are marked. With the continual growth in number of the Calabi-Yau data, one might be led to wander whether there might be an infinite number. While this is unsettled, there is an important conjecture of Yau [4] that

CONJECTURE 2 (Yau) *There is a finite number of (topological types of) Calabi-Yau threefolds in the sense that there is a finite number of possible values to the data (2.22).*

So far, this full data, viz.,

$$\{(h^{1,1}, h^{2,1}) ; [c_2]_r ; d_{rst}\} , \quad r, s, t = 1, \dots, h^{1,1} , \quad (2.35)$$

is really only known for the CICYs,

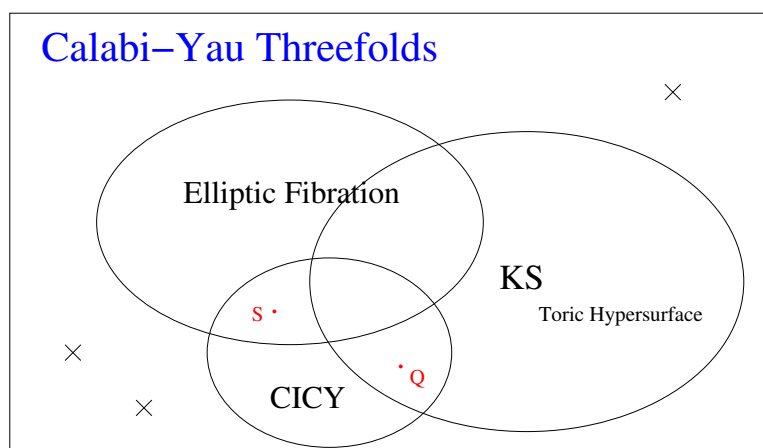


Figure 2.5: The landscape of compact smooth Calabi-Yau 3-folds.

<http://www-thphys.physics.ox.ac.uk/projects/CalabiYau/cicylist/> ,
and very partially, for the KS data:

<http://www.rossealtman.com/>

and it would be interesting to study the statistics thereof.

2.6 Epilogue: Recent Developments

Whereas the original triadophilia, which we recall to be the physicists' search for smooth compact Calabi-Yau 3-folds with $\chi = \pm 6$, saw its *fin-de-siècle* ebb by the aforementioned explosion of other string vacua and by the enormity of the KS data (there are more than 10^6 in the list with $\chi = \pm 6$), there had been renewed interest over the past decade in an extension of more physical importance.

Using the tangent bundle T_M in (1.5) gave, by (1.7), GUT theories with E_6 gauge group. By taking V not being T_M , but, for example, a stable $SU(4)$ or $SU(5)$ bundle, one could obtain the more interesting commutant $SU(10)$ or $SU(5)$ GUTs. This has come to be known as “non-standard” embedding and has with the developments in the theory of stable bundles on Calabi-Yau manifolds become an industry of realistic model building (cf. e.g., [119]).

One can do even better. With the incorporation of Wilson lines, i.e., representations of the fundamental group $\pi_1(M)$, should it be non-trivial, $SO(10)$ and $SU(5)$ can be further broken to the exact standard model group and instead of Hodge numbers (which are cohomologies valued in T_M its duals and exterior powers), one computes the more general bundle-cohomologies valued in V , projected by the $\pi_1(M)$ -representations.

QUESTION 2 *In summary, the mathematical problem becomes*

- *Find a smooth, compact Calabi-Yau 3-fold M with non-trivial fundamental group $\Gamma = \pi_1(M)$. This is usually done by finding an “upstairs” CY 3-fold \widetilde{M} with a freely acting discrete symmetry Γ so that “downstairs” $M \simeq \widetilde{M}/\Gamma$;*
- *Find a stable holomorphic $SU(4)$ or $SU(5)$ vector bundle V with index ± 3 on M (cf. Theorem 3);*
- *Compute the cohomology groups $H^*(M, \wedge^i V)$ which must match the table in (1.6). This done by constructing \widetilde{V} (of index $\pm 3|\Gamma|$) on \widetilde{M} equivariant under Γ and computing the equivariant cohomologies $H^*(\widetilde{M}, \wedge^i \widetilde{V})^\Gamma$ together with the projection of a chosen representation of Γ .*

This is a rich and interesting story in algebraic geometry and in physics and we do apologize that a subject deserving an entire book by itself - a feeble attempt was made in [120] as a quick introduction - has been relegated to an epilogue. However, venturing to the landscape of the extra data of bundles over Calabi-Yau manifolds will clearly be incompatible with the limitations of space and energy.

The problem, due to its physical significance, galvanized Burt Ovrut¹² to launch an ongoing programme by teaming up with card-carrying geometers

¹² The relentlessness with which Burt pursues this ultimate Triadophilia – of not only 3 generations but the exact spectrum and precise properties of the standard model – is truly inspiring. I deeply appreciate the guidance he has given me over the years.

Ron Donagi and Tony Pantev at UPenn during the early years of the millennium. It was supported by one of the earliest inter-disciplinary grants for algebraic geometry/theoretical physics by the USNSF [118], a collaboration at whose fruiting stages I was fortunate to join. The first answer to the above question, called the “Penn Model”, was found in [121], built on a particular bundle of extension type on a quotient of the Schoen manifold, by tuning parameters in constituent line bundles in the exact sequence and exploiting the double elliptic-fibration structure of S .

Again, with the advances in computer algebra, the above problem can be algorithmized [49] over the various datasets (CICYs [50], elliptic fibration [122] and some preliminary cases of the KS set [94, 95]), with a few more exact solutions produced [123], before a tour-de-force scan over Whitney sums of line-bundles within the regions of stability inside the Kähler cone was performed over the CICY list [124]. Over an impressive consortium of some 10^{10} candidates which would have made KS proud, [124] found about 200 exact solutions to the problem, whereby giving 200 possibilities of (heterotic) string compactifications on smooth compact Calabi-Yau 3-folds endowed with (poly-)stable holomorphic vector bundles whose cohomologies give the *exact* charged matter content of the MSSM ¹³.

It is interesting that this 1 in a billion factor of reduction is very much in line with independent model-building results from type II strings on branes [125]. Recently it has been suggested that even within the CICY list alone, there might be 10^{23} bundles ¹⁴ giving the exact standard model matter content [127]. Indeed, the string landscape is far more vast [129] than the initial quick estimates of 10^{500} [128]. The statistics of string vacua is very much an active field [126] and one could, as with fields of cosmogony or exo-planets, take either the anthropocentric view that there is a fundamental selection rule rendering our universe “special” or the more existentialist one that we are simply a stochastic point in a multitude of universes.

¹³ As always with these constructions, the uncharged matter corresponds to $H^*(M, V \otimes V^\vee)$, which give scalar moduli in the field theory.

¹⁴ Tristan Hübsch very charmingly calls it “a mole of models” and we almost entitled the paper as such.

3

The Non-Compact Calabi-Yau Landscape

“At the end of the lecture, an arcane dialogue took place between the speaker [Calabi] and some members of the audience, Ambrose and Singer if I remember correctly. There followed a period of tense silence. Professor Struik broke the ice. He raised his hand and said: ‘Give us something to take home!’ Calabi obliged, and in the next five minutes he explained in beautiful simple terms the gist of his lecture. Everybody filed out with a feeling of satisfaction.”

– Gian-Carlo Rota, *Ten Lessons I wish I had given*

We have now taken a long stroll in the garden of Calabi-Yau manifolds, one of whose key definitions is its Ricci-flat metric, without a single mention of the metric. This, as mentioned from the outset, is not due to negligence but to the fact (and challenge!) that no analytic Ricci-flat Kähler metric has ever been found on a compact Calabi-Yau n -fold (other than the trivial case of tori $T^{2n} \simeq \mathbb{C}^n/\Lambda$ where the flat metric on \mathbb{C}^n is inherited from the discrete quotient). One could try to pull-back the Fubini-Study metric on \mathbb{P}^4 onto the quintic as a natural course of action, but would find the resulting metric

to be positively curved.

Relaxing the condition of compactness usually grants us liberty, as for instance in the familiar setting of Liouville’s theorem on bounded entire functions. In other words, one could think of local models of Calabi-Yau manifolds when one works on some affine patch. In this sense, in the following we will use the words “non-compact”, “affine”, and “local” inter-changeably.

What is the simplest non-compact Calabi-Yau n -fold? Clearly, it is just \mathbb{C}^n , which is not only Ricci flat, but completely flat. Therefore, as the quintic was the *point d’appui* in the previous chapter, \mathbb{C}^3 will be so for our present one. In particular, $\mathbb{C}^3 \simeq \mathbb{R}^6$ is a cone over the round sphere S^5 (just like the more familiar case of \mathbb{R}^3 being a cone over S^2) in that its flat metric ¹ can be written as

$$ds^2(\mathbb{C}^3) = dr^2 + r^2 ds^2(S^5) , \quad (3.1)$$

where r is the radial coordinate of the cone with $r = 0$ being at the origin. One might be misled to think all that this is too trivial but we will soon see a richness in both the mathematics and the physics.

3.1 Another $10 = 4 + 2 \times 3$

While local Calabi-Yau manifolds enjoy a wealth of usefulness in many contexts, in parallel to §1.2 from the Prologue, we take the point of view of its rôle in building the standard model from string theory. Our non-compactness began with the late Joe Polchinski’s discovery of Dirichlet branes, or **D-branes** as dynamical objects in string theory [105]. In a nutshell, a Dp-brane is, by

¹ In the few times when I met Calabi when I was a postdoc at the University of Pennsylvania he struck me as a gentleman of the Old School. I remember when Serge Lang came to give a colloquium (in his 70s) and in his typically flamboyant style turned to Calabi in the middle of his talk when he came to a certain manifold - having repeatedly cross-examined various members of the audience throughout the lecture, and even jokingly told a poor chap to get out when he could not provide a correct answer - “You, Calabi! is it Ricci flat?!” Eugenio calmly answered with his usual charm and diplomacy, “Sorry, I am afraid I was asleep.”

convention, a $(p + 1)$ -dimensional space-time object (one of whose dimension is time) whose world-volume supports a $(p + 1)$ form so that a charge can be obtained by integration. One can see the form as the connection of a $U(1)$ -bundle on the D p -brane. Importantly a stack of N D-branes (i.e., N of them placed in parallel and with separation taken to the zero limit), the gauge group is “enhanced” from $U(1)^N$ to $U(N)$. This is all we will need from the vast theory of D-branes.

It is therefore clear the importance which the D3-brane plays: its world-volume is $3 + 1$ dimensional, and, for our *local* purposes, is $\mathbb{R}^{1,3}$ which gives us a *brane-world*² scenario [109]. The 6 directions perpendicular to a stack of N D3-branes, will again be Calabi-Yau, albeit non-compact. In this set-up, in contrast to the *compactification* scenario of the previous chapter, the (supersymmetric) standard model lives on the $\mathbb{R}^{1,3}$ of the D3-brane, interacting with the transverse or bulk dimensions only via gravity.

3.1.1 Quiver Representations & a Geometer’s AdS/CFT

While the setup of the D-brane’s correspondence between gravity in the bulk and gauge theory on the world-volume goes under the rubric of [holography](#) or [AdS/CFT](#), the challenge of captivating the interest of an algebraic geometer is the one which we will embrace here. Once we phrase at least some of the subject purely in term of the mathematics, we will then see how there too is a plethora of combinatorial data.

In order to venture into this landscape of non-compact Calabi-Yau spaces. We need a few preliminary concepts from representation theory.

DEFINITION 4 A *quiver* $\mathcal{Q} = (\mathcal{Q}_0, \mathcal{Q}_1, W)$ is a finite directed graph with the set of vertices \mathcal{Q}_0 and arrows \mathcal{Q}_1 , the cardinalities of which are N_0 and N_1 respectively:

² The curvature of the brane and back-reactions with the background metric, for our algebro-geometric purposes, will be neglected throughout.

- \mathcal{Q} is equipped with a representation, meaning that we attach $V_i \simeq \mathbb{C}^{n_i}$ to each node for some positive integer n_i , whence each arrow $(X_{ij} \in \mathcal{Q}_1) \in \text{hom}(V_i, V_j)$ can be considered as an $n_j \times n_i$ matrix; we allow self-adjointing arrows, $\phi_i = X_{ii}$, as well as cycles which are closed loops $X_{i_1 i_2} X_{i_2 i_3} \dots X_{i_k i_1}$ formed by the arrows.
- \mathcal{Q} is also furnished by relations; this is imposed by the *superpotential* W which is a polynomial in all the arrows treated as formal matrix variables:

$$W = \sum_{k=1}^{N_2} c_k \text{Tr}(\prod X_{ij}) \dots \text{Tr}(\prod X_{i'j'}) \quad (3.2)$$

summed over possible cycles or products therein with coefficients $c_k \in \mathbb{C}$. The formal polynomial relations amongst the arrows are determined by the vanishing of the Jacobian $\partial_{X_{ij}} W$. We let the number of monomial terms in W be N_2 .

The term quiver was coined by Gabriel [148] because its nodes, like the holster for the weapon, is a holder for arrows.

Indeed, even the pure mathematics community is using the term “superpotential”, which originates in supersymmetric gauge theories and string theory³. The allowance for loops and cycles significantly complicates the representation theory of \mathcal{Q} but this is necessary for the physics. The integers N_0 , N_1 and N_2 will play an interesting combinatorial rôle for a wide class (almost all which we will consider) of quivers. To the above quiver data, one associates a 4-dimensional supersymmetric gauge theory with gauge group

³ There is an underlying 4-dimensional supersymmetric gauge theory, whose action, in $\mathcal{N} = 1$ superspace is

$$S = \int d^4x \left[\int d^2\theta d^2\bar{\theta} \Phi_i^\dagger e^V \Phi_i + \left(\frac{1}{4g^2} \int d^2\theta \text{Tr} \mathcal{W}_\alpha \mathcal{W}^\alpha + \int d^2\theta W(\Phi) + \text{c.c.} \right) \right],$$

where V is the vector multiplet and Φ , the hypermultiplet. The effective potential in terms of the scalars is

$$V(\phi_i, \bar{\phi}_i) = \sum_i \left| \frac{\partial W}{\partial \phi_i} \right|^2 + \frac{g^2}{4} \left(\sum_i q_i |\phi_i|^2 \right)^2$$

whose vanishing is precisely the vacuum defined by the D- and F-terms being 0.

$\mathcal{G} = \prod_{i=1}^{N_0} U(n_i)$ under the dictionary:

Node i : Factor $U(n_i)$ in \mathcal{G}

Arrow $i \rightarrow j$: a so-called bi-fundamental field X_{ij} transforming as $(\square, \bar{\square})$ of $U(N_i) \times U(N_j)$

Loop $i \rightarrow i$: a so-called adjoint field $\varphi_i = X_{ii}$ of $U(N_i)$

Cycle $i_1 \rightarrow i_1 \rightarrow \dots \rightarrow i_k \rightarrow i_1$: Gauge Invariant Operator (GIO) created by concatenating along a path, via matrix multiplication and finishing with an overall trace: $\text{Tr}(X_{i_1 i_2} X_{i_2 i_3} \dots X_{i_k i_1})$; a term such as $\text{Tr}(\prod X_{ij})$ is called a Single-trace GIO while products thereof $\text{Tr}(\prod X_{ij}) \dots \text{Tr}(\prod X_{i'j'})$ are Multi-trace GIO

2-Cycle $X_{ij} X_{jk}$: Mass term

Superpotential (3.2): Superpotential in the Lagrangian with couplings c_i ; and the set of polynomials $\{\partial_{X_{ij}} W\}$ are the F-Terms

The list of labels $\vec{n} = (n_1, n_2, \dots, n_{N_0})$ is called the dimension vector and for the simplest case when all $n_i = 1$, the arrows are just complex numbers and the quantum field theory has gauge group $U(1)^{N_0}$. Finally, recall

DEFINITION 5 *The incidence matrix of \mathcal{Q} is an $N_0 \times N_1$ integer matrix $d_{i\alpha}$ where $i = 1, \dots, N_0$ indexes the nodes and $\alpha = 1, \dots, N_1$, the arrows, such that each arrow $i \rightarrow j$ gives a new column in $d_{i\alpha}$, with -1 at row i and $+1$ at row j , and 0 otherwise.*

Then $\sum_{\alpha} d_{j\alpha} |X_{ij}|^2 - \zeta_i$ are known as *D-terms*, where $\zeta_i \in \mathbb{C}$ are so-called Fayet-Iliopoulos (FI) parameters⁴. Note that unlike the F-terms, these are non-holomorphic, as they involve the complex conjugates of X_{ij} .

⁴ In general, one assigns charges q_{α} to the fields and sum over $q_{\alpha} |X_{i\alpha}|^2$ but for our present purposes of $U(1)^{N_0}$ theories, the incidence matrix serves to encode the charges. Moreover, the FI-parameters exist only for the $U(1)$ gauge group factors.

What does all of this have to do with geometry? There is a key object in geometric representation theory ⁵, coming from a quiver [134, 135].

DEFINITION 6 *The representation variety $\mathcal{M}(\mathcal{Q})$ is the GIT quotient of the representations $Rep(\mathcal{Q}) = \bigoplus_{i,j} \text{hom}(\mathbb{C}^{n_i}, \mathbb{C}^{n_j})$, with relations from W , quotiented by the complexified group $\mathcal{G}_{\mathbb{C}} = \prod_i GL_n(\mathbb{C})$*

$$\mathcal{M}(\mathcal{Q}) = \text{Spec} \mathbb{C}[Rep(\mathcal{Q}) / \langle \partial_{X_{ij}} W \rangle]^{G_{\mathbb{C}}} \simeq \langle \partial_{X_{ij}} W \rangle // \mathcal{G}_{\mathbb{C}} ,$$

where Spec is the maximal spectrum (set of maximal ideals) of the quotient ring.

From the point of view of geometric representation, $\mathcal{M}(\mathcal{Q})$ can be construed as the centre of the path algebra of \mathcal{Q} .

In physics, $\mathcal{M}(\mathcal{Q})$ is called the *vacuum moduli space (VMS)* of the gauge theory ⁶ because solving the F-terms and D-terms amounts to finding the space of solutions which the vacuum expectation values of the scalars parametrize the supersymmetric vacuum.

The rest of the this chapter is concerned with

QUESTION 3 *When is the representation variety $\mathcal{M}(\mathcal{Q})$ an affine variety that is (local) Calabi-Yau M ? In particular, what is the relation between \mathcal{Q} and M when $\dim_{\mathbb{C}}(M) = 3$?*

⁵ Strictly speaking a *quiver variety* in the sense of [135] is a more general and decorated (in the sense of extra data) notion, and $\mathcal{M}(\mathcal{Q})$ really ought to be called the King variety, after [134]. I had suggested this to fellow numerologist Alastair King but he, in his humility, insisted that it be called the representation variety.

⁶To be more precise, \mathcal{M} here defined is the mesonic, Higgs branch of the moduli space because the gauge invariants are built from taking traces. We could contract with other invariant tensors, for instance, contracting with Levi-Civita symbols to obtain the GIOs would give the baryonic moduli space. The Jacobian variety $\langle \partial_{X_{ij}} W \rangle$ is itself also interesting and the equations $\partial_{X_{ij}} W = 0$, which are collectively the F-terms, gives the so-called *master space* [136, 142]

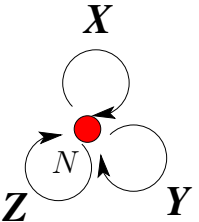
The skeptical reader may wonder why we have chosen to present varieties in this seeming convoluted way through representation of quivers. Other than the fact that it is the central way to understand it in physics, we are assured by the universality of quiver moduli space [134, 137–141]:

THEOREM 7 *Given any scheme \mathcal{M} , there exists a quiver \mathcal{Q} and an ideal \mathcal{J} in the path-algebra $k\mathcal{Q}$ over the ground field k whose moduli space of all indecomposable $k\mathcal{Q}/\mathcal{J}$ -modules (and even with dimension vector $(1, 1, \dots, 1)$), is isomorphic to \mathcal{M} .*

In our language, we can always find some \mathcal{Q} and W so that the VMS $\mathcal{M}(\mathcal{Q})$ is a required variety.

3.1.2 The Archetypal Example

We have certainly bombarded the reader with volley of definitions and abstractions. It is illustrative to take a look at a simple example, which will help to anchor us. Let us take the “clover” quiver with a specific cubic superpotential:



$$W = \text{Tr}(XYZ - XZY) , \quad (3.3)$$

In the above, there is a single node labelled N . Thus, our 3 arrows X, Y, Z are $N \times N$ matrices. The F-terms are obtained from the partials of W with respect to the variables X, Y, Z : one note about taking a derivative by a matrix variable is that within the trace, we can cyclically permute the variables by property of matrix trace, so that we can by convention move the variable to be differentiated to the last position (this matrix derivative is sometimes called the cyclic derivative). Performing this we obtain $\partial_X W = YZ - ZY$, $\partial_Y W = ZX - XY$ and $\partial_Z W = XY - YX$. On the other

hand $\text{Tr}(X)$, $\text{Tr}(Y)$, $\text{Tr}(Z)$ are clearly the 3 minimal generators for the GIOs. Hence,

$$\mathcal{M}(\mathcal{Q}) \simeq \text{Spec}(\mathbb{C}[\text{Tr}(X), \text{Tr}(Y), \text{Tr}(Z)] / \langle [X, Y], [Y, Z], [X, Z] \rangle) . \quad (3.4)$$

While the space may look rather complicated, the case of $N = 1$ should be immediately clear to us. Here, X, Y, Z are just complex numbers and the F-terms provide no extra relations. Hence, $\mathcal{M}(\mathcal{Q})$ is parametrized freely by 3 complex variables, i.e.,

$$\mathcal{M}(\mathcal{Q}_{N=1}) = \text{Spec}\mathbb{C}[X, Y, Z] = \mathbb{C}^3 , \quad (3.5)$$

and we have retrieved our simplest non-compact Calabi-Yau threefold. In general, one can check (though the defining equations become quite involved) that $\mathcal{M}(\mathcal{Q}_{N \geq 1}) \simeq (\mathbb{C}^3)^N / \mathfrak{S}_N$, the N -th symmetric product of \mathbb{C}^3 , i.e., the direct product of N copies of \mathbb{C}^3 , quotiented by the action of the symmetric group by permutations.

The strategy used above to compute $\mathcal{M}(\mathcal{Q})$ explicitly is generally applicable [143] (formalized in [144] and algorithmized in [145]) to obtaining $\mathcal{M}(\mathcal{Q})$:

PROPOSITION 5 *The VMS $\mathcal{M}(\mathcal{Q})$ is realized as an affine algebraic variety by the following algorithm*

1. Let GIO_{\min} be the set of minimal (Eulerian) cycles in \mathcal{Q} , i.e., $\Phi_{r=1, \dots, k}$, each of which is a polynomial in X_{ij} and k , the total number of such cycles;
2. Consider the ring map ⁷ from the quotient ring by the Jacobian ideal by Φ_r as

$$\mathbb{C}[X_{ij}] / \langle \partial W \rangle \xrightarrow{\theta} \mathbb{C}[\phi_r] ;$$

⁷ As coordinate rings the map should go in the reverse direction so that as varieties the map goes as indicated, but we beg the readers' indulgence so that it is clear that the *image* is an affine variety in \mathbb{C}^k .

3. \mathcal{M} is the image of this map, as an affine variety in \mathbb{C}^k .

In the above example for $N = 1$, we have $\Phi : \mathbb{C}[X, Y, Z] \rightarrow \mathbb{C}^3$. Later we will study more involved examples.

Though the above exercise may seem trivial, there is highly non-trivial mathematics and physics even for this example. The quiver with superpotential given in (3.3) is called $\mathcal{N} = 4$ **super-Yang-Mills** theory in $(3 + 1)$ -dimensions. It is the unique conformal, supersymmetric, quantum field theory with maximal supersymmetry in 4-dimensions, and on it countless articles and books have been written. The insight of [108] was that it is precisely the world-volume theory on the D3-brane and there is a “holographic” duality between this gauge theory and the gravity in the bulk Calabi-Yau. More precisely, the D3-branes furnish an asymptotic metric of $AdS_5 \times S^5$ the information of the full string theory on which is holographically projected onto the world-volume gauge theory. The anti-de Sitter space (AdS) and the world-volume conformal field theory (CFT) is what engendered the name “AdS/CFT”. This S^5 factor is none other than the S^5 in (3.1). We will return to this point later in the chapter.

Maldacena’s duality is a set of precise statements on relating correlation functions and partition functions, in a particular limit of large N . Our algebraic geometer’s AdS/CFT, that $\mathcal{M}(\mathcal{Q}) \simeq \mathbb{C}^3 = \text{Cone}(S^5)$, already remarkable, is only a tip of the iceberg of correspondences. But since this is a book on Calabi-Yau varieties and not on QFTs, we will content ourselves with playing on this oasis of a tip.

The point is that because the position of the brane is specified by a point in the transverse non-compact Calabi-Yau space M , the physical moduli, given by the vacuum expectation values (VEVs) of the scalar fields of the world-volume gauge theory, parametrize M by furnishing its coordinates. Now, the gauge theory on the brane is encoded by a quiver with representa-

tion variety $\mathcal{M}(Q) = \text{VMS}$. Therefore, tautologically, by construction,

$$M \simeq \mathcal{M}(Q) = \text{VMS} . \quad (3.6)$$

Therefore, string theory provides a natural answer to Question 3.

3.2 Orbifolds and Quotient Singularities

So far, our non-compact landscape consists of a single point, \mathbb{C}^3 . What is the next natural candidate? Since we are working locally, we are at liberty to allow certain singularities. There is a class of generalization of manifolds which was called V-manifolds [146] but now better known as **orbifolds**. These are perfectly adapted to our present needs.

Briefly, one considers the action of a discrete, finite group $G \curvearrowright \mathbb{C}^n$ with a fixed locus, usually taken to be just a point, the origin, and form the quotient: the very fact there is a fixed locus means that the quotient is not smooth, quite contrary to what one is used to. Indeed, in our discussion of projective spaces and toric varieties in the previous chapter, we remove the origin (Stanley-Reisner ideal) before the quotient so as to avoid singularities.

In order to preserve Calabi-Yau-ness, we must at least work within $SU(n)$ holonomy, i.e., we should only consider orbifolds of the form

$$\mathcal{M} \simeq \mathbb{C}^n / G , \quad G \text{ discrete, finite, subgroup of } SU(n) . \quad (3.7)$$

It turns out that the condition is not sufficient for \mathcal{M} to be local Calabi-Yau, but is a necessary starting point.

In dimension ⁸ $n = 1$, we essentially have only \mathbb{C} quotiented by a cyclic group so that the result is a pizza wedge but with the origin singular.

⁸ In *real* dimension 1, there is only $\mathbb{R}/(\mathbb{Z}/2\mathbb{Z})$, which is just a half-line with the point at the origin a singular point, coming from the real axis folded over.

In dimension $n = 2$, we are considering \mathbb{C}^2 quotiented by discrete, finite, subgroups of $SU(2)$, whose classification goes back (at least) to Klein [147]

Group	Name	Size
$A_n \simeq \mathbb{Z}/(n+1)\mathbb{Z}$	Cyclic	$n+1$
D_n	Binary Dihedral	$4n$
E_6	Binary Tetrahedral	24
E_7	Binary Octahedral (Cube)	48
E_8	Binary Icosahedral (Dodecahedron)	120

(3.8)

For reference, we give all the explicit 2×2 generators for the groups in (B.9) in the Appendix.

To see this, we recall that $SU(2)$ is the lift of $SO(3)$ by its centre $\mathbb{Z}/2\mathbb{Z}$, so we only need the regular symmetries in $SO(3)$, which are the two infinite families of the symmetries of the regular n -gon: the cyclic group of size n and dihedral groups of size $2n$; as well as the symmetries of the 5 Platonic solids: the tetrahedron T , the cube C , the octahedron O , the dodecahedron D and the icosahedron I . However, C - O and D - I are graph dual to each other and share the same symmetry so we only have the 3 exceptional symmetry groups, viz., the alternating group \mathfrak{A}_4 of size 12, the permutation group \mathfrak{S}_4 of size 24, as well as \mathfrak{A}_5 of size 60. Now all these groups need to be lift to $SU(2)$, and become their binary binary counterparts, except the cyclic case which is Abelian whereby affording no lift. The fact we have named the groups ADE is a whole story by itself to which we will devote the next subsection.

Geometrically, $\mathbb{C}^2/(G \subset SU(2))$ should correspond to an interesting set of surface singularities. To write their affine equations as hypersurfaces in \mathbb{C}^3 is simple enough: one only needs to write down the list of generators of invariants under the group action (by a classical theorem of Hilbert-Noether, the ring of invariants is finitely generated) and find the defining relation amongst them. This is a traditional problem in *polynomial invariant theory* and the textbook [149] offers a great account from a computational/Gröbner basis perspective (q.v. Appendix B.0.2).

The Ordinary Double Point: Let us illustrate the above discussions with the simple case of $A_1 = \mathbb{Z}/2\mathbb{Z}$. Let the coordinates of \mathbb{C}^2 be u, v and let $A_1 \curvearrowright \mathbb{C}^2$ by $(u, v) \rightarrow (-u, -v)$. Note that as a matrix group, the generator is $\begin{pmatrix} -1 & 0 \\ 0 & -1 \end{pmatrix}$ and we have to make sure that the generators, and hence all group elements, be unitary and have determinant 1, so as to guarantee the group is properly a subgroup of $SU(2)$.

Clearly, the basic invariants are $x = u^2$, $y = v^2$ and $z = uv$; in the sense that any other invariant of A_1 is a polynomial in these 3. There is a single relation amongst the invariants, viz., $xy = z^2$, so we can write the equation defining \mathbb{C}^2/A_1 , embedding into \mathbb{C}^3 with coordinates (x, y, z) as

$$\mathbb{C}^2/A_1 \quad : \quad \{xy = z^2\} \subset \mathbb{C}[x, y, z] . \quad (3.9)$$

This is perhaps the most well-known algebraic singularity and is known as the *ordinary double point*.

Doing the same for all the groups in (3.8) gives the list of well-known du Val singularities [150], and as with A_1 , one can readily check that the affine equations of these as hypersurfaces $F(x, y, z)$ in \mathbb{C}^3 are:

$$\begin{aligned} A_n &: xy + z^n = 0 \\ D_n &: x^2 + y^2z + z^{n-1} = 0 \\ E_6 &: x^2 + y^3 + z^4 = 0 \\ E_7 &: x^2 + y^3 + yz^3 = 0 \\ E_8 &: x^2 + y^3 + z^5 = 0 . \end{aligned} \quad (3.10)$$

One checks, by solving simultaneously for $F = \partial_x F = \partial_y F = \partial_z F = 0$, that the origin $(x, y, z) = (0, 0, 0)$ is a solution, meaning that it is a singular point.

Desingularization: As with all singularities, the standard procedure is to smoothen (or variously called desingularize, or resolve) it. In performing resolution of a singularity M to a smooth variety \widehat{M} , one compares the

canonical bundle $K_{\widehat{M}}$ of \widehat{M} with the canonical sheaf K_M

$$K_{\widehat{M}} = f^*(K_M) + D \quad (3.11)$$

where $f : \widehat{M} \rightarrow M$ is the *resolution map* and the “extra” divisor D is called the *discrepancy*. Now M , being local Calabi-Yau, has $K_M = \mathcal{O}_M$, and if the discrepancy is 0 and $K_{\widehat{M}} = \mathcal{O}_{\widehat{M}}$ would mean that \widehat{M} is Calabi-Yau. Such a resolution has a cute name:

DEFINITION 7 *When the discrepancy divisor $D = 0$ and the canonical sheaf naturally pulls back as $K_{\widehat{M}} = f^*(K_M)$, the resolution $f : \widehat{M} \rightarrow M$ is called crepant.*

That is, we have dropped the “dis” in “discrepant”, as a play on the English. It is these resolutions that we need for our Calabi-Yau purposes.

The list (3.10) is exhaustive in that we have (cf. [151, 152])

THEOREM 8 *The list (3.10) admit crepant resolutions to smooth K3 surfaces and vice versa, they are all (up to analytic isomorphism) the local models for K3 surfaces.*

The situation is even better, explicit metrics are known for many of these [154], for the A_n series it is the celebrated Eguchi-Hanson metric [153]. In fact, for A_1 which we discussed above, the double point, the quotient \mathbb{C}^2/A_1 is the total space of the cotangent bundle over S^2 , and the Ricci flat metric for it was one of the very first to be constructed [153].

3.2.1 McKay Correspondence

The specialness of the ADE list is remarkable from many approaches in mathematics and this meta-pattern [155] appears in so many mysterious

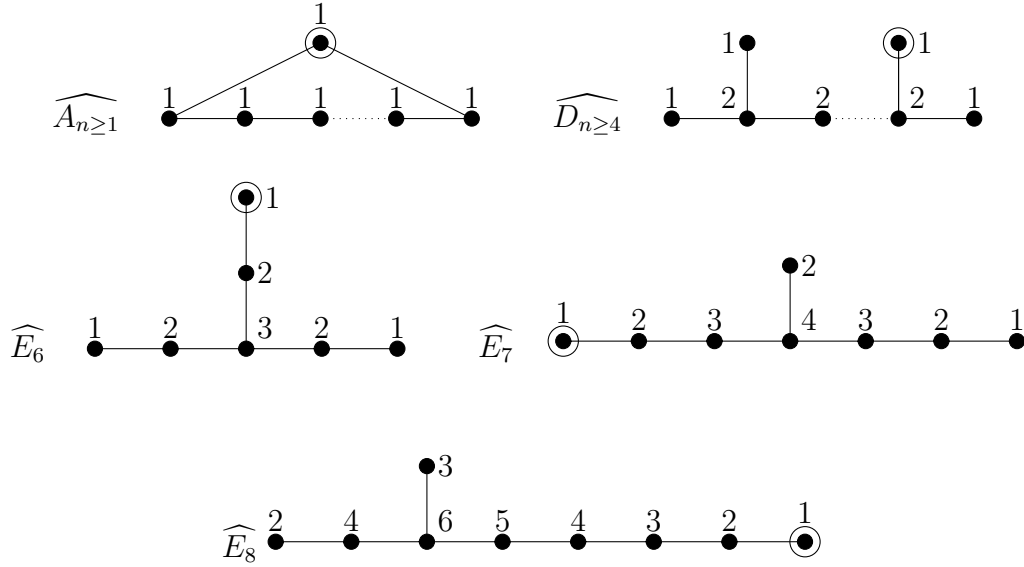


Table 3.1: The extended (affine) ADE diagrams, with integer labels being the Coxeter numbers. The affine nodes are circled explicitly; without this node, the diagram is the Dynkin diagram of the ordinary ADE Lie algebra.

and inter-connected ways that it has inspired an entire discipline of *ADE-ology* [156, 157], a highlight of which is the McKay Correspondence on whose brief exposition we cannot resist but to give.

Take our discrete finite subgroup $G \subset SU(2)$, it has a defining 2 complex-dimensional representation $\mathbf{2}$, which for the non-Abelian cases is irreducible and for the Abelian A_n -series, is the direct sum of 2 (conjugate) one-dimensional representations. John McKay⁹ performed an experiment: tensor $\mathbf{2}$ with all the irreducible representations (irreps) r_i of G , decompose this into irreps as

$$\mathbf{2} \otimes \mathbf{r}_i = \bigoplus_j a_{ij}^{\mathbf{2}} \mathbf{r}_j \tag{3.12}$$

and note the multiplicities $a_{ij}^{\mathbf{2}} \in \mathbb{Z}_{\geq 0}$. He subsequently noticed that [158] if

⁹ John’s super-human ability to notice patterns from unthinkably disparate branches of mathematics, whereby giving profound new insight, is legendary. Yet of all his correspondences, he seems most proud of the ADE one.

one were to interpret a_{ij} as the **adjacency matrix** of a finite graph, they are precisely the Dynkin diagrams of the affine ADE Lie algebras, as shown in Figure 3.1.

Just to briefly recall some rudiments to clarify this amazing fact, we have

DEFINITION 8 *For a finite directed graph with n nodes, the **adjacency matrix** a_{ij} is an $n \times n$ matrix of non-negative integers whose (i, j) -th entry counts the number of arrows from node i to node j .*

In the Dynkin diagram case, each line is understood to represent a bi-directional pair of arrows $i \leftrightarrow j$. Next, an affine Lie algebra is an infinite dimensional extension of the ordinary Lie algebra whose Dynkin diagram has one more “affine” node which we circle in the Figure. Finally, of the complete set of semi-simple Lie algebras, the ADE ones are the *simply-laced*, i.e., there are no double or triple bonds, so that all simple roots are at 60 or 90 degrees from each other.

As is typical of correspondences from John McKay, the above is remarkable in that it relates two seemingly unrelated fields, here that of Lie algebras and of finite groups. To this we can add geometry. It turns out that in the resolution of the singularities in (3.10), one performs blow-up and the exceptional curves are \mathbb{P}^1 s whose intersection matrix is precisely a_{ij} [151]. Thus, we have returned to our initial discussion about moduli space of quivers

PROPOSITION 6 *The representation variety $\mathcal{M}(\mathcal{Q})$ for the affine Dynkin diagrams considered as quivers (the superpotentials are fixed and can be found in e.g. [160]) are the affine hypersurfaces in (3.10), which are local Calabi-Yau 2-folds, i.e., K3 surfaces.*

This beautiful web of relations quickly found its place in string theory [159–162], with the word “quiver” introduced into physics by [161] and the general method of computation set out in [162] and algorithmized in [163].

Recall our example of \mathbb{C}^3 . It can be thought of as an orbifold of \mathbb{C}^3 with the trivial group $G = \mathbb{I}$ and this gave us $\mathcal{N} = 4$ super-Yang-Mills theory in 4 dimension. The discrete subgroups of $SU(2)$, then, furnish orbifolds of the form $\mathbb{C} \times (\mathbb{C}^2/G)$ and these will give McKay quivers (each node also with an added self-adjointing loop due to the \mathbb{C} factor) which correspond to a special class of $\mathcal{N} = 2$ supersymmetric QFTs in 4 dimensions.

3.2.2 Beyond ADE

As so we can generalize. A discrete subgroup G of $SU(3)$ would give an orbifold of the form $\mathbb{C}^3/(G \subset SU(3))$. Luckily, crepant resolutions also exist for these are they are indeed locally Calabi-Yau 3-folds [164, 165]. However, unlike the $n = 2$ case where the crepant solution to K3 surfaces is unique, the $n = 3$ case exist but is not unique and the resolutions are related to each other by flop transitions.

The $SU(3)$ subgroups were first classified at the turn of the twentieth century when matrix groups were still known as colineation groups [166]. Again, the classification scheme follows the dichotomy: (1) infinite-families, and (2) finite exceptional cases. In addition to the obvious cases of the $SU(2)$ subgroups which embed non-transitively (with an block-matrix structure) as well as the Abelian case of $\mathbb{Z}/p\mathbb{Z} \times \mathbb{Z}/q\mathbb{Z}$, the extra $SU(3)$ groups are

$$\begin{array}{c|c} \text{Infinite Series} & \Delta(3n^2), \Delta(6n^2) \\ \hline \text{Exceptionals} & \Sigma_{36 \times 3}, \Sigma_{60 \times 3}, \Sigma_{168 \times 3}, \Sigma_{216 \times 3}, \Sigma_{360 \times 3} \end{array} \quad (3.13)$$

The two infinite families Δ of size $3n^2$ and $6n^2$ are certain non-Abelian extensions of $A_n \times A_n$ and the sizes of the 5 exceptionals (the analogue of the symmetries of the Platonic solids) are marked as subscripts.

Using GAP [35], the representations for all these groups were worked out in [163] and using the orthonormality of finite group characters, one can invert the generalization of (3.12) (with a chosen defining representation \mathbf{R} of G)

as

$$\mathbf{R} \otimes \mathbf{r}_i = \bigoplus_j a_{ij}^{\mathbf{R}} \mathbf{r}_j \quad \Rightarrow \quad a_{ij}^{\mathbf{R}} = \frac{1}{|G|} \sum_{\gamma=1}^r r_\gamma \chi_\gamma^{\mathbf{R}} \chi_\gamma^{(i)} \overline{\chi_\gamma^{(j)}} \quad (3.14)$$

where $\chi_\gamma^{(i)}$ are the entries in the finite character table of G , with (i) indexing the irreps/rows and γ , the conjugacy classes/columns; the number of irreps and number of conjugacy classes are both equal to a positive integer r and r_γ is the size of the γ -th conjugacy class.

Using this, the analogues of the McKay ADE quivers were drawn (cf. Fig. 5 in cit. *ibid.*). In the physics, they correspond to $\mathcal{N} = 1$ super-conformal field theories in 4-dimensions. In the mathematics, they are quivers whose $\mathcal{M}(\mathcal{Q})$ are non-compact Calabi-Yau 3-folds.

Our non-compact landscape has therefore grown from a single example of \mathbb{C}^3 to an infinite number. On the physics side, there is a long programme to try to seriously construct the standard model from branes at singularities [109, 125, 168–177].

To close the discussion on orbifolds, for $n > 3$ in (3.7), the situation is much more complicated. Very little is known about which groups admit crepant resolution to Calabi-Yau manifolds. Nevertheless, the $n = 4$ case has also been classified in [166] and the McKay quiver for these, studied in [167].

3.3 Toric Calabi-Yau Varieties

As with the compact case, the combinatorics of toric geometry gives us the most fruitful method of construction. The geometer need not be alarmed by the title of this subsection, while there are no compact Calabi-Yau manifolds which are toric (in fact they do not even admit any continuous isometries), the fact that we are only concerned with non-compact Calabi-Yau manifolds in this chapter salvages the situation [19] (cf. [21] for a more immediate

treatment). Since we are dealing with a local, affine variety, the toric variety is described by a single cone. We again refer to Appendix A.2 for notation and a rapid discussion on such cones.

The vanishing of the first Chern class translates to the fact that the end-points of the generators of the cone are co-hyperplanar. That is, an affine toric variety of complex dimension n is defined by a rational polyhedral cone in \mathbb{R}^n , but for an affine Calabi-Yau manifold, the end-points lie on a hyperplane and therefore a lattice $(n - 1)$ -polyhedron suffices to encode it. In summary,

THEOREM 9 *An affine (local) toric Calabi-Yau 3-fold M is represented by a toric diagram \mathcal{D} that is a convex lattice polygon, defined up to $GL(2; \mathbb{Z})$. In particular, this gives an infinite number of toric Calabi-Yau 3-folds.*

Now, \mathbb{C}^n is the prototypical example of an affine toric variety, so let us illustrate the above theorem with our familiar \mathbb{C}^3 . The cone for \mathbb{C}^3 has 3 generators, viz., the standard basis of \mathbb{R}^3 , which are clearly coplanar. Therefore, the toric diagram for \mathbb{C}^3 can simply be taken, after $GL(2; \mathbb{Z})$, to be the lattice triangle: $\{(0, 0); (0, 1); (1, 0)\}$.

Next, it should be noted that the Abelian orbifolds to which we alluded earlier are all toric varieties, though the non-Abelian ones are not. Specifically, letting the coordinates of \mathbb{C}^3 be (x, y, z) , the 2 generators of $\mathbb{Z}/p\mathbb{Z} \times \mathbb{Z}/q\mathbb{Z}$ with $p, q \in \mathbb{Z}_+$ can be chosen as

$$(x, y, z) \rightarrow (x, \omega_p y, \omega_p^{-1} z), \quad (x, y, z) \rightarrow (\omega_q x, \omega_q^{-1} y, z) \quad (3.15)$$

to ensure that the group embeds into $SU(3)$, where ω_p and ω_q are the primitive p -th and q -th roots of unity respectively. In particular, \mathbb{C}^3 itself and $\mathbb{C}^3/(\mathbb{Z}/r\mathbb{Z})$ for $r \in \mathbb{Z}_{\geq 2}$ are all toric varieties (the $\mathbb{C}^3/(\mathbb{Z}/2\mathbb{Z})$ case is actually just $\mathbb{C} \times \mathbb{C}^2/(\mathbb{Z}/2\mathbb{Z})$ since there will always be one coordinate fixed). The toric diagram for this Abelian orbifold is the lattice right-angle triangle whose legs (catheti) are of length p and q . Consequently, by choosing large

enough p and q , any toric diagram is a sub-diagram of that of the Abelian orbifold.

3.3.1 Cone over \mathbb{P}^2

We return to our Question 3 of relating the quiver and the Calabi-Yau 3-fold, which in the toric context translates to

QUESTION 4 *What quiver with superpotential \mathcal{Q} has its representation variety (VMS) $\mathcal{M}(\mathcal{Q})$ that is an affine toric Calabi-Yau 3-fold with toric diagram \mathcal{D} (a lattice convex polygon)?*

So far, we know the clover quiver (3.3) corresponds to \mathbb{C}^3 , or $\mathcal{D} = \{(0, 0); (0, 1); (1, 0)\}$, the (minimal) lattice triangle. Also, we know that lattice triangle with legs (p, q) corresponds to the McKay quiver for $\mathbb{Z}/p\mathbb{Z} \times \mathbb{Z}/q\mathbb{Z}$, which turns out to be the clover repeated pq number of times, with all nodes tri-valent. In physics, this is known as a *brane-box model* [178].

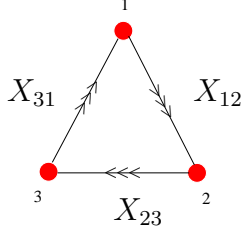
It is expedient to illustrate all of this with a simple but important example. Consider the action on $\mathbb{C}^3[x, y, z]$ by a $\mathbb{Z}/(3\mathbb{Z})$ action

$$(x, y, z) \longrightarrow (\omega_3 x, \omega_3 y, \omega_3 z), \quad \omega_3^3 = 1. \quad (3.16)$$

This is an $SU(3)$ action since the matrix $\text{Diag}(\omega_3, \omega_3, \omega_3)$ is special unitary. There are 3 irreps for the Abelian group $\mathbb{Z}/(3\mathbb{Z})$, all of dimension one, $\mathbf{1}$, $\mathbf{1}_{\omega_3}$, and $\mathbf{1}_{\omega_3^2}$ and the action corresponds to a 3-dimensional reducible representation $R_3 = \mathbf{1}_{\omega_3}^{\oplus 3}$. The quiver can then be obtained from the analogue of (3.12), viz.,

$$R_3 \otimes \mathbf{r}_i = \bigoplus_j a_{ij} \mathbf{r}_j \quad \Rightarrow \quad \text{Adjacency Matrix: } a_{ij} = \begin{pmatrix} 0 & 3 & 0 \\ 0 & 0 & 3 \\ 3 & 0 & 0 \end{pmatrix}, \quad (3.17)$$

which says there are 9 arrows and 3 nodes with triplets going in a cycle. We label the nodes from 1 to 3 and let $X_{ij}^{\alpha=1,2,3}$ denote the triplet of arrow from node i to j . The superpotential W can also be found by projection on the clover using [162] and we have the quiver data



$$W = \sum_{\alpha,\beta,\gamma=1}^3 \epsilon_{\alpha\beta\gamma} X_{12}^{(\alpha)} X_{23}^{(\beta)} X_{31}^{(\gamma)}, \quad (3.18)$$

with arrows $X_{12}^{(\alpha)}, X_{23}^{(\beta)}, X_{31}^{(\gamma)}$ and the completely antisymmetric Levi-Civita symbol $\epsilon_{\alpha\beta\gamma}$. Note that the dimension vector is $(1, 1, 1)$ and the $(1, 2, 3)$ are just index labels for the nodes.

Now, let us check that $\mathcal{M}(\mathcal{Q})$ is as promised. In order to do so, we apply Proposition 5 and to make everything crystal clear, we will again resort to Macaulay2 [32] for our illustration ¹⁰. We begin by ordering the variables as

$$(X_{12}^1, X_{12}^2, X_{12}^3, X_{23}^1, X_{23}^2, X_{23}^3, X_{31}^1, X_{31}^2, X_{31}^3) \rightarrow (X_1, X_2, \dots, X_9) \quad (3.19)$$

and define the ring of the 9 arrow variables

```
R=ZZ/101[X_{1}..X_{9}];
```

Next, there are clearly $3^3 = 27$ GIOs (minimal loops) $X_{12}^\alpha X_{12}^\beta X_{12}^\gamma$, which we index as y_1, y_2, \dots, y_{27} (recall that 101 is just a prime of convenient choice):

```
S=ZZ/101[y_{1}..y_{27}];
```

```
gios = {
```

```
  X_{1}*X_{4}*X_{7}, X_{1}*X_{4}*X_{8}, X_{1}*X_{4}*X_{9},
```

```
  X_{1}*X_{5}*X_{7}, X_{1}*X_{5}*X_{8}, X_{1}*X_{5}*X_{9},
```

¹⁰ The map θ is actually a projection, and one can compactify the whole algorithm in one fell swoop using elimination, as is detailed in §2.1 of [179]. However, for illustrative purposes we will use the ring map presented in the text here.

$$\begin{aligned}
& X_{\{1\}}*X_{\{6\}}*X_{\{7\}}, X_{\{1\}}*X_{\{6\}}*X_{\{8\}}, X_{\{1\}}*X_{\{6\}}*X_{\{9\}}, \\
& X_{\{2\}}*X_{\{4\}}*X_{\{7\}}, X_{\{2\}}*X_{\{4\}}*X_{\{8\}}, X_{\{2\}}*X_{\{4\}}*X_{\{9\}}, \\
& X_{\{2\}}*X_{\{5\}}*X_{\{7\}}, X_{\{2\}}*X_{\{5\}}*X_{\{8\}}, X_{\{2\}}*X_{\{5\}}*X_{\{9\}}, \\
& X_{\{2\}}*X_{\{6\}}*X_{\{7\}}, X_{\{2\}}*X_{\{6\}}*X_{\{8\}}, X_{\{2\}}*X_{\{6\}}*X_{\{9\}}, \\
& X_{\{3\}}*X_{\{4\}}*X_{\{7\}}, X_{\{3\}}*X_{\{4\}}*X_{\{8\}}, X_{\{3\}}*X_{\{4\}}*X_{\{9\}}, \\
& X_{\{3\}}*X_{\{5\}}*X_{\{7\}}, X_{\{3\}}*X_{\{5\}}*X_{\{8\}}, X_{\{3\}}*X_{\{5\}}*X_{\{9\}}, \\
& X_{\{3\}}*X_{\{6\}}*X_{\{7\}}, X_{\{3\}}*X_{\{6\}}*X_{\{8\}}, X_{\{3\}}*X_{\{6\}}*X_{\{9\}} \quad];
\end{aligned}$$

The superpotential expands to a six-term cubic

$$W = X_{23}^1 X_{31}^2 X_{12}^3 - X_{23}^1 X_{31}^3 X_{12}^2 + X_{23}^3 X_{31}^1 X_{12}^2 + X_{23}^2 X_{31}^3 X_{12}^1 - X_{23}^3 X_{31}^2 X_{12}^1 - X_{12}^3 X_{23}^2 X_{31}^1. \quad (3.20)$$

Using our relabelling and taking the partial derivatives with respect to all 9 variables, we have the Jacobian ideal in R

$$\begin{aligned}
\text{jac} = \{ \\
& -X_{\{6\}}*X_{\{8\}}+X_{\{5\}}*X_{\{9\}}, X_{\{6\}}*X_{\{7\}}-X_{\{4\}}*X_{\{9\}}, \\
& -X_{\{5\}}*X_{\{7\}}+X_{\{4\}}*X_{\{8\}}, X_{\{3\}}*X_{\{8\}}-X_{\{2\}}*X_{\{9\}}, \\
& -X_{\{3\}}*X_{\{7\}}+ X_{\{1\}}*X_{\{9\}}, X_{\{2\}}*X_{\{7\}}-X_{\{1\}}*X_{\{8\}}, \\
& -X_{\{3\}}*X_{\{5\}}+X_{\{2\}}*X_{\{6\}}, X_{\{3\}}*X_{\{4\}}-X_{\{1\}}*X_{\{6\}}, \\
& -X_{\{2\}}*X_{\{4\}}+X_{\{1\}}*X_{\{5\}} \quad];
\end{aligned}$$

We are now ready to perform the map θ :

$$M = \ker(\text{map}(R/\text{jac}, S, \text{gios}));$$

Note that we use the kernel rather than the image in Macaulay2 since, we mentioned in the footnote to Proposition 5, the map between varieties is in the opposite direction from that between coordinate rings. As an ideal in S , M is the affine variety $\mathcal{M}(\mathcal{Q})$. First, $\dim(M)$ returns 3, which is good. Next, we can see, using

$$\text{minimalPresentation}(M)$$

what it actually is. This minimal presentation strips of trivial linear relations and reduces the the number of variables in S . In all, only 10 variables are left and V is realized as the (non-complete) intersection of 27 quadrics in \mathbb{C}^{10} , which the astute algebraic geometer would recognize. There is a standard Veronese embedding of $v : \mathbb{P}^2 \hookrightarrow \mathbb{P}^9$ of degree 3

$$v : \mathbb{P}^2 \hookrightarrow \mathbb{P}^9 \quad (3.21)$$

$$; [z_0 : z_1 : z_2] \longrightarrow [z_0^3 : z_0^2 z_1 : z_0 z_1^2 : z_1^3 : z_0^2 z_2 : z_0 z_1 z_2 : z_1^2 z_2 : z_0 z_2^2 : z_1 z_2^2, z_2^3] ,$$

since there are exactly 10 degree 3 monomials in 3 variables. In fact, these are precisely the 10 generators of the ring of invariants under the action of the $G = \mathbb{Z}/3\mathbb{Z}$ in (3.16) and there are 27 quadratic relations amongst them (the 27 quadrics returned from the minimal presentation).

Rephrasing all this in the affine language $M = \text{Spec}\mathbb{C}[x, y, z]^G$, the spectrum of the G -invariant polynomial ring. That is, $M \simeq \mathbb{C}^3/(\mathbb{Z}/3\mathbb{Z})$, the orbifold as desired. Furthermore, the cubics furnish the degree 3 sections of a line bundle over \mathbb{P}^2 , and thence, the orbifold is

$$\mathbb{C}^3/(\mathbb{Z}/3\mathbb{Z}) = \text{Cone}(\mathbb{P}^2) \simeq \text{Tot}(\mathcal{O}_{\mathbb{P}^2}(-3)) , \quad (3.22)$$

the total space of the anti-canonical bundle over \mathbb{P}^2 . We can intuitively think of this as the negative curvature of the cone cancelling the positive curvature of \mathbb{P}^2 , giving a zero-curvature space which is Calabi-Yau.

Finally, as an Abelian orbifold, M is toric, and the toric diagram can be retrieved readily. The 10 exponents of the invariant cubics from (3.21) are $\{ (3, 0, 0), (2, 1, 0), (1, 2, 0), (0, 3, 0), (2, 0, 1), (1, 1, 1), (0, 2, 1), (1, 0, 2), (0, 1, 2), (0, 0, 3) \}$ (one can check that as vectors they are co-planar). The dual cone σ^\vee to the cone σ spanned by these 10 vectors can be readily found, again using SageMath [38], as was done in the digression in §2.4.2:

```
sigma = Cone([
    [3, 0, 0], [2, 1, 0], [1, 2, 0], [0, 3, 0], [2, 0, 1],
    [1, 1, 1], [0, 2, 1], [1, 0, 2], [0, 1, 2], [0, 0, 3] ]);
```

and then `sigma.dual().rays()` returns $\{(1, 0, 0), (0, 1, 0), (0, 0, 1)\}$, which is the toric diagram: its endpoints are coplanar – by appropriate $GL(2; \mathbb{Z})$ we can make the toric diagram as $\mathcal{D} = \{(1, 0), (0, 1), (-1, -1)\}$. Viewed from the plane on which the respective endpoints are coplanar, σ and σ^\vee are simply Δ_2 and Δ_2° in (2.28) respectively, or, the top and bottom of Figure 2.3.

3.3.2 The Conifold

If the toric diagram \mathcal{D} for \mathbb{C}^3 is the minimal lattice triangle $\{0, 0\}, (1, 0), (0, 1)\}$, then one might wonder to what space – call it \mathcal{C} – the next simplest case of $\mathcal{D} = \{(0, 0), (1, 0), (0, 1), (1, 1)\}$, the minimal square, might correspond. The non-triangular shape already precludes the possibility of it being an orbifold of \mathbb{C}^3 and we seem to have the beginning of another interesting family of toric Calabi-Yau 3-folds (simply enlarging the square indeed gives orbifolds of \mathcal{C}).

The defining equation of \mathcal{C} can be readily found through toric methods, as in the previous subsection. We first restore the third coordinate of the toric cone, say by adding height one for the z direction $\{(0, 0, 1), (1, 0, 1), (0, 1, 1), (1, 1, 1)\}$ (there are of course many $GL(\mathbb{Z})$ -equivalent ways of doing this). Next, we treat these vectors as exponents to 3 variables (x, y, z) , giving us the monomials $\{u, v, s, t\} := \{z, xz, yz, xyz\}$ which satisfy the single quadric relation

$$\{ut = vs\} \subset \mathbb{C}[u, v, s, t], \quad (3.23)$$

In summary, this hypersurface in \mathbb{C}^4 , with $(0, 0, 0, 0)$ as its singular point, is an affine, toric, Calabi-Yau 3-fold, called the **conifold**. In fact, just like the ordinary double point (3.9) is the total space of the cotangent bundle over S^2 (as a local K3 surface), this is the total space of the cotangent bundle over S^3 . The metric (the 3-complex-dimensional analogue of Eguchi-Hanson [153]), was found in [180]. It is also a conical metric in the sense that the Calabi-Yau metric can be put in the form of (3.1), but now the base,

instead of being S^5 , is a 5-manifold known rather esoterically as $T^{1,1}$ [180]. For a summary table of some of the most studied toric Calabi-Yau 3-folds and their toric diagrams, see p9 of [181]. Further pedagogical material on toric Calabi-Yau 3-folds, quivers and related physics and mathematics can also be found in cit. *ibid*.

The conifold is one of the central objects in the mathematics and physics of mirror symmetry and geometric transitions and deserves a monograph by itself. Sadly, due to spacetime constraints as well as the theme of this book, we shall only make two remarks.

Geometric Transitions: We can explicitly find the conifold – and indeed any of the affine varieties in this chapter – inside the compact ones from the previous chapter. This justifies the name “local” to which we alluded in the beginning of the chapter. For instance, \mathcal{C} can be a local singularity of our familiar quintic Q from §2.1. Suppose a particular quintic (in the moduli space of complex structures, which we recall to be possible choices of monomials) looked like

$$\bar{Y} := \{z_3g(z_0, \dots, z_4) + z_4h(z_0, \dots, z_4) = 0\} \subset \mathbb{P}_{[z_0:\dots:z_4]}^4, \quad (3.24)$$

where g and h are homogeneous quartic polynomials in the projective coordinates. Unlike the generic quintic, or the Fermat quintic, \bar{Y} is singular, with its singular locus given as

$$\text{Sing}(\bar{Y}) = \{z_3 = z_4 = g(z_0, \dots, z_4) = h(z_0, \dots, z_4) = 0\} \quad (3.25)$$

that solves to $4^2 = 16$ points (nodes), being the intersection of two quartics in the 3 remaining homogeneous variables. These nodes can be

1. Resolved to Y by blow-up;
2. Smoothed to \tilde{Y} by adding generic quintic monomials.

From Y to \tilde{Y} is a geometric transition of the conifold type. In relation to Conjecture 2, it is believed by an optimism known as **Reid's Fantasy** (after Miles Reid), that all Calabi-Yau 3-folds can be related to each other by versions of such geometric transitions.

Sasaki-Einstein Manifolds: The other emblematic aspect of the conifold is its conical form of the metric, analogous to \mathbb{C}^3 in (3.1). This important property is one of a class of manifolds known as *Sasaki-Einstein*. In general, suppose we have a Kähler n -fold M with Kähler form ω which is a cone over a $(2n - 1)$ -dimensional real manifold X . The metric takes the form

$$ds^2(M) = dr^2 + r^2 ds^2(X) , \quad (3.26)$$

with $r \in \mathbb{R}_{\geq 0}$ the radial coordinate for the cone where $r = 0$ is the tip. The base $(2n - 1)$ -manifold is called Sasakian when M is Kähler. If in addition M is Calabi-Yau, then X is called Sasaki-Einstein.

The Kähler form ω can be written, for η a global one-form on X , as $\omega = -\frac{1}{2}d(r^2\eta) = \frac{1}{2}i\partial\bar{\partial}r^2$. Moreover, X has a Killing vector field R called the **Reeb vector**, defined, for the complex structure \mathcal{I} on M , as $R := \mathcal{I}\left(r\frac{\partial}{\partial r}\right)$.

Now, when M is furthermore toric Calabi-Yau, meaning that we have an integrable torus action \mathbb{T}^n which leaves ω invariant, everything becomes even more explicit and the metric can be elegantly written down [182]. Taking $\partial/\partial\phi_i$ to be the generators of the torus action, with ϕ_i to be the angular coordinates, allows for the introduction of symplectic coordinates y_i defined as $y_i := -\frac{1}{2}\langle r^2\eta, \frac{\partial}{\partial\phi_i} \rangle$, with $\langle \cdot, \cdot \rangle$ the usual bilinear pairing between forms and vector fields.

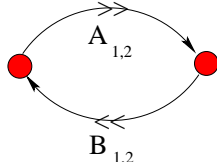
Subsequently, the Kähler form and the metric become, in these symplectic coordinates

$$\omega = dy_i \wedge d\phi_i , \quad ds^2 = G_{ij}dy_i dy_j + G^{ij}d\phi_i d\phi_j , \quad (3.27)$$

where G^{ij} is the inverse of $G_{ij} := \partial_i \partial_j G$ for some symplectic potential G determined from the complex structure as $\mathcal{I} = \begin{bmatrix} 0 & -G^{ij} \\ G_{ij} & 0 \end{bmatrix}$. There is a long programme to understand the geometry of Sasaki-Einstein cones in relation to the world-sheet conformal field theory, generating such beautiful results as the equivalence of the minimization of the volume of the base X and the maximization of certain central charge in the field theory [183–185].

Now, with non-compact manifolds, it is difficult to have a canonical notion of Hodge numbers and other such topological quantities. Thus, while we have an infinite number of data points, it is hard to have a succinct analogue of the Hodge-pair plot of Figure 2.4. With a compact Sasaki-Einstein base, however, one *does* have an ordinary sense of Euler and Betti numbers. The statistical studies of these, versus the normalized volumes for toric Calabi-Yau 3- and 4-folds coming from reflexive polytopes (cf. the 16 polygons of Figure 2.3 and the analogous 4319 polyhedra) was initiated in [186].

The Conifold Quiver: Returning to our question of quiver representations, what (\mathcal{Q}, W) has \mathcal{C} as its moduli space? This problem was solved by [187] in one of the earliest examples of AdS/CFT beyond \mathbb{C}^3 . The required data is a 2-noded quiver (with dimension vector (N, N)), with 4 arrows ($A_{1,2}$ and $B_{1,2}$, which are bi-fundamentals under $SU(N) \times SU(N)$) and 2-term quartic superpotential (upon expanding out the antisymmetric symbol ϵ):



	$SU(N)$	$SU(N)$
$A_{i=1,2}$	\square	$\bar{\square}$
$B_{j=1,2}$	$\bar{\square}$	\square

$$\begin{aligned}
 W &= \text{Tr} \left(\sum_{i,j,k,l=1,2} \epsilon_{il} \epsilon_{jk} A_i B_j A_l B_k \right) \\
 &= \text{Tr} (A_1 B_1 A_2 B_2 - A_1 B_2 A_2 B_1) .
 \end{aligned}
 \tag{3.28}$$

One can check the VMS quite simply in this case. Taking $N = 1$, we again have $W = 0$ so no further quotients by the Jacobian ideal is needed. There

are 4 minimal loops: $u = A_1B_1$, $t = A_2B_2$, $v = A_1B_2$ and $s = A_2B_1$, and they satisfy the one equation, the hypersurface in (3.23), as required for the defining quadric of \mathcal{C} . Taking $N > 1$ would have given us the symmetric product $\mathcal{C}^N/\mathfrak{S}_N$.

3.3.3 Bipartite Graphs and Brane Tilings

Having gained some confidence with examples, one might wonder whether there exists, on returning to the original Question 3 of this chapter, an algorithm of translating between the quiver data and the Calabi-Yau data. For orbifolds, we saw that we needed the character table of the finite group and then happily using McKay’s method. Surely, the rich combinatorics of toric varieties should facilitate this translation. Indeed, the method was given in [188] and algorithmized in [189], wherein the direction $\mathcal{Q} \rightarrow \mathcal{D}$, from the quiver (with superpotential) data to the toric diagram, was called, rather unimaginatively, the *forward algorithm* and the direction $\mathcal{D} \rightarrow \mathcal{Q}$, the *inverse algorithm*.

The forward algorithm is more or less by direct computation, using a toric version of what was done in §3.3.1. The inverse algorithm uses the facts that (1) every toric diagram is a sub-diagram of that of $\mathbb{C}^3/(\mathbb{Z}/p\mathbb{Z} \times \mathbb{Z}/q\mathbb{Z})$ for sufficiently large p, q meaning that geometrically every affine toric Calabi-Yau 3-fold is a partial resolution of the said orbifold (corresponding to node deletion in its toric diagram); (2) the quiver for the orbifold is known and it is simply the generalized McKay quiver with superpotential; and (3) the desired quiver can be obtained by deletion of the nodes which corresponds to removal of arrows (Higgsing in the field theory).

This inverse algorithm of “geometrical engineering” (a whimsical but very appropriate term first coined in [190]) the quiver/physics from the given Calabi-Yau geometry turns out to be computationally expensive, with the bottle-neck being finding the dual cone for a given convex lattice polyhedral cone, which is exponential in complexity. The break-through came

in the mid-2000s when it was realized [191, 192] that a seemingly frivolous relation for the quiver \mathcal{Q} is actually of deep physical and mathematical origin and consequence: whenever $\mathcal{M}(\mathcal{Q})$ is toric, it was noted that

$$N_0 - N_1 + N_2 = 0 \tag{3.29}$$

for N_0 , the number of nodes, N_1 , the number of arrows, and N_2 , the number of monomial terms in the superpotential. In our running examples, for \mathbb{C}^3 , this is $1 - 3 + 2 = 0$, for \mathcal{C} , this is $2 - 4 + 2 = 0$, for $\text{Cone}(\mathbb{P}^2)$, this is $3 - 9 + 6 = 0$.

Over the years, the *School of Hanany*¹¹ pursued the mapping between toric Calabi-Yau manifolds and quiver representations relentlessly. In brief, (3.29) is the Euler relation for a torus, and the quiver data (and superpotential) can be re-packaged into a bipartite tiling (called [brane tiling](#) or [dimer model](#)) of the doubly-periodic plane. This bipartite-ness is profound and involves a plethora of subjects ranging from scattering amplitudes, to dessin d'enfants, to cluster mutation, etc. [203–209].

The bipartite tiling perspective on quiver representations and Calabi-Yau moduli spaces has grown into a vast field itself [193–200], on which there are excellent introductory monographs [210–212], a short invitation by means of a conference report [181], and an upcoming book [213]. Again, with an apology we leave the curious reader to these references as well as two bird's-eye-view summary diagrams in Appendix C.

For now we will only summarize the method of translating between the quiver data and the bipartite graph data:

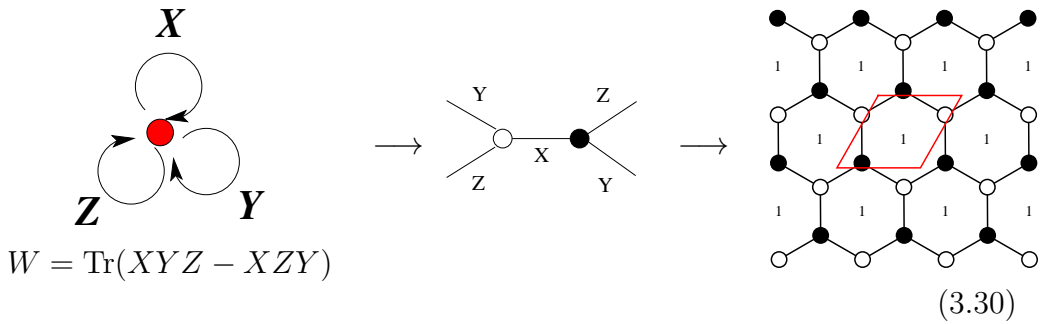
1. Consider a monomial term in W , if it comes with a plus (respectively minus) sign, draw a black (respectively white) node (the choice of

¹¹ I am very honoured to be the primogenitus of this happy and industrious family whose siblings are unusually close and to whom Amihay Hanany, due to his calm demeanour, his insightfulness and his paterfamilias air almost biblical, is known affectionately as “the Prophet”.

colour is, of course, purely by convention), write all the variables in the monomial clockwise (respectively counter-clockwise) as edges around the node;

2. Connect all the black/white nodes by these edges. Because W has the property (this comes from the fact that the VMS is a toric variety, corresponding to a so-called *binomial ideal*, q.v., Appendix A.2) that each variable appears exactly twice with opposite sign, we end up with a bipartite graph \mathcal{B} ;
3. The condition (3.29) dictates that \mathcal{B} is a bipartite graph on T^2 , or, equivalently, a tiling of the doubly periodic plane;
4. Each node in \mathcal{B} is a term in W and thus a GIO, and edge is perpendicular to an arrow in \mathcal{Q}_1 obeying orientation and each face in \mathcal{Q} corresponds to a node in \mathcal{Q}_0 ; in other words, \mathcal{B} is a dual graph of \mathcal{Q} ;
5. In particular, being the dual, \mathcal{B} has $N_2/2$ pairs of black/white nodes, N_1 edges and N_0 inequivalent (polygonal) faces.

Note that while the quiver has two pieces of information, the adjacency matrix and the superpotential, the tiling encodes both in one. We illustrate the above procedure with our archetypal example of \mathbb{C}^3 :



We have marked the fundamental domain of T^2 with the red parallelogram; therein, there is 1 pair of black-white nodes, each of valency 3, corresponding respectively to the $+XYZ$ and $-XZY$ terms in W . The edge together give the honeycomb tiling of the doubly periodic plane, with a single inequivalent face which is a hexagon marked “1”.

The set of relations in (3.30) is only a corner of an intricate web of correspondence which we summarize in Figure C.1 in Appendix C. For further reference, the situation for our other favourite example, the conifold \mathcal{C} , is shown in Figure C.2 in the said appendix.

These explorations by physicists have generated sufficient interest in the mathematics community that teams of “card-carrying” algebraic geometers and representation theorists [214–224] have formalized the statement into

THEOREM 10 *Let \mathcal{Q} be a quiver with superpotential, which is graph dual to a bipartite graph drawn on T^2 according to the steps above, then the (coherent component of, i.e., the top dimensional irreducible piece of) the moduli space $\mathcal{M}(\mathcal{Q})$ is an affine toric Calabi-Yau 3-fold.*

A systematic probe of this toric landscape was initiated in [201] and updated using the latest algorithms and computer power in [202], marching upwards in incremental area of \mathcal{D} .

We remark, therefore, that we have an infinite number of affine toric Calabi-Yau 3-folds, coming from (1) a lattice convex polygon \mathcal{D} as a toric diagram; or (2) a bipartite graph \mathcal{B} on T^2 as a quiver with superpotential. Mapping between these two sets is intricate, it is generally believed that set (2) surjects onto set (1) and the orbit of quivers \mathcal{Q} or dimers \mathcal{B} mapping to the same \mathcal{D} are related to each other by cluster mutation (or known as Seiberg duality in the field theory). As mentioned, we leave the full detail this toric-bipartite story to the wonderful reviews of [210,211], the upcoming book [213], or, for the impatient, the rapid report in [181].

3.4 Cartography of the Affine Landscape

We have taken our stroll in the landscape of non-compact, or affine, Calabi-Yau 3-folds, through the eyes of quiver representations, which *ab initio* may

seem convoluted but turned out to luxuriate in an extraordinary wealth of mathematics and physics. Indeed, the relaxation of compactness gave us not only explicit Ricci-flat metrics but also many infinite families of manifolds, exemplified by orbifolds and toric varieties.

Let us part with one last small but fascinating family, the del Pezzo surfaces, which we have encountered in many different circumstances (cf. Appendix A.3). These Fano surfaces are all of positive curvature, so a complex cone over them (think of these projective varieties simply affinized) with the tip at the origin, can be judiciously chosen to make the cone Calabi-Yau. Computationally, we can “affinize” any compact variety projective M to a non-compact one \hat{M} rather easily by promoting the homogeneous coordinates of the projective space into which M embeds to affine coordinates, i.e.,

$$M \subset \mathbb{P}^n_{[z_0:z_1:\dots:z_n]} \longrightarrow \hat{M} \subset \mathbb{C}^{n+1}_{(z_0,z_1,\dots,z_n)} . \quad (3.31)$$

In this sense, \hat{M} is a complex cone over M (not to be confused with the real cone which we discussed throughout the chapter for Sasaki-Einstein manifolds) with the origin of \mathbb{C}^{n+1} as the tip.

In general, in this affinization M and \hat{M} cannot both be Calabi-Yau, one compact, and the other non-compact. This is our case here, M is a Fano surface and \hat{M} is the affine Calabi-Yau 3-fold. We already saw this in §3.3.1 with the cone over \mathbb{P}^0 , which we recall is the first of the del Pezzo family (including Hirzebruch zero). In this sense $Tot(\mathcal{O}_{\mathbb{P}^2}(-3))$ is a wonderful affine Calabi-Yau 3-fold, it is an orbifold, it is toric, and it is a del Pezzo cone.

Adhering to the notation of the Appendix, we can write dP_0 for \mathbb{P}^2 . It turns out that $dP_{0,1,2,3}$ and $\mathbb{F} = \mathbb{P}^1 \times \mathbb{P}^1$ are all toric, with their toric diagrams being number 1, 3, 6, 10 and 4 respectively in Figure 2.3. The higher ones with more blow-up points, $dP_{4,5,6,7,8}$ are not toric varieties, though their associated quivers were found in [225] using exceptional collections of sheafs. As a historical note, the Calabi-Yau metrics for these del Pezzo cones - undoubtedly part of the tradition of the Italian School of algebraic geometry - were found by Calabi himself shortly after Yau’s proof.

3.4.1 Gorenstein Singularities

Before closing, we make a brief remark about the singular nature of our manifolds. In this chapter, except \mathbb{C}^3 , all the affine Calabi-Yau varieties are singular (at least) at the origin. We saw in §3.2 that orbifolds are by construction so. Algebraic singularities in geometry is a complicated business and much effort has been devoted to their smoothing or resolutions.

The class of singularities of our concern are called **Gorenstein**, which is a rather tamable situation. The formal definition of Gorenstein-ness is intimidating and will take us too far into the inner sanctum of commutative algebra. Roughly, a Gorenstein singularity is one outside of which there exists a global holomorphic form, or, from a sheaf-theoretical point of view, the affine scheme is Gorenstein if its canonical sheaf is a line bundle (of degree 0). In other words, Gorenstein-ness is local Calabi-Yau-ness.

Luckily, there is an explicit computation that checks this crucial condition [227]:

THEOREM 11 (R. Stanley) *The numerator to the Hilbert series of a graded Cohen-Macaulay domain R is palindromic iff R is Gorenstein.*

Recalling the basics of Hilbert series from Appendix B.0.2, we can see this theorem in action. The Hilbert series for \mathbb{C}^3 is just $1/(1-t)^3$ from (B.5), the numerator is 1 and is trivially palindromic. For the conifold \mathcal{C} , it is $\frac{(1-t^2)}{(1-t)^4}$ (coming for 4 generators obeying a single quadratic relation) and the numerator upon cancellation is $1+t$, which is palindromic.

The Hilbert series for $\mathbb{C}^3/(\mathbb{Z}/3\mathbb{Z})$, using (B.8), is $\frac{1+7t+t^2}{(1-t)^3}$ and the numerator is palindromic: the coefficients of the lowest and highest term are both 1. In fact, for dP_n , the Hilbert series is $\frac{1+(7-n)t+t^2}{(1-t)^3}$ [228]. We have included all the Hilbert series (Molien series) for the discrete finite ADE subgroups of $SU(2)$ in (B.9) in the appendix.

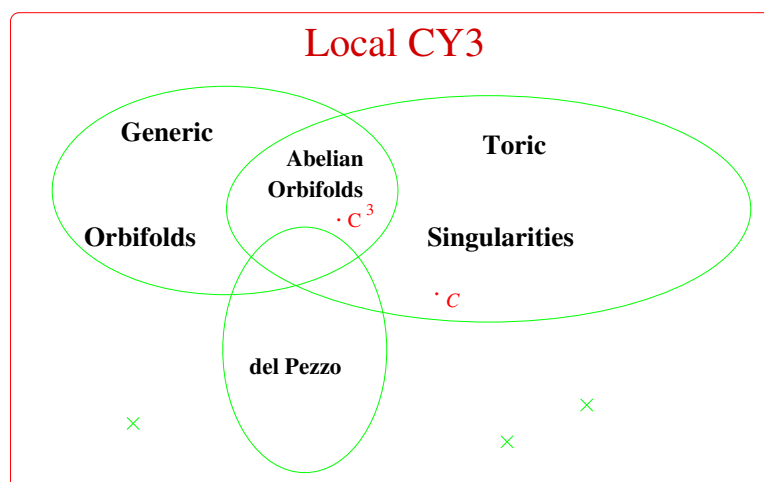


Figure 3.1: The landscape of non-compact, affine, local Calabi-Yau 3-folds.

In general, once we have some affine variety M , we can use the Gröbner basis methods detailed in the appendix to find the Hilbert series, and need only check the palindromy of the numerator to see whether M is “local Calabi-Yau”.

3.4.2 The non-Compact Landscape

As we reach the end of our promenade, it is expedient to recall the vista of the non-compact Calabi-Yau 3-folds, in analogy to the Venn diagram in Figure 2.5 of §2.5. We show the landscape of non-compact Calabi-Yau 3-folds in Figure 3.1. As in the compact case, the Venn diagram is only topologically relevant and the size of the bubbles are not significant. Several bubbles are meant to encapture an infinite number of spaces.

The analogue of the simplest starting point quintic Q is here \mathbb{C}^3 , from which we have Abelian orbifolds of the form $\mathbb{C}^3/(\mathbb{Z}/p\mathbb{Z} \times \mathbb{Z}/q\mathbb{Z})$ for any $p, q \in \mathbb{Z}_{\geq 1}$, of which there is already an infinite number. Next, we have orbifolds of \mathbb{C}^3 by discrete finite subgroups of $SU(3)$, which, in addition to the ADE subgroups of $SU(2)$, there are two infinite families, the delta-series, as well as a number of exceptionals.

The Abelian orbifold $\mathbb{C}^3/(\mathbb{Z}/3\mathbb{Z})$ is the cone (total space of the anticanonical bundle) over $dP_0 = \mathbb{P}^2$, the first member of the very special family of del Pezzo surfaces. It is also a toric variety, as are all Abelian orbifolds. This toric family is again infinite in number: any convex lattice polygon is the toric diagram of an affine, toric Calabi-Yau 3-fold. The prototypical example in this toric class is \mathcal{C} , the conifold, or the quadric hypersurface in \mathbb{C}^4 .

Of course, unlike local K3 surfaces, whose algebraic models can *only* be the ADE singularities, local Calabi-Yau 3-folds have no known complete characterization, the families chosen in the above Venn diagram are those which have been intensely studied, by mathematicians and physicists alike, and in particular, realize as the moduli space of quiver representations. The crosses outside the bubbles are supposed to denote the plethora of other local Calabi-Yau models on which, though most certainly infinite in number, there have not been too intense an investigation.

Nunc Dimitis: With our tantalizing pair of plots of the Calabi-Yau landscape in Figures 2.5 and 3.1 let us pause here. We have taken a promenade in the land of CY_3 , mindful of the intricate interplay between the mathematics and physics, emboldened by the plenitude of data and results, and inspired by the glimpses towards the yet inexplicable.

We have devoted a duo of chapters on cartography, first on the compact and second on the non-compact, gaining familiarity with the terrain of CI-CYs, KS hypersurfaces, orbifolds, del Pezzo cones, lattice polytopes, etc. The landscape of Calabi-Yau manifolds will certainly continue to provoke further exploration, especially with the advance of ever new mathematics, physics and computing.

Assured by the abundance of data and the increasing computing power to calculate requisite quantities, we are perhaps simultaneously daunted by the complexities involved in the analysis, in the algorithmic sense of “complexity”. In the ensuing chapter, we shall speculate as to what might be done when confronted with the furrowed mountains of the Calabi-Yau landscape.

4

Machine-Learning the Landscape

“Die Physik ist für die Physiker eigentlich viel zu schwer.”

– David Hilbert

And so we have partaken our excursion into the landscape of compact and non-compact Calabi-Yau manifolds, and like the keen geologist, soiled our hands with fascinating samples for scrutiny and experimentation, rather than the artist, whose primary concern is an impression of the magnificent vista. Thus prepared, we enter the last chapter, where with the plenitude of data collected, we can speculate upon its treatment. We mentioned at the very outset of the preface that a *Zeitgeist*, cultural and intellectual, seems to be curiously present, which breathes its *spiritus movens* onto scientific progress. Indeed, were we to examine our Scientific Age, it is doubtless that the omnipresence of data is what propels much of research, from exoplanets to the human genome to the outpouring particle-jets at CERN.

It is natural, therefore, to ask whether the most cutting-edge techniques from Data Science can be applied to the landscape of Calabi-Yau manifolds,

or indeed, to algebraic geometry. This was initiated in [229, 230], and has since been taken to various industrious and profitable ventures by many authors [231–249]. In this final chapter, we shall let our imagination take the reins and be no longer like the meticulous naturalists, but rather the fearless frontiersmen, and roam freely in the landscape which we had charted in the previous chapters.

We have followed the colourless skein of history throughout the book, keeping track of the discovery of the manifolds and the compilation of the datasets in tune with the contemporaneous developments in mathematics and physics. It is interesting to note that the first annual “Strings” conference began in the 1980s, from which offshoots of “String Phenomenology” and “String Mathematics” emerged in the early 2000s and in 2017/8, began the new series of “String Data”. The reader is also referred to the “String-Data Cooperation” on Github, inaugurated by Sven Krippendorf et al. in Munich: <https://github.com/stringdata>

which should grow to a marvellous repository of the data which we have discussed so far and much more beyond.

4.1 The Typical Problem

Reviewing the previous two chapters we are encouraged by the ever growing database of geometries ¹, mostly freely available online, as well as the computer software, especially the open-source SageMath umbrella [38], designed to calculate many of the requisite quantities.

Much of these data have been the brain-child of the marriage between physicists and mathematicians, especially incarnated by applications of computational algebraic geometry, numerical algebraic geometry and combina-

¹ In this book we have only focused on Calabi-Yau 3-folds for concreteness, there are many other datasets which have been established, ranging from the closely related bundles over CY 3-folds, generalization of CICYs, etc., to diverse subjects as the ATLAS of finite groups, etc., as mentioned in the Preface.

torial geometry to problems which arise from the classification in the physics and recast into a finite, algorithmic problem in the mathematics. In principle, as far as addressing problems such as searching for the right bundle cohomology to give the Standard Model - which we recall was what inspired the field of Calabi-Yau data from the late 1980s - is concerned, one could scan through configurations, find large clusters of computers ² and crunch away.

However, we had repeatedly alluded to the fact, even when demonstrating the powers of the likes of `Macaulay2` [32] and `SageMath` [38] in the foregoing discussions, that most of the core algorithms are exponential in running time and in memory usage. This is the case for establishing Gröbner bases (due to getting all pairs of S-polynomials), for finding dual cones (due to finding all subsets of facets to check perpendicularity), for triangulation of polytopes (due to collecting all subsets of lattice points on the polytope), etc., which are the crux of the computational methods. Even parallelizable computations in numerical algebraic geometry [34, 145] suffer from the need to find a large number of paths in homotopy continuation.

Confronted with this limitation, it would be helpful to step back and re-examine the desired result [229, 230]. One finds that regardless of the origin and the intent, the typical problem in computational algebraic geometry is one of the form

$$\boxed{\begin{array}{ccc} & \textit{INPUT} & \textit{OUTPUT} \\ \boxed{\text{integer tensor}} & \longrightarrow & \boxed{\text{integer}} \end{array}} \quad (4.1)$$

We see this in all the cases presented hitherto (note that where the output is a list of integers, we can just focus on one at a time, conforming to the paradigm of (4.1)), e.g.,

- Computing the Hodge number of a CICY.

² I remember a wonderful quote from Dan Freedman's lectures when I was a PhD student at MIT, on addressing a difficult calculation, he, in his usual dry sense of humour, said, "this is a problem perfectly adapted to large parallel clusters of graduate students."

Input: an integer matrix whose row size ranges from 1 to 12, column size, from 1 to 15, and whose entries are from 0 to 5;

Output: a non-negative integer $h^{2,1}$ or a positive integer $h^{1,1}$.

- Computing the cohomologies of a line bundle L over a CICY M .

Input: the CICY configuration matrix as above, plus a vector of the integer (negative also allowed) degrees of L ;

Output: a list of non-negative integers, the rank $h^*(M, L)$ of the cohomology of L .

- Computing the Hodge numbers and Chern classes of a KS Calabi-Yau 3-fold.

Input: an integer polytope, specified either by a list of integer 4-vectors or by the coefficients of the hyperplane inequalities defining the polytope;

Output: integers $(h^{1,1}, h^{2,1})$, integer coefficients of c_2 (expanded into the basis of Kähler classes).

- Computing the triple intersection numbers of a hypersurface in weighted projective \mathbb{P}^4 .

Input: a 5-vector of co-prime positive integers;

Output: a list (totally symmetric 3-tensor) of non-negative integers.

- Computing the quiver from given affine toric Calabi-Yau 3-fold.

Input: the list of integer vertices of a convex lattice polygon, the toric diagram \mathcal{D} ;

Output: the integer adjacency matrix of the quiver as well as the list of non-negative integer exponents of the monomial terms to include in the superpotential.

- Computing the number of cluster mutation/Seiberg dual phases of a quiver (whose moduli space of representations, the VMS, is toric Calabi-Yau 3-fold).

Input: the Kasteleyn adjacency matrix of the bipartite graph (brane-tiling) on the doubly periodic plane;

Output: a positive integer.

The list goes on and on.

4.2 WWJD

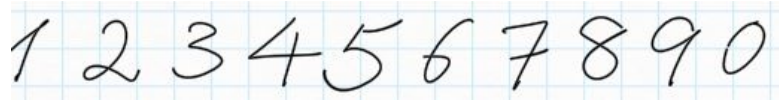
As we enter the Age of Data Science and Artificial Intelligence (AI), one cannot resist how one might address problems of the type presented at the end of the previous section, without recourse to traditional methods, which are known to be computationally expensive. Indeed, WWJD? **What Would JPython/Jupyter Do?**

The joke is perhaps so esoteric that it might be lost on most. First, JPython, or its successor, Jython, is the implementation of the Python Programming language [252] for the JAVA platform and Jupyter [253] is an open-source project whose core language consists of Julia, Python, and R, whose interface is where Python and SageMath [38] are usually run.

According to card-carrying computer scientists and data scientists, these are the platforms of their preference, and Python, together with C++, the programming languages of choice, one higher and one slightly lower level. Second, in some circles, especially amongst American Evangelical Christians, many wear T-shirts with the acronym WWJD, or “What Would Jesus Do”, as a constant reminder on how to lead one’s life ³.

³ Though Catholics like myself may find this gauche, I do appreciate the nobility of the sentiment. Nevertheless, I beg the reader for a moment’s indulgence on my speculations on theology. Perhaps a key difference between the Catholic and the Protestant is in the former’s tormenting sense of worthlessness in failing to imitate Christ and the latter’s over-optimism in being able to do so. To quote Miguel de Unamuno who so eloquently puts it, “. . . Protestantism, absorbed in this preoccupation with justification . . . ends by neutralizing and almost obliterating eschatology; it abandons the Nicene symbol, falls into an anarchy of creeds, into pure religious individualism and a vague esthetic, ethical, or

So, what would one versed in Python do? Let us make an analogy. Suppose we are given the hand-written digits



(4.2)

and we wish to let the computer recognize them. The input is an image, which is nothing but a $m \times n$ matrix (indexing the pixels in a 2-dimensional grid) each entry of which is a 3-vector of a real value between 0 and 1, denoting the percentage of RGB values. Or, if we only wish to keep black-white (gray-scale) information as is sufficient for this case, each entry is then a real number between 0 and 1. In fact, it is even sufficient to only keep the information of whether each pixel is occupied so that the input is an $m \times n$ matrix of 0s and 1s. The output is an integer from 0 to 9. In the computer science literature, this is called a *10-channel output*.

As mathematicians or theoretical physicists, what might instinctively come to mind in order to solve this problem is to find a clever Morse function as we scan the input matrix row-wise and column-wise and detect the critical points, which is different because the topologies of the digits are all different. Or, perhaps, one could compute the persistent homology, as it has become fashionable of late, of the pixels as a point-cloud of data. The downside to all of these is that (1) the computation is very expensive, and (2) there is too much variation: how I write the digits will differ substantially (though not overwhelmingly) from how you would write them.

Upon reflection, this is rather like the situation of our concern: the computation, such as Gröbner bases, is too expensive and the input has some variation in configuration, e.g., CICY matrices are defined only up to permutations and splitting-equivalence, or a polytope is only defined up to $GL(n; \mathbb{Z})$.

How does your smartphone, or, indeed, Google, treat (4.2)? With today's

cultured religiosity. What we may call "other-worldliness" (Jenseitigkeit) was obliterated little by little by "this-worldliness" (Diesseitigkeit) . . ."

access to data, one can readily proceed to repositories wherein there is a plenitude of writing samples. For example, the NIST (National Institute of Standards) database [254] has some 10^6 actual samples, classified in the form

$$\begin{array}{l}
 6 \rightarrow 6, 8 \rightarrow 8, 2 \rightarrow 2, 4 \rightarrow 4, 8 \rightarrow 8, 7 \rightarrow 7, 8 \rightarrow 8, \\
 0 \rightarrow 0, 4 \rightarrow 4, 2 \rightarrow 2, 5 \rightarrow 5, 6 \rightarrow 6, 3 \rightarrow 3, 2 \rightarrow 2, \\
 9 \rightarrow 9, 0 \rightarrow 0, 3 \rightarrow 3, 8 \rightarrow 8, 8 \rightarrow 8, 1 \rightarrow 1, 0 \rightarrow 0, \dots
 \end{array}
 \tag{4.3}$$

from which we see large (and in some sense also small) variation in handwriting. The likes of smartphones then performs the four-step procedure

1. Acquire data: the collection of known cases (input \rightarrow output), such as (4.3), is commonly called [training data](#);
2. Machine-Learn: this is the core algorithm which is slowly dominating all fields of human endeavour, from patient diagnoses, to LHC particle data analysis, to speech and hand-writing recognition, etc. This chapter will be devoted to an invitation to this subject for mathematicians and theoretical physicists ⁴;
3. Validate: once the machine/AI has “learnt” the training data, we can take a set of so-called [validation data](#), which, importantly, the machine has *not* seen before. This is in the same format as the training data, with given input and output. Thus we can see how the machine performs on by checking the predicted output with the actual output;
4. Predict: If the validation is well-behaved, then the machine-learning is successful and we can use it to predict new output on input hithertofore unseen.

⁴ Indeed, for this audience which is versed in the elements of differential and algebraic geometry and/or quantum field theory and general relativity, the tools in the subject of machine-learning should present no conceptual challenge. This is part of the appeal of the field, it is remarkably simple but extraordinarily powerful and universally applicable, so powerful, in fact, that there is still much which seem almost magical and await statements of formal theorems and rigorous proofs.

We now move to a rapid introduction to machine-learning and the reader is referred to the canonical textbooks in [257]. Of course, the entire field of machine-learning has been around for decades and has been an indispensable tool in many areas of science. The famous discovery of the Higgs boson, for instance, could not have been made, without machine-learning the patterns of particle jets. Back in the early days, the human eye had to disentangle hundreds of trajectories in cloud chambers, the amount of data now clearly precludes this possibility.

The explosion in the last decade or so of machine-learning is due to an important advancement in hardware: the gaming industry has brought about the proliferation of graphic processing units (GPUs) in addition to the standard CPU, even to the personal computer. Each GPU is a processor specialized in tensor transformations. Essentially, every personal device now has become somewhat a super-computer with thousands of parallel cores. This ready availability of the mini-super-computer has thus given a new incarnation to machine-learning whose algorithms have existed for decades but have been seriously hindered by the limitations of computing power.

Theoretical physics has been no exception in taking advantage of this explosion of technology [256]. The novelty of [229,230] is the proposal that the machine-learning paradigm can, too, be applied to fields of pure mathematics such as algebraic geometry.

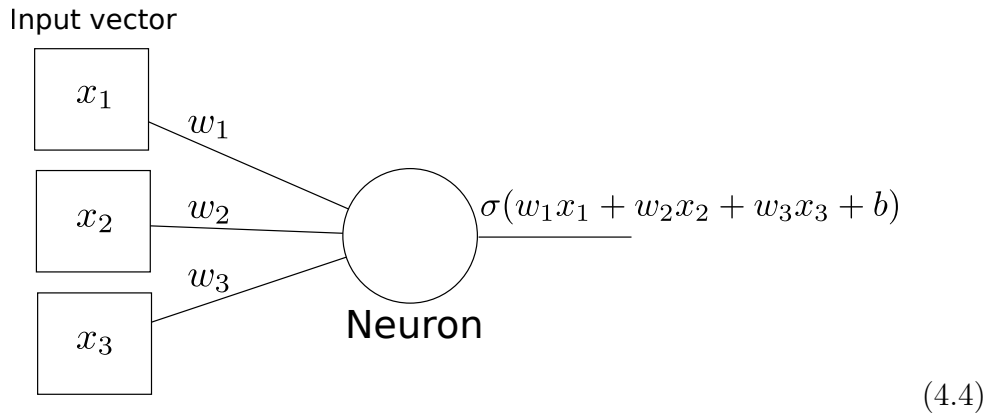
4.3 Rudiments of Machine-Learning

The steps outlined above in addressing (4.3) should remind the reader of first-year undergraduate statistics, it is what one does in **regression**. In fact, machine-learning is but a massive generalization of regression. In this spirit, we begin with

DEFINITION 9 A *neuron* or **perceptron** is a function $f(\sum_I w_I x_I + b)$

which is preferably but not necessarily analytic, whose argument is x_I , a tensor for some multi-index i and whose range is typically in $[0, 1] \subset \mathbb{R}$. The parameters w_I are called weights and b , the bias or off-set.

The multi-index is so that if the input is a vector, we have a single index, if it is a matrix, then I is a pair of indices, etc. We will loosely call w_I a weight vector because it has a single multi-index. The range is usually in $[0, 1]$ in order to imitate the “activation” of an animal neuron, which “fires” or not according to stimuli. Thus, standard choices of f are the hyperbolic tangent $\tanh(\cdot)$, the sigmoid $\sigma(x) := (1 + e^{-x})^{-1}$, or the rectified linear unit function $\text{ReLU}(x) := \max(0, \alpha x)$ for some $\alpha \in \mathbb{R}^\times$. Schematically, the perceptron looks like (for vector input x_I , and sigmoid function, for example)



The bias b is included to offset the resulting weighted sum so as to stay in the *active region*. To be more explicit, consider the sigmoid activation function. If we have a large input vector, without a bias, applying a sigmoid activation function will tend to map the output to 1 due to the large number of entries in the sum, which may not be the correct response we expect from the neuron. We could just decrease the weights, but training the neuron can stagnate without a bias due to the vanishing gradient near $f(x) = 1$ and 0.

What is astounding that this idea of imitating the neuron in order to facilitate computation dates as far back as 1957, at the very dawn of computers [255]: Cadmium Sulfide photo-voltaic cells the size of a wall were

linked up and stimulated in order to learn/produce pixelated images. The nomenclature “perceptron”, with its charming “-tron” ending probably gives away its 1950-60s origin.

With the neuron, the “training” proceeds as follows.

- The **training data**: $D = \{(x_I^{(j)}, d^{(j)})\}$ with input x_I and *known* output $d^{(j)}$ where j indexes over the number of data points;
- Find the standard deviation

$$SD := \sum_j \left(f\left(\sum_I w_I x_I^{(j)} + b\right) - d^{(j)} \right)^2 \quad (4.5)$$

and minimize with respect to the parameters w_i and b , whereby fixing them;

- the neuron is now “trained” and we can validate against *unseen* data.

Of course, this is precisely (non-linear) regression for model function f . We remark that this, and most of ensuing discussions, is **supervised learning**, in the sense that there are distinct pairs of inputs and outputs. The machine is “supervised”, as it were, to associate specific inputs with outputs. There is also unsupervised learning, where the machine can attempt to find patterns at will.

4.3.1 MLP: Forward Propagating Neural Networks

Next, we can generalize the neuron to

DEFINITION 10 *A collection of neurons is known as a **layer** where the weight vector w_I is promoted to a weight matrix. We denote the output of*

the i -th neuron in this layer as f_i such that

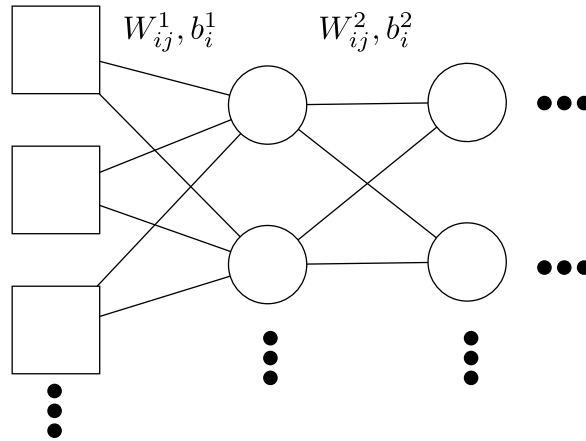
$$f_i := f\left(\sum_I W_{iI}x_I + b_i\right).$$

We can certainly string a sequence of layers in the next generalization by extending to several layers:

DEFINITION 11 A **multi-layer perceptron (MLP)** is a sequence of layers where the output of the previous layers is the input to the next layer, applying a different weight matrix and bias vector as we propagate through. All internal layers between the input and output layers are referred to as hidden layers. Denoting the output of the i -th neuron in the n -th layer as f_i^n , with $f_I^0 = x_I$ as the input vector,

$$f_i^n = f(W_{ij}^n f_j^{n-1} + b_i^n).$$

Schematically, the MLP looks like



(4.6)

where the left-most layer is the input layer, the right-most, the output layer and every thing in between, hidden layers.

The MLP is the simplest type of a **neural network**, consisting of only

forward-propagating layers, as one goes from left to right sequentially in the layers as indicated in (4.6). In general, a neural network is any finite directed graph of neurons and could consist of backward as well as forward propagation, even cycles in the graph are perfectly allowed. If there are several (or many) hidden layers, the neural network is usually called *deep* and the subsequent machine learning is referred to as **Deep Learning**.

Backward Propagation: Allowing for backward propagation gives us the flexibility to adjust the weights and biases of a neural network when training. To do so, we can define a **cost function**, standard examples of which include mean squared error and cross-entropy (for categorical and binary data). Back propagation then achieves parameter adjustments by minimising the cost function. It is so named as adjustments are first made to the last layer and then successive layers moving backwards.

To illustrate, consider a neural network with M layers and a mean squared error cost function, as in the standard deviation in (4.5),

$$E := \frac{1}{N} \sum_{train} (\bar{\sigma}^M - \bar{t})^2, \quad (4.7)$$

where N is the number of training entries to which we sum and \mathbf{t} , the expected output for a given entry. Taking derivatives, shifts in the last weight matrix become:

$$\frac{\partial E}{\partial W_{ij}^M} = \frac{2}{N} \sum_{train} (\sigma_i^M - t_i) \sigma_i'^M \sigma_j^{M-1}. \quad (4.8)$$

Likewise, working backwards, shifts in the second to last weight matrix:

$$\frac{\partial E}{\partial W_{ij}^{M-1}} = \frac{2}{N} \sum_{train} \sum_u (\sigma_u^M - t_u) \sigma_u'^M W_{ui}^M \sigma_i'^{M-1} \sigma_j^{M-1}. \quad (4.9)$$

Defining $\Delta_i^M := (\sigma_i^M - t_i) \sigma_i'^M$ and $\Delta_i^m := \sum_u \Delta_u^{m+1} W_{ui}^{m+1} \sigma_i'^m$, we can write

by induction, for an arbitrary layer m ,

$$\frac{\partial E}{\partial W_{ij}^m} = \frac{2}{N} \sum_{train} \Delta_i^m \sigma_j^{m-1}, \quad \frac{\partial E}{\partial b_i^m} = \frac{2}{N} \sum_{train} \Delta_i^m. \quad (4.10)$$

By utilising our neural network's final output and the expected output, we can calculate the Δ s successively, starting from the last layer and working backwards. We shift the weight values in the direction the gradient is descending to minimise the error function. Thus shifts are given by

$$\Delta W_{i,j}^m = -\eta \frac{\partial E}{\partial W_{ij}^m}, \quad \Delta b_i^m = -\eta \frac{\partial E}{\partial b_i^m}, \quad (4.11)$$

where η is the *learning rate*, which is effectively a proportionality constant fixing the magnitude of shifts in gradient descent. Care must be taken when choosing the learning rate. A rate too small leads to slow convergence and the possibility of becoming trapped in a local minimum. A rate too large leads to fluctuations in errors and poor convergence as the steps taken in parameter space are too large, effectively jumping over minima.

Note that parameter shifts are dependent on the gradient of the activation function. For activation functions such as sigmoid or tanh this then drives the output of a neuron to its minimal or maximal value, as parameter shifts become increasingly small due to the vanishing gradient. This is advantageous in an output layer where we may want to use binary classification. However, if neurons in hidden layers are driven to their min/max too early in training, it can effectively make them useless as their weights will not shift with any further training. This is known as the *flat spot problem* and is why the ReLU activation function has become increasingly popular.

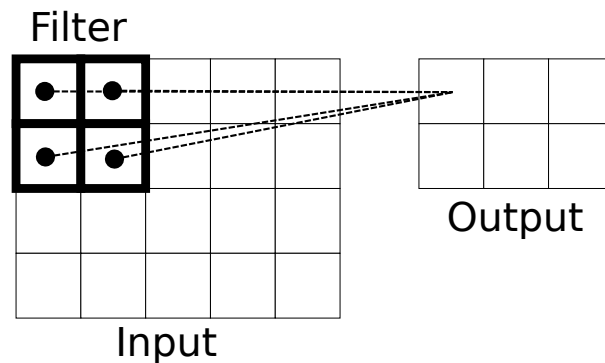
4.3.2 Convolutional Neural Networks

The MLP is one commonly used neural network. For image/tensor processing, another widely used one is the *Convolutional neural network* (CNN)

which is an alternative type of network that thrives when inputs contain translational or rotational invariance, whereby making them particularly useful for image recognition.

Like a fully connected, feed-forward layer, convolution layers use a set of neurons which pass a weighted sum through an activation function. However, neurons in convolution layers do not receive a weighted sum from all the neurons in the previous layer. Instead, a *kernel* (not to be confused with the kernel of matrix; this is more of a kernel in the sense of a discrete transform) restricts the contributing neurons.

To be more explicit, consider a two dimensional input (matrix). A *kernel* will be a grid sized $n \times n$ which convolves across the input matrix, taking the smaller matrix the grid is covering as the input for a neuron in the convolution layer, as exemplified by the following which is a size 2×2 kernel



The output generated by convolving the kernel across the input matrix and feeding the weighted sums through activations is called a feature map. Importantly, the weights connecting the two layers must be the same, regardless of where the kernel is located. Thus it is as though the kernel window is scanning the input matrix for smaller features which are translationally invariant. For instance, when the kernel window moves one unit to the right, the connected neuron in the output layer will be the centre square in the top row.

In the running examples of the handwritten digit recognition problem, the network may learn to associate rounded edges with a zero. What these features are in reality relies on the weights learned during training. A single convolution layer will usually use several feature maps to generate the input for the next layer.

Over-fitting: In any statistical model, it is important that one does not over-fit, i.e., to allow for so many parameters in the model so as to render any dataset to be able to be fitted to any desired model; this must be avoided. For the neural network, *over-fitting* occurs during training when accuracy against the training dataset continues to grow but accuracy against unseen data stops improving. The network is not learning general features of the data any more and the complexity of the net architecture has more computing potential than required. The opposite problem is *under-fitting*, using too small a network which is incapable of learning data to high accuracy.

An obvious solution to over-fitting is early stopping, cutting the training short once accuracy against unseen data ceases to improve. However, we also wish to delay over-fitting such that this accuracy is as large as possible after stopping.

A common solution is called *Dropout*, which is a technique where neurons in a given layer have a probability of being switched off during one training round. This forces neurons to learn more general features about the dataset and can decrease over-fitting [258].

4.3.3 Support Vector Machines

In the above we have outlined the neural-network approach to machine-learning. There are other approaches, such as support vector machines (SVMs), decision trees, etc., the most widely used being SVMs. In contrast to neural networks, SVMs take a more geometric approach. They can

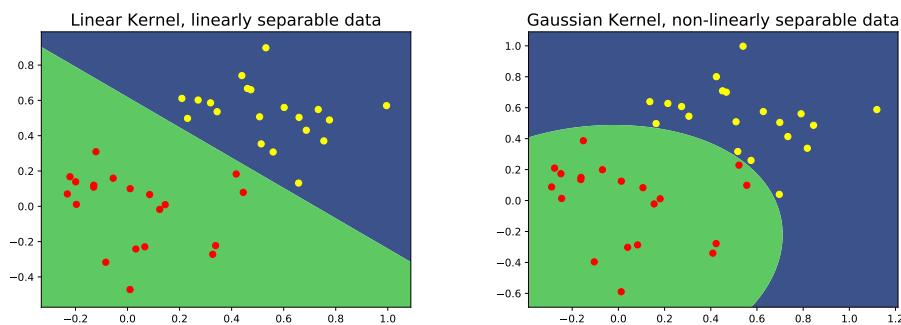


Figure 4.1: Example SVM separation boundary using different kernels.

act as both classifiers and regressors which we shall introduce sequentially.

SVM Classifiers: While a neural network classifier essentially fits a large number of parameters (weights and biases) to obtain a desired function $f(\mathbf{v}_{\text{in}}) \in [0, 1]$, a SVM tries to establish an optimal hyperplane separating clusters of points in the *feature space*, the n -dimensional Euclidean space to which the n -dimensional input vector belongs. Points lying on one side of the plane are identified with one class, and vice versa for the other.

Thus, a vanilla SVM is only capable of acting as a binary classifier for linearly separable data. This is somewhat restrictive, but the approach can be generalised to non-linearly separable data via the so called *kernel trick* and likewise can be extended to deal with multiple classes [259]. We illustrate this in Figure 4.1. We wish to separate points \mathbf{x}_i with a hyperplane based on a classification of true/false, which we represent with the labelling $y_i = \pm 1$; this is so-called binary feature.

First define a hyperplane

$$\{x \in \mathbb{R}^n | f(\mathbf{x}) = \mathbf{w} \cdot \mathbf{x} + b = 0\}, \quad (4.13)$$

where \mathbf{w} is the normal vector to the hyperplane. Then we have that

DEFINITION 12 Support vectors are the points in the feature space lying closest to the hyperplane on either side which we denote as \mathbf{x}_i^\pm .

The **margin** is the distance between these two vectors projected along the normal \mathbf{w} , i.e.,

$$\text{Margin} := \mathbf{w} \cdot (\mathbf{x}_i^+ - \mathbf{x}_i^-) / |\mathbf{w}| . \quad (4.14)$$

There is typically not a unique hyperplane we could choose to separate labelled points in the feature space, but the most optimal hyperplane is one which maximises the margin. This is because it is more desirable to have points lie as far from the separating plane as possible, as points close to the boundary could be easily misclassified. Note that condition defining a hyperplane (4.13) is not unique as a rescaling $\alpha(\mathbf{w} \cdot \mathbf{x} + b) = 0$ describes the same hyperplane. Thus we can rescale the normal vector such that $f(\mathbf{x}_i^\pm) = \pm 1$ and the margin reduces to

$$\text{Margin} = \frac{2}{|\mathbf{w}|} . \quad (4.15)$$

Moreover, with such a rescaling, the SVM acts as a classifier on an input \mathbf{x} through the function $\text{sgn}(f(\mathbf{x})) = \pm 1$. In particular, for each point (x_i, y_i) , $y_i = 1$ if $\mathbf{w} \cdot \mathbf{x}_i + b \geq 1$ and $y_i = -1$ if $\mathbf{w} \cdot \mathbf{x}_i + b \leq -1$, so that the product $y_i \times (\mathbf{w} \cdot \mathbf{x}_i + b)$ is always ≥ 1 for each i . Maximising the margin thus corresponds to minimising $|\mathbf{w}|$, with the constraint that each point is correctly classified. This wholly defines the problem which can be stated as

$$\text{Min } \frac{1}{2} |\mathbf{w}|^2 \text{ subject to } y_i \times (\mathbf{w} \cdot \mathbf{x}_i + b) \geq 1. \quad (4.16)$$

This is a quadratic programming problem with well known algorithms to solve it. Reformulating this problem with Lagrange multipliers:

$$\begin{aligned} L &= \frac{1}{2} |\mathbf{w}|^2 - \sum_i \alpha_i (y_i (\mathbf{w} \cdot \mathbf{x}_i + b) - 1) \Rightarrow \\ \frac{\partial L}{\partial \mathbf{w}} &= \mathbf{w} - \sum_i \alpha_i y_i \mathbf{x}_i = 0, \quad \frac{\partial L}{\partial b} = - \sum_i \alpha_i y_i = 0, \end{aligned} \quad (4.17)$$

leads to the *dual problem* upon substitution:

QUESTION 5 Solve the quadratic programming:

$$\begin{aligned} \text{Min} \quad & \frac{1}{2} \sum_{i,j} \alpha_i \alpha_j y_i y_j \mathbf{x}_i \cdot \mathbf{x}_j - \sum_j \alpha_j , \\ \text{subject to} \quad & \alpha_j \geq 0, \quad \sum_j \alpha_j y_j = 0 . \end{aligned} \quad (4.18)$$

With our classifying function now being $\text{sgn}(f(\mathbf{x})) = \text{sgn}(\sum_i (\alpha_i y_i \mathbf{x}_i \cdot \mathbf{x}) + b)$.

The Python package `Cvxopt` implements a quadratic computing algorithm to solve such problems.

The dual approach is much more illuminating as it turns out the only α_i which are non-zero correspond to the support vectors [259] (hence the name support vector machine). This makes SVMs rather efficient as unlike a neural network which requires a vast amount of parameters to be tuned, a SVM is fully specified by its support vectors and is ignorant of the rest of the data. Moreover the quadratic programming optimisation implemented via `Cvxopt` ensures the minimum found is a global one.

The dual approach also enables us to generalise to non-linearly separable data rather trivially. In theory, this is achieved by mapping points in the feature space into a higher dimensional feature space where the points are linearly-separable, finding the optimal hyperplane and then mapping back into the original feature space. However, in the dual approach, only the dot product between vectors in the feature space is used.

Therefore, in practice we can avoid the mapping procedure as we only need the effective dot product in the higher dimensional space, known as a kernel. Hence, by replacing $\mathbf{x}_i \cdot \mathbf{x}$ with $\text{Ker}(\mathbf{x}_i, \mathbf{x})$ we can deal with non-linearly separable data at almost no extra computational cost. This is known as the *kernel trick* which just replaces the usual dot product to common

kernels such as

$$\begin{aligned} \text{Gaussian: } \text{Ker}(\mathbf{x}_i, \mathbf{x}) &= \exp\left(\frac{-|\mathbf{x}_i - \mathbf{x}|^2}{2\sigma}\right), \\ \text{Polynomial: } \text{Ker}(\mathbf{x}_i, \mathbf{x}) &= (1 + \mathbf{x}_i \cdot \mathbf{x})^n . \end{aligned} \quad (4.19)$$

We remark that SVMs reduces to our familiar linear regressor by finding a function $f(\mathbf{x}) = \mathbf{w} \cdot \mathbf{x} + b$ to fit to the data. Analogous to the above discussion, one can frame this as an optimisation problem by choosing the flattest line which fits the data within an allowed residue ϵ . Likewise one can make use of Lagrange multipliers and the kernel trick to act as a non linear regressor as well.

Note in the above discussion we have avoided the concept of slack. In order to avoid overfitting to the training data, one can allow a few points in the training data to be misclassified in order to not constrain the hypersurface too much, allowing for better generalisation to unseen data. In practice this becomes quantified by replacing the condition $\alpha_i \geq 0$ with $0 \leq \alpha_i \leq C$, where C is the cost variable [259].

SVM Regressors: Having discussed SVM as a classifier, its role as a regressor is similar. The optimisation problem for a linear SVM regressor follows from finding the flattest possible function $f(\mathbf{x}) = \mathbf{w} \cdot \mathbf{x} + b$ which fits the data within a residue ϵ . As $|\nabla f|^2 = |\mathbf{w}|^2$, this flatness condition reduces to the problem:

$$\text{Min } \frac{1}{2} |\mathbf{w}|^2 \text{ subject to } -\epsilon \leq y_i - (\mathbf{w} \cdot \mathbf{x}_i + b) \leq \epsilon . \quad (4.20)$$

Again, introducing Lagrange multipliers

$$\begin{aligned} L &= \frac{1}{2} |\mathbf{w}|^2 - \sum_i \alpha_i (y_i - (\mathbf{w} \cdot \mathbf{x}_i + b) + \epsilon) + \sum_i \alpha_i^* (y_i - (\mathbf{w} \cdot \mathbf{x}_i + b) - \epsilon) \Rightarrow \\ \frac{\partial L}{\partial \mathbf{w}} &= \mathbf{w} - \sum_i (\alpha_i - \alpha_i^*) y_i \mathbf{x}_i = 0, \quad \frac{\partial L}{\partial b} = \sum_i (\alpha_i - \alpha_i^*) y_i = 0, \end{aligned} \quad (4.21)$$

leads to the dual problem:

QUESTION 6 *Solve the optimization problem*

$$\begin{aligned} \text{Min } & \frac{1}{2} \sum_{i,j} (\alpha_i - \alpha_i^*)(\alpha_j - \alpha_j^*) y_i y_j \mathbf{x}_i \cdot \mathbf{x}_j + \epsilon \sum_i (\alpha_i + \alpha_i^*) + \sum_i y_i (\alpha_i^* - \alpha_i) \\ \text{subject to } & \alpha_i, \alpha_i^* \geq 0, \quad \sum_i (\alpha_i - \alpha_i^*) = 0. \end{aligned} \quad (4.22)$$

Thus, as with the classifier, this optimisation problem can be implemented with `Cvxopt`. As the dual problem again only contains a dot product between two entries in the feature space, we can use the kernel trick to generalise this approach to fit non-linear functions.

Hyperparameter Optimisation As a final remark to our lightning introduction to machine-learning, we discuss parameters and hyperparameters. Indeed, while both neural networks and SVMs are trained algorithmically as outlined above, certain variables must be set by hand prior to training. These are known as **hyperparameters**. Examples include net architecture (number of hidden layers and neurons in them) and dropout rate for feedforward neural networks, kernel size and number of feature maps for convolution layers and the cost variable, kernel type and kernel parameters for SVMs.

Several methods exist to optimise these parameters. For the case of a few hyperparameters, one could search by hand, varying parameters explicitly and training repeatedly until an optimal accuracy is achieved. A grid search could also be used, where each parameter is scanned through a range of values. However, for a large number of hyperparameters permitting a large number of values this quickly becomes an extremely time consuming task. Random searches can often speed up this process, where parameter values are drawn from a random distribution across a sensible range. Finally, random search coupled with a *genetic algorithm* is very much favoured, which effectively begins as a random search but then makes an informed decision

of how to *mutate* parameters to increase accuracy.

4.4 Machine-Learning Algebraic Geometry

Armed with an arsenal of technique, we return to the theme of this book, viz., Calabi-Yau data. We have seen in §4.1 a list of typical problems in computational algebraic geometry, inspired by physical need, all of which can *in principle* be addressed by brute-force methods ranging from Gröbner bases to polytope triangulations, all of which are exponential in complexity.

It is therefore natural to pose the adventurous query

QUESTION 7 *Can AI / machine-learning help with algebraic geometry ?*

Indeed, can machines help with problems in pure mathematics and theoretical physics, *without* explicit knowledge of the actual methods involved. We know a plethora of cases which *has* been computed by traditional methods and wish to extrapolate to where computing power hinders us, by essentially bypassing - in a mysterious way, as we shall see - the frontal attacks offered by the likes of Gröbner bases. This is precisely in analogy of the handwritten digit problem: to recognize a new, esoteric written digit is hard but furnished with tens of thousands of samples already classified by experience, to predict this new digit to good accuracy does not seem impossible. After all, there is inherent pattern, however big the variance, in written digits (or, for that matter, any manuscript).

There are inherent patterns in problems in mathematics, should some of these problems, too, not be amenable to this philosophy?

Of course, this philosophy is not new. It is simply the process of forming a conjecture. There is a long tradition of experimental mathematics from which countless conjectures have been posited, many leading to the most

profound consequences. Consider the greatest mind of the 18th century, that of K. F. Gauß which can be considered as the best neural network of the time. By looking at the distribution of primes, supposedly in his teens, Gauß was able to predict that the prime-counting function $\pi(x) \sim x/\log(x)$, a fact which had to wait over a century to be proven by de la Vallée-Poussin and Hadamard, using complex analysis, a method entirely unknown to the 18th century.

The minds of the calibre of Gauß are rare, but neural networks of increasing sophistication now abound. Could the combined efforts of AI at least stochastically achieve some correct predictions? In this section, we will see that many, if not most of the problems discussed in this book, could indeed be machine-learnt to great accuracy .

4.4.1 Warm-up: Hypersurface in Weighted \mathbb{P}^4

Let us warm up with the simplest of the input configurations, viz., that of hypersurfaces in $W\mathbb{P}^4$, discussed in §2.3.1, which is specified by a single 5-vector of co-prime positive integers. To make things even simpler, suppose we wish for a *binary query* of whether $h^{2,1}$ is larger than a certain value, say 50. We know that $h^{2,1} \in [1, 491]$ with the histogram shown in Figure 2.2; 50 is a reasonable division point. In terms of geometry we are looking for manifolds which have a relatively large/small number of complex structure deformations, a question of physical interest as well.

Our data, therefore, is of the form $\{x_i \rightarrow y_i\}$:

$$\{1, 1, 1, 1, 1\} \rightarrow 1, \quad \{1, 1, 1, 1, 2\} \rightarrow 1, \quad \dots, \quad \{2, 2, 3, 3, 5\} \rightarrow 0, \dots \quad (4.23)$$

totalling 7555. The first entry, is the quintic Q in regular \mathbb{P}^4 and its $h^{2,1} = 101$ gives a positive hit (denoted as 1) on $h^{2,1} > 50$. Further down the list, the degree 15 hypersurface in $W\mathbb{P}^4[2, 2, 3, 3, 5]$ has $h^{2,1} = 43$, giving us the negative hit (denoted as 0). As mentioned in §2.3.1, the $h^{2,1}$ values were

calculated meticulously by [69, 70] using Landau-Ginzberg methods (even on SageMath (linked to Macaulay2 or Singular), the computation using sequence-chasing is not straight-forward) and the results, though known, quite escapes the human eye in any discernable pattern.

Since all results are known and the data is labelled, a standard procedure is called **cross validation** where we *split* the data into the (1) training set and (2) validation set, establish a machine-learning algorithm, and check how well the predicted result, trained on the training set, behaves on the complementary validation set. That is, the training set is used to train models whereas the validation set remains entirely unseen by the machine-learning algorithm.

Accuracy measures computed on the training set thus give an indication of the model's performance in recalling what it has learned. More importantly, accuracy measures computed against the validation set give an indication of the models performance as a predictor. Common measures of the goodness of fit include (q.v. [260])

DEFINITION 13 *Let $y_{i=1,\dots,N}$ be the actual output for input x_i in the validation set, and let y_i^{pred} be the values predicted by the machine-learning model on x_i , then*

(naive) precision *is the percentage agreement of y_i with y_i^{pred}*

$$p := \frac{1}{N} |\{y_i = y_i^{pred}\}| \in [0, 1];$$

root mean square error (RMS) $\left(\frac{1}{N} \sum_{i=1}^N (y_i^{pred} - y_i)^2 \right)^{1/2}$;

coefficient of determination $R^2 := 1 - \frac{\sum_{i=1}^N (y_i - y_i^{pred})^2}{\sum_{i=1}^N (y_i - \bar{y})^2} \in [0, 1]$

where \bar{y} is the mean over y_i ;

cosine distance considering y_i and y_i^{pred} as vectors \vec{y} and \vec{y}^{pred} respectively, compute the cosine of the angle between them so that 1 is complete agreement, -1 , worst fit and 0, random correlation:

$$d_C := \frac{\vec{y} \cdot \vec{y}^{pred}}{|\vec{y}| |\vec{y}^{pred}|} \in [-1, 1] ;$$

In the cases of categorical data where y_i belong to finite, discrete categories, such as the binary case at hand. there are a few more measures. First, we define

DEFINITION 14 Let $\{x_i \rightarrow y_i\}$ be categorical data, where $y_i \in \{1, 2, 3, \dots, k\}$ take values in k categories. Then, the $k \times k$ **confusion matrix** has 1 added to its (a, b) -th entry, whenever there is an actual value of $y = a$ but is predicted to $y^{pred} = b$.

Ideally, of course, we want the confusion matrix to be diagonal. In the case of binary y_i as in (4.23), the 2×2 confusion matrix takes the rather familiar form and nomenclature

		Actual	
		True (1)	False (0)
Predicted Classification	True (1)	True Positive (tp)	False Positive (fp)
	False (0)	False Negative (fn)	True Negative (tn)

(4.24)

In the binary case, we have to be careful about **imbalanced** data. For instance, consider the case where only 0.1% of the data is classified as true. In minimising its cost function on training, the machine-learning algorithm could naively train a model which just predicts false for *any* input. Such a model would still achieve a 99.9% accuracy as defined by p in Definition 13, but it is useless in finding the special few cases in which we are interested. Thus, naive p is meaningless and we need more discriminatory measures.

DEFINITION 15 For binary data, two commonly used measures of goodness of fit, in furtherance to naive accuracy are

F-Score: $F := \frac{2}{\frac{1}{\text{TPR}} + \frac{1}{\text{Precision}}}$ where [262], using the confusion matrix (4.24),

$$\begin{aligned} \text{TPR} &:= \frac{tp}{tp+fn} , & \text{FPR} &:= \frac{fp}{fp+tn} , \\ \text{Accuracy } p &:= \frac{tp+tn}{tp+tn+fp+fn} , & \text{Precision} &:= \frac{tp}{tp+fp} . \end{aligned}$$

where TPR (FPR) stands for true (false) positive rate.

Matthew's Correlation Coefficient: Using the confusion matrix (4.24), the Matthew's coefficient is the square root of the normalized chi-squared:

$$\phi := \sqrt{\frac{\chi^2}{N}} = \frac{tp \cdot tn - fp \cdot fn}{\sqrt{(tp+fp)(tp+fn)(tn+fp)(tn+fn)}} .$$

The definition is also generalizable to $k \times k$ confusion matrices [261].

We must guarantee that both F_1 and ϕ are close to 1, in addition to p being close to 1, in order to conclude that the machine-learning model has predicted to satisfaction.

In addition to these measures of accuracy, we have notion of a confidence interval for the fit.

DEFINITION 16 The Wilson confidence interval is $[\omega, \omega_+]$ where

$$\omega_{\pm} := \frac{p + \frac{z^2}{2n}}{1 + \frac{z^2}{n}} \pm \frac{z}{1 + \frac{z^2}{n}} \left(\frac{p(1-p)}{n} + \frac{z^2}{4n^2} \right)^{1/2} .$$

Here n is the sample size, p is the accuracy or probability of correct prediction within the sample, $z = \sqrt{2} \text{Erf}^{-1}(2P - 1)$ is the probit for a normal distribution.

This is a confidence interval in the sense that with probability P , the Wilson interval contains the mean of the accuracy from the population.

Finally, we define a crucial quantity in machine-learning which helps with the visualization of how well the algorithm is behaving:

DEFINITION 17 *Let $\{x_i \rightarrow y_i\}_{i=1,\dots,N}$ be N data-points. We choose cross-validation by taking a percentage γN of the data randomly for a chosen $\gamma \in (0, 1]$ as training data \mathcal{T} , the complement $(1-\gamma)N$ data-points will be the validation data \mathcal{C} . The performance of the machine-learning algorithm, measured by any of the goodness of fit from Definitions 13 and 15, upon training on \mathcal{T} and validated on \mathcal{C} , is a function $L(\gamma)$ of γ . The **Learning curve** is the plot of $L(\gamma)$ against γ .*

In practice, γ will be chosen at discrete intervals, for instance in increments of 10% until the full dataset is attained for training. Furthermore, we repeat each random sample γN a number of times, so the learning curve has error bars associated with each of its points.

Learning Curves for $W\mathbb{P}^4$ -Hypersurfaces: After this long digression on clarifying terminology, let us now return to the problem of machine-learning (4.23). Let us take 25% random samples as training data \mathcal{T} , establish a neural network which is a simple MLP with 3 hidden layers: a linear layer of size 5×50 (i.e., a 5×50 matrix transformation of the 5-vector input), followed by an element-wise sigmoid transformation, and then a linear layer of size 50×10 , before summing up to an integer. This choice is purely ad hoc and merely to illustrate. A more serious thing to do would be, as mentioned above, to optimize the network structure and the hyperparameters such as the sizes of the matrices in the linear layers.

To be completely explicit, we will explain the Python [252] code in detail, as we have always done with software throughout the book. As mentioned, the great thing about SageMath [38] is that its core language is Python-based and we even execute Python from within SageMath (by, for instance, calling `sage -ipython` as with our early Macaulay2 [32] example in the previous chapters). One could also run a Jupyter notebook from which one can run

the ensuing code, after all, WWJD is our guiding question.

We begin with the usual preamble of calling the necessary Python packages: 'numpy' for numerical recipes, 'scipy' for scientific computing, 'matplotlib.pyplot' for plotting, 'pandas' for data analysis and 'random' for random number generation:

```
import numpy as np
import scipy as sp
import matplotlib.pyplot as plt
import pandas as pd
import random
```

Next, we load the key packages, Tensorflow, the premium Python package for neural networks as well as keras, which is the high-level interface (wrapper) for Tensorflow. From keras, a few standard ones of its layers (most of which we will not use for this example but keep here for illustration) and network structures

```
import tensorflow as tf
import keras
from keras.models import Sequential,load_mod
from keras.layers import Dense,Activation,Dropout
from keras.layers import Conv1D,Conv2D,MaxPooling1D,MaxPooling2D,Flatten
```

Suppose now we have organized the data in the form (importing from <http://hep.itp.tuwien.ac.at/~kreuzer/CY/> on the 'CY/4d' tab, for instance):

```
dataX = [[1, 1, 1, 1, 1], [1, 1, 1, 1, 2], [1, 1, 1, 1, 3],
         [1, 1, 1, 2, 2], [1, 1, 1, 1, 4], ... ];
dataY = [1, 1, 1, 1, 1, ...];
```

`dataX` is the *ordered* list of 5-vector weights of WP^4 and `dataY`, whether the corresponding CY3 has $h^{2,1} > 50$. Note that there are 2867 cases of 1 and 4688 of 0, so this is a fairly balanced problem; it so happens in the ordering of the configurations, the first quite a few (the first being the quintic) all have $h^{2,1} > 50$.

From this we split (achieved by the set difference) the data into training \mathcal{T} and validation \mathcal{C} sets as a 25-75% split, and then convert \mathcal{T} and \mathcal{C} into arrays for pre-processing:

```
trainingindex = random.sample([k for k in range(len(dataX))],
                              round(len(dataX)/4) );
validateindex = list(set([k for k in range(len(dataX))]) -
                    set(trainingindex));

trainingX = np.array([dataX[a] for a in trainingindex]);
trainingY = np.array([dataY[a] for a in trainingindex]);

validateX = np.array([dataX[a] for a in validateindex]);
validateY = np.array([dataY[a] for a in validateindex]);
```

Finally, we are ready to establish our simple neural network:

```
network = Sequential()
network.add(Dense(50,activation=None,input_dim=5))
network.add(Activation('sigmoid'))
network.add(Dense(10,activation=None))
network.add(Dense(1))
```

A few points of explanation. The `Sequential()` specification indicates that the neural network is a MLP. The first (input) layer, `Dense()`, is a fully-connected layer meaning that the input 5-vector will be mapped to 50 nodes in a fully-connected way, i.e., the weight-matrix will be dotted with the

vector, and then, added with a bias, will return a 50-vector. The specification of `activation = None` means it is defaulted to the linear function $f(x) = x$.

The output of the input layer is fed to the first hidden layer, which is an element-wise sigmoid function $\sigma(x)$ defined under Definition 9, which is then sent to the second hidden layer, again a linear, fully-connected layer, this time outputting a 10-vector, before finally sent to the output layer which sums everything into a single number by the `Dense(1)`. Note that only the input layer requires a specification of its input-shape (of dimension 5) and the network will then automatically deal with the subsequent dimensions.

Having established the network structure, we can train simply by compiling and then fitting

```
network.compile(loss='mean_squared_error', optimizer = 'adam',
                metrics=['accuracy'])
network.fit(trainingX,trainingY,batch_size=32,epochs=100,verbose=1,
            validation_data=(validateX,validateY))
```

In the above, the `batch_size` specifies that the training data is passed in groups of 32 at a time and the `epochs` means that the data will be passed through the network 100 times to optimize the parameters. Finally, we can use the fitted network to check the validation data by ‘predicting’:

```
predictY = network.predict(validateX,verbose = 1)[: ,0]
```

where the `[: ,0]` is merely an artefact of the the output format of `network.predict()`, which is an array whose every entry is of the form such as `array([1.07], dtype=float32)`, so that we extract only the 0-th entry, viz., the number itself.

This last point is actually rather important: the predicted result is a floating number (real number up to, here, 32 significant digits). Nowhere did we specify in the network structure that the result should be an integer

0 or 1. The optimization performed only finds the best fit over the reals. Therefore, the final answer needs to be rounded. For instance, the error can be obtained by doing

```
error=0;
for a in range(len(train_predict)):
    if(np.round(train_predict[a] - validatey[a]) != 0):
        error+=1;
```

The error turns out to be 375 here.

Let us pause a moment to reflect upon the above calculation. The neural network randomly saw 25% of the 7555 cases of whether $h^{2,1} > 0$, and when optimized, it predicted on the remaining *unseen* 75% of the cases with only 375 errors, i.e., to an accuracy of $1 - 375/(7555 \cdot 75\%) \simeq 93.3\%$, which is rather remarkable, considering the total computation time was less than a minute on an ordinary laptop. Trying to compute over 5,600 Hodge numbers for a $W\mathbb{P}^4$ -hypersurface (even estimating whether $h^{2,1} > 50$ has no short-cut) would have taken the computer many many hours. The power of machine-learning algebraic geometry can thus be appreciated!

Before we go on to do more pedantic statistics, it is a comforting fact for the *Mathematica* aficionado that as of version 11.2+ (timely released in 2017), machine-learning has been built into the core operating system and being such a high-level language, allows the above to be condensed into a few lines of code. Suppose we have the data

```
datah21 = {
    {1, 1, 1, 1, 1} -> 1, {1, 1, 1, 1, 2} -> 1, {1, 1, 1, 1, 3} -> 1,
    {1, 1, 1, 2, 2} -> 1, {1, 1, 1, 1, 4} -> 1, ...
};
```

from which we obtain \mathcal{T} and \mathcal{C} as

```
training = RandomSample[dataah21, 2000];
validation = Complement[dataah21, training];
```

Then, the same neural network can be specified by

```
net = NetChain[{ LinearLayer[100], ElementwiseLayer[LogisticSigmoid],
  ElementwiseLayer[Tanh], LinearLayer[100], SummationLayer[]},
  "Input" -> {5}];
```

with training done by

```
net = NetTrain[net, training, MaxTrainingRounds -> 100];
```

and validation done by

```
actual = Table[validation[[i, 2]], {i, 1, Length[validation]}];
predict = Table[Round[net[validation[[i, 1]]]],
  {i, 1, Length[validation]}];
```

The reader is highly encouraged to vary all the code above to adapt to his/her own needs as well as explore the multitude of possibilities of which our naive example has touched only the surface.

The learning curve for this problem is presented in Figure 4.2. We have repeated, at each incremental interval of 5%, the training/prediction 10 times, which gives us the error bars. There is a large error when the seen training data is less than 10%, as expected – the network simply has not seen enough data to make a valid prediction. However, starting at 20%, as discussed above, we are already looking at 96% precision with Matthew's ϕ -coefficient around 0.9. The curve is slowly but steadily climbing to around 97% precision and $\phi \sim 0.92$ at around 80% seen data. All of this is indeed reassuring. The neural network can estimate a solution to our complex structure problem to very high precision and confidence at orders of magnitude less computation time.

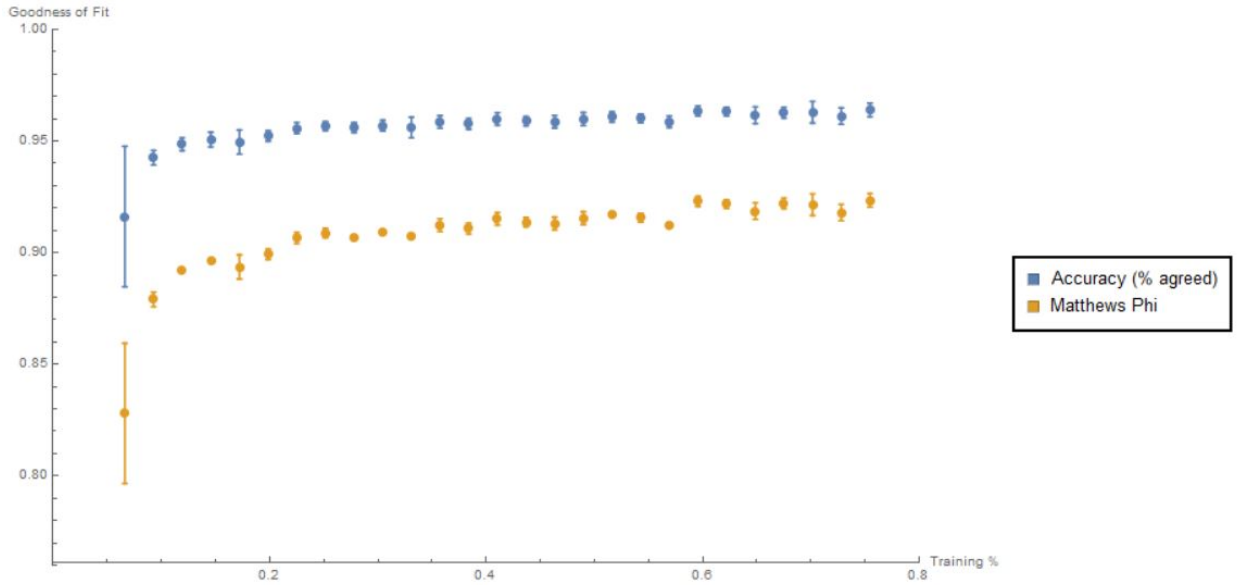


Figure 4.2: Learning curve for neural network machine-learning whether $h^{2,1} > 50$ for a hypersurface Calabi-Yau 3-fold in $W\mathbb{P}^4$.

4.4.2 Learning CICYs

Emboldened by the success in the warm-up, we can proceed to more sophisticated inputs. A CICY, we recall, is an integer matrix with number of rows ranging from 1 to 12 and number of columns, from 1 to 15, and whose entries are 0 to 5. As far as the computer is concerned, this is a 12 array of arrays (by down-right padding with zeros) with 6 discrete entries. In other words, it is a 12×15 pixelated image with 6 shades of grey (or 6 different colours). For instance, this very colourful representation [229] for the CICY which is the complete intersection of 8 equations in $(\mathbb{P}^1)^5 \times (\mathbb{P}^2)^3$ would be

$$\left(\begin{array}{cccccccc|c}
 1 & 1 & 0 & 0 & 0 & 0 & 0 & 0 & 0 \\
 1 & 0 & 1 & 0 & 0 & 0 & 0 & 0 & 0 \\
 0 & 0 & 0 & 1 & 0 & 1 & 0 & 0 & 0 \\
 0 & 0 & 0 & 0 & 1 & 0 & 1 & 0 & 0 \\
 0 & 0 & 0 & 0 & 0 & 0 & 0 & 2 & 0 \\
 0 & 1 & 1 & 0 & 0 & 0 & 0 & 0 & 1 \\
 1 & 0 & 0 & 0 & 0 & 1 & 1 & 0 & 0 \\
 0 & 0 & 0 & 1 & 1 & 0 & 0 & 1 & 0 \\
 \hline
 & & & & & & & & 0 \\
 & & & & & & & & 0
 \end{array} \right)_{12 \times 15} \rightsquigarrow \text{Image} \tag{4.25}$$

where purple is 0, green, 1 and red, 2. This is a CY3 with Hodge pair $(h^{1,1}, h^{2,1}) = (8, 22)$ (and thus $\chi = -28$); that $h^{1,1}$ is equal to the number of product projective spaces means it is favourable. For the reader's amusement, the *average* CICY as an image was drawn in *cit. ibid.*

With such an image, one could use a convolutional network to process it, much like hand-writing recognition. While we will not do so here, the point of presenting the manifold in this way is to emphasize the fact that the computer knows absolutely nothing about the algebraic geometry, or even that the image should correspond to a geometry. We can associate the image with an integer (such as the topological numbers) to the image much as one associates a value to a hand-written scribble. Yet with enough samples of correct values we can teach the machine how to “guess” the right values. This is doable because there is inherent pattern in algebraic geometry, regular enough to be “learnt”.

In [229, 230], the analogous neural network approach to testing CICY Hodge numbers as the one presented in detail above for WP^4 was performed. A more insightful and comprehensive analysis ⁵ specifically for CICYs was then done in [249]. The input data is a CICY configuration (image) and one can try the following structures to study not just whether one of the Hodge numbers exceeds a value, but the precise value of, say, $h^{1,1}$. This is obviously of great importance as we are actually going to let the machine calculate the exact value of a topological invariant simply by experience:

Neural network regressor: the output is continuous (i.e., some real number which we will then round up); Optimal neural network hyperparameters were found with a genetic algorithm, leading to an overall architecture of five hidden layers with 876, 461, 437, 929, and 404 neurons, respectively. The algorithm also found that a ReLU (rectified linear unit) activation layer and dropout layer of dropout 0.2072 be-

⁵ Though I am very much an amateur to data science, I must use this opportunity to thank my former Masters student Kieran Bull from Oxford, who was the torch-bearer for [249]. With admiration I joke with him that he eats 2000 lines of Python for breakfast, and, in retrospect, he probably did.

tween each neuron layer give optimal results.

SVM: the output is one of the possible values for $h^{1,1}$, viz., an integer ⁶ between 0 and 19, inclusive; here the hyperparameters were found to be a Gaussian kernel with $\sigma = 2.74, C = 10, \epsilon = 0.01$.

Neural network classifier: the output is a 20-channel classifier (like handwritten digits being a 10-channel classifier) with each neuron mapping to 0 or 1. The optimal architecture can be found to be four convolution layers with 57, 56, 55, and 43 feature maps, respectively, all with a kernel size of 3×3 . These layers were followed by two hidden fully-connected layers and the output layer, the hidden layers containing 169 and 491 neurons. ReLU activations and a dropout of 0.5 were included between every layer, with the last layer using a sigmoid activation.

Importantly, training with a laptop took on the order of 10 minutes and execution on the validation set, seconds. The actual Hodge computation of the CICYs, on the other hand, was a stupendous task.

The performance is again quite satisfactory, for a 25%-75% split of training versus validation (the machine has only seen 1/4 of the data!) and we have the various accuracy measures for the 3 above methods as

	Accuracy	RMS	R^2	ω_-	ω_+
NN Regressor	0.78 ± 0.02	0.46 ± 0.05	0.72 ± 0.06	0.742	0.791
SVM Reg	0.70 ± 0.02	0.53 ± 0.06	0.78 ± 0.08	0.642	0.697
NN Classifier	0.88 ± 0.02	-	-	0.847	0.886

(4.26)

In the above, the error bars come from repetition over 100 random samples, the dashes for the RMS and R^2 are because these are only defined for continuous variables, and ω_{\pm} give the Wilson confidence interval. Moreover, we have put in bold face the best performance.

Reassured by the prediction based only on 1/4 of seen data, the learning

⁶ An artefact of the CICY dataset is that $h^{1,1} = 0$ is a marker for a trivial CY3, such as the direct product $(T^2)^3$.

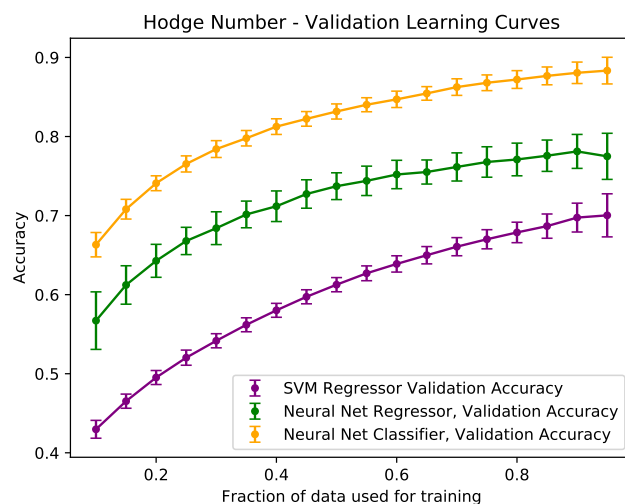


Figure 4.3: Hodge learning curves generated by averaging over 100 different random cross validation splits. The accuracy quoted for the 20 channel (since $h^{1,1} \in [0, 19]$) neural network classifier is for complete agreement across all 20 channels.

curves for the above 3 different methods are presented in Figure 4.3. We see that interestingly the SVM seems to be the best performer, quite quickly reaching 90% accuracy. For reference, we also demonstrate, in Figure 4.4, the comparative performance amongst the 3 methods at 20% seen training data, for each of the 20 values of $h^{1,1}$, checked against the 80% unseen validation data. We recall from Figure 2.1 that the distribution for $h^{1,1}$ is approximately Gaussian, peaked at 7, for CICYs.

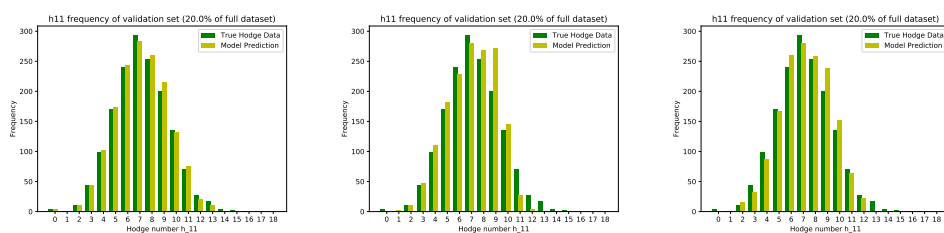


Figure 4.4: The histogram of predicted versus actual CICY $h^{1,1}$ at 20%-80% training-validation split, for (1) the neural network classifier, (2) regressor, and the SVM regressor.

4.4.3 Outlook

Encouraged by our string of successes, one might be led astray by optimism. Whilst there is, by definition, patterns in all fields of mathematics, machine-learning is not some omnipotent magical device, nor an oracle capable of predicting any pattern. Otherwise, we might as well use it to guess the position of the Riemann zeros or similar such questions of profound consequences. Indeed, one would expect problems in number theory not particularly amenable to our paradigm.

We therefore finish with a sanity check that machine-learning is not a magic black-box predicting all things. A reprobate ⁷ example which should be doomed to failure is the primes. Indeed, if a neural network could guess some unexpected pattern in the primes, this would be a rather frightening prospect for mathematics. Suppose we have a sequence of labelled data

$$\begin{aligned}
 \{2\} &\rightarrow 3 ; \\
 \{2, 3\} &\rightarrow 5 ; \\
 \{2, 3, 5\} &\rightarrow 7 ; \\
 \{2, 3, 5, 7\} &\rightarrow 11 ; \dots
 \end{aligned}
 \tag{4.27}$$

One can easily check that even with millions of training data, any neural network or SVM would be useless in prediction and that we are better off with a simple regression against the $n \log(n)$ curve in light of the Prime Number Theorem.

This principle of algebraic geometry being more susceptible to AI than number theory could be approximately understood. At the most basic level, every computation in algebraic geometry, be it a spectral sequence or a Gröbner basis, reduces to finding kernels and cokernels of sets of matrices (over \mathbb{Z} or even over \mathbb{C}), albeit of quickly forbidding dimensions ⁸. Ma-

⁷ In Calvinist heresy, a reprobate is a soul doomed for condemnation. I am grateful to my wife Dr. Elizabeth Hunter He, an expert on Reformation history, for teaching me this.

⁸ The recent work [233] shows that one needs to be careful even within algebraic geometry, as bundle-cohomology appears to be harder to learn than ordinary cohomology

trix/tensor manipulation is exactly the heart of any machine-learning – after all, this why the Python package is called TensorFlow – and what AI is good at. Number theory, on the other hand, ultimately involves patterns of prime numbers which, as is well known, remain elusive.

However apparent the power of machine-learning, much of it does remain mysterious: of all the intricate connections amongst the neurons or optimization of kernels and hyperplanes, what exactly is doing what? As Yau critiques, “there are no theorems in machine-learning”. Indeed, for a pure mathematician of his calibre, getting a topological invariant correct 95% of the time may not be precise enough. Nevertheless, getting such a quick estimate *entirely bypassing the expensive steps such as polytope triangulation or finding a Gröbner basis or finding the ranks of all the matrices in an exact sequence* is salient enough for practical purposes that the endeavour is well worth pursuing. One concrete line of attack might be

Let P be a problem in algebraic geometry with a simple answer (such as an integer), reduce its computation to its constituent parts (typically finding kernels and cokernels of matrix maps ⁹), test which of these is being out-performed by the likes of a neural network or SVM, and how.

On the other hand, from a purely applicability point of view for the physics, the potential is enormous. For instance, we mentioned earlier that while there are 473,800,776 reflexive polytopes, each of which gives a certain Hodge pair according to (2.33), but to compute the Chern numbers and the intersection form requires full triangulation of the polytope. This was done for on the order of 10^4 cases in [64, 98] of low or high $h^{1,1}$ - which is only a tiny fraction of the total set - and the vast majority is beyond computational ability due to triangulation being expensive. Could one training on these

and topological invariants.

⁹ Even finding the Gröbner basis, in a chosen basis of monomials in the variables, reduces to tensor manipulation. In the case of toric varieties, the problem can be entirely phrased in combinatorics of polytopes whose vertices are extracted from the exponents of monomials [23].

known cases in a supervised machine learning and predict what c_2 and d_{rst} would most likely be and thus complete the topological data for the KS set? Or indeed, even on a simpler level, predict how many triangulations - and hence different candidate CY_3 manifolds - there should be? Recently, an estimate of the number triangulations for the full KS set was nicely performed in [248] and an astounding 10^{10^5} was proposed.

If one has the c_2 and d_{rst} , one could pursue many serious phenomenological questions. For example, certainly properties of the d_{rst} (so-called “Swiss-cheese” [250]) single out manifolds which can be used in cosmology. However, the computation to decide whether a manifold is Swiss-cheese is very computationally intensive [251]. Machine-learning the dataset in distinguishing such manifold while not be impeded by the expensive steps would be much desired.

As mentioned in the end of the first Chapter, Calabi-Yau compactifications is only a small portion of the heterotic landscape. More sophisticated methods now use stable holomorphic vector bundles on manifolds with non-trivial fundamental group in obtaining the *exact* standard model. This is a much richer and phenomenologically interesting landscape of geometries which involve the much more intractable task of computing bundle-value cohomology groups. Machine learning for these have been considered in [233, 245].

What about beyond Calabi-Yau geometry? We know the string landscape extends far beyond Calabi-Yau manifolds and touch deeply upon G_2 -manifolds, generalized Kähler manifolds, and beyond. The paradigm of machine-learning algebraic geometry is clearly of interest to physicists and mathematicians alike, and applicable to varieties other than Calabi-Yau manifolds. What can they say about computing topological or rational invariants in general?

We leave all these tantalizing challenges to the dedicated reader.

4.5 Epilogue

Though the area of machine-learning geometry and applying the latest results from data science to treat the landscape is still in its infancy, and much of its inner workings is still perplexing, its power is apparent and its potential, vast. This new paradigm should prove useful as both a *classifier* and *predictor* of geometrical quantities. The ability to rapidly obtain results stochastically, before embarking on to intensively compute from first principles is at once curious and enticing. What we have sacrificed in complete confidence and analytical result, we have gained by improving the computation time by many orders of magnitude.

To quote Boris Zilber, Professor of Mathematical Logic at Merton College, Oxford, “you have managed syntax without semantics.” This is an astutely appropriate analogy, not only for our present context but also for AI research in general. The prowess of machine-learning is precisely its not taking a reductionist framework where all intermediate quantities are computed analytically from first principles - much like our earlier comment of trying to recognize hand-writing by setting up Morse functions - but by gathering large quantities of data to probabilistically find latent patterns.

It is interesting that the last decades of the 20th century, theoretical physicists had to learn algebraic geometry, now, in the dawn of the 21st, it is AI which can be put to “learn” some tricks of the trade. We are reminded of many species of primates who have learnt to effectively use herbal medicine by trial and error without any idea of chemical composition. Perhaps confronting the vast landscape of mathematics and theoretical physics, the human mind is still learning by tentation.

Postscriptum

Thus concludes our excursion of the *terra sancta* of Calabi-Yau manifolds. From the compact landscape of CICYs and KS hypersurfaces, to the non-compact vista of quiver representations and Sasaki-Einstein cones, from the computational algebraic geometry of topological invariants, to the combinatorics of convex polytopes and rational cones, from the plethora of data compiled into readily accessible webpages to the *terra incognita* of machine-learning algebraic geometry, I hope the reader has beheld the richness of the grounds, fertile with mathematics, physics and data science.

Though from these alluring terrains we now pause to return to our mundanities, our orisons shall continue to drift to this lofty pursuit which transcends disciplines, and so it is only fitting to close with an excerpt from the master himself, the “Ode to Time and Space” by Prof. S.-T. Yau:

...

大哉大哉，宇宙之謎。美哉美哉，真理之源。
時空量化，智者無何。管測大塊，學也洋洋。

丘成桐先生：時空頌

Appendix A

Some Rudiments of Complex Geometry

In this appendix, we give a lightning recapitulation of the key concepts from complex geometry which we use throughout the text. Other than the canonical texts [13,14], the reader is also referred to brief, self-contained expositions in [20,21], both of which do a wonderful job in rapid initiation.

For a compact, smooth, differential manifold M of dimension n , we can define differential p -forms $\eta^{(p)} \in \Omega^p := \bigwedge^p T_M^\vee$, the p -th antisymmetric power of the cotangent bundle T_M^\vee , as well as a differential operator $d : \Omega^p \rightarrow \Omega^{p+1}$ satisfying $d^2 = 0$. Whence, we have the (de Rham) cohomology group $H_{dR}^p(M) = \ker(d) / \text{Im}(d)$.

Next, we recall the following sequence of specializations by imposing incremental structures:

Riemannian M is endowed with a positive-definite symmetric metric g ;

With this metric, we can define the Hodge star operator $\star : \Omega^p \rightarrow \Omega^{n-p}$ as $\star(dx^{\mu_1} \wedge \dots \wedge dx^{\mu_p}) := \frac{\epsilon^{\mu_1 \dots \mu_n}}{\sqrt{|g|}} g_{\mu_{p+1}\nu_{p+1}} \dots g_{\mu_n\nu_n} dx^{\nu_{p+1}} \wedge \dots \wedge dx^{\nu_n}$ so

that a Laplacian Δ can be defined:

$$\Delta_p = dd^\dagger + d^\dagger d = (d + d^\dagger)^2, \quad d^\dagger := (-1)^{np+n+1} \star d \star .$$

Importantly, Harmonic p -forms can be put into 1-1 correspondence with elements of cohomology, that is, $\Delta_p \eta^p = 0 \xleftrightarrow{1:1} \eta \in H_{dR}^p(M)$.

Complex M is further endowed with a complex structure $J : T_M \rightarrow T_M$, inducing the split $\Omega^p = \bigoplus_{r+s=p} \Omega^{r,s}$ so that we have (p, q) -forms with p -holomorphic and q -antiholomorphic indices. Clearly, n needs to be even at this point. Subsequently, the operator d also splits to $d = \partial + \bar{\partial}$, together with $\partial^2 = \bar{\partial}^2 = \{\partial, \bar{\partial}\} = 0$.

Hermitian The Riemannian metric on M further obeys $g(J_-, J_-) = g(-, -)$, so that in local coordinates $g_{\mu\nu} = g_{\bar{\mu}\bar{\nu}} = 0$ and we only have the mixed components $g_{\mu\bar{\nu}}$. This is the Hermitian metric. At this point we can define **Dolbeault Cohomology** $H_{\bar{\partial}}^{p,q}(X)$ as the cohomology of $\bar{\partial}$ (we could equivalently use ∂) with Laplacian $\Delta_{\partial} := \partial\partial^\dagger + \partial^\dagger\partial$ and similarly $\Delta_{\bar{\partial}}$.

Kähler With the Hermitian metric one can define a Kähler form $\omega := ig_{\mu\bar{\nu}} dz^\mu \wedge dz^{\bar{\nu}}$ such that $d\omega = 0$. This in particular implies that $\partial_\mu g_{\nu\bar{\lambda}} = \partial_\nu g_{\mu\bar{\lambda}}$ so that $g_{\mu\bar{\nu}} = \partial\bar{\partial}K(z, \bar{z})$ for some scalar function (the Kähler potential) $K(z, \bar{z})$. Now, the Laplacian becomes $\Delta = 2\Delta_{\partial} = 2\Delta_{\bar{\partial}}$, and we have **Hodge decomposition**

$$H^i(M; \mathbb{C}) \simeq \bigoplus_{p+q=i} H^{p,q}(M) = \bigoplus_{p+q=i} H^q(M, \bigwedge^p T_M^\vee), \quad i = 0, 1, \dots, n . \tag{A.1}$$

In the above, we have written ordinary complex-valued cohomology in terms of Dolbeault cohomology in the first equality and in terms of bundle-valued cohomology in the second, where T_M^\vee is the cotangent bundle of M , dual to the tangent bundle T_M , and \wedge^p gives its p -th wedge (anti-symmetric tensor) power.

The Ricci curvature 2-form also assumes a particularly simple form for

M Kähler, which in local coordinates, is

$$R = -i\partial\bar{\partial} \log \det(g_{\mu\bar{\nu}}) dz \wedge d\bar{z} . \quad (\text{A.2})$$

This is a $(1, 1)$ -form which as a real 2-form is closed. Thence, we can define the **Chern classes** $c_k(M) = c_k(T_M) \in H^{2k}(M)$ as

$$\det \left(\mathbb{I}_{n \times n} + \frac{it}{2\pi} R \right) = \sum_{k=0}^{n/2} c_k(M) t^k . \quad (\text{A.3})$$

As we will always take a more algebraic rather than differential approach, we can think of the Chern classes more axiomatically [13]. In the above we defined the Chern classes of M , understood as those of the tangent bundle T_M ; they can be defined for arbitrary bundles.

DEFINITION 18 *Let E be a complex vector bundle of rank r over our manifold M (i.e., locally, $E \simeq M \times \mathbb{C}^r$), then the Chern classes $c_k(E) \in H^{2k}(M; \mathbb{Z})$, together with their associated formal sum (the total Chern class)*

$$c(E) := c_0(E) + c_1(E) + \dots + c_r(E) ,$$

obey the axiomata

- *Leading term: $c_0(E) = 1$ for any E ;*
- *Naturality: if $f : N \rightarrow M$ is a continuous morphism from manifold N to M and $f^*(E) \rightarrow N$ is the pull-back vector bundle, then*

$$c_k(f^*E) = f^*c_k(E) ;$$

- *Whitney sum: If $F \rightarrow X$ is another complex bundle on M , then*

$$c(E \oplus F) = c(E) \wedge c(F) \quad \rightsquigarrow \quad c_k(E \oplus F) = \sum_{i=0}^k c_i(E) \wedge c_{k-i}(F) ;$$

- *Normalization:* For complex projective space $\mathbb{C}\mathbb{P}^n$, let H be the Poincaré dual to the hyperplane class $\mathbb{C}\mathbb{P}^{n-1} \subset \mathbb{C}\mathbb{P}^n$, then for the degree 1 bundle $\mathcal{O}_{\mathbb{P}^n}(1)$ whose transition functions are linear (the dual $\mathcal{O}_{\mathbb{P}^n}(-1)$ is the tautological bundle),

$$c(\mathcal{O}_{\mathbb{P}^n}(1)) = 1 + H .$$

We remark that the Whitney sum generalized to short exact sequence of bundles (a *splitting principle* due to Grothendieck) gives

$$0 \rightarrow E \rightarrow G \rightarrow F \rightarrow 0 \quad \Rightarrow \quad c(G) = c(E) \wedge c(F) . \quad (\text{A.4})$$

Furthermore, for the *dual bundle* E^\vee , we have that

$$c_i(E^\vee) = (-1)^i c_i(E) . \quad (\text{A.5})$$

We can reorganize the Chern class into a *character* from $(\oplus, \otimes) \rightarrow (+, \wedge)$ called the *Chern character* $\text{Ch}(\)$.

$$\text{Ch}(E \oplus F) = \text{Ch}(E) + \text{Ch}(F) , \quad \text{Ch}(E \otimes F) = \text{Ch}(E) \wedge \text{Ch}(F) , \quad (\text{A.6})$$

The total Chern class does not enjoy this nice property, For a line bundle (i.e., rank 1) L , the Chern character is $\text{Ch}(L) := \exp(c_1(L))$, and more generally for a rank r bundle E , using the splitting principle into line bundles, $E = \bigoplus_{i=1}^r L_i$, we have that

$$\text{Ch}(E) := \sum_{i=1}^r \exp(c_1(L_i)) = \sum_{m=0}^{\infty} \frac{1}{m!} \sum_{i=1}^r c_1(L_i)^m = \text{Ch}_0(E) + \text{Ch}_1(E) + \dots$$

where

$$\begin{aligned} \text{Ch}_0(E) &= \text{rk}(E), \\ \text{Ch}_1(E) &= c_1(E), \\ \text{Ch}_2(E) &= \frac{1}{2}(c_1(E)^2 - 2c_2(E)), \\ \text{Ch}_3(E) &= \frac{1}{6}(c_1(E)^3 - 3c_1(E)c_2(E) + 3c_3(E)) , \dots \end{aligned} \quad (\text{A.7})$$

The recasting of Ch_i in terms of the c_i is evidently an exercise in Newton symmetric polynomials. The Chern character of more sophisticated combinations such as antisymmetric products, crucial in physics, can be similarly obtained (cf. Appendix A of [119]).

Finally, we will also be making use of the Todd class. It is yet another combination of the Chern classes, which is multiplicative over \otimes , i.e., $\text{Td}(E \oplus F) = \text{Td}(E) \wedge \text{Td}(F)$,

$$\begin{aligned} \text{Td}(E) &= 1 + \text{Td}_1(E) + \text{Td}_2(E) + \text{Td}_3(E) + \dots, \text{ where} \\ \text{Td}_1(E) &= \frac{1}{2}c_1(E), \\ \text{Td}_2(E) &= \frac{1}{12}(c_2(E) + c_1(E)^2), \\ \text{Td}_3(E) &= \frac{1}{24}(c_1(E)c_2(E)) , \dots \end{aligned} \tag{A.8}$$

One can invert the above to obtain, for instance, the top Chern class, from an identity of Borel-Serre (cf. 3.2.5 of [17])

$$\sum_{i=0}^r (-1)^i \text{Ch}(\bigwedge^i E^\vee) = c_r(E) \text{Td}(E)^{-1}. \tag{A.9}$$

A.1 Covariantly Constant Spinor

In brief, the authors of [110] take the effective 10-dimensional action

$$S \sim \int d^{10}x \sqrt{g} e^{-2\Phi} \left[R + 4\partial_\mu \Phi \partial^\mu \Phi - \frac{1}{2}|H'_3|^2 - \frac{1}{g_s^2} \text{Tr}|F_2|^2 \right] + SUSY \tag{A.10}$$

of the heterotic string (where we write only the bosonic part and $+SUSY$ is understood to be the supersymmetric completion) and considers ¹ the

¹ One way to think of supersymmetry, regardless of experimental results and from a philosophical point of view, is to ask “are complex numbers part of reality?” We know that the complex numbers complete the reals in a canonical way, and has become indispensable even to engineers. Supersymmetry completes QTFs in a canonical way, and should likewise

supersymmetric variation δ on the various fields:

$$\begin{aligned}
\text{gravitino} & \quad \delta_\epsilon \Psi_{m'=1,\dots,10} = \nabla_{m'} \epsilon - \frac{1}{4} H_{m'}^{(3)} \epsilon \\
\text{dilatino} & \quad \delta_\epsilon \lambda = -\frac{1}{2} \Gamma^{m'} \partial_{m'} \Phi \epsilon + \frac{1}{4} H_{m'}^{(3)} \epsilon \\
\text{adjoint Yang-Mills} & \quad \delta_\epsilon \chi = -\frac{1}{2} F^{(2)} \epsilon \\
\text{Bianchi} & \quad dH^{(3)} = \frac{\alpha'}{4} [\text{Tr}(R \wedge R) - \text{Tr}(F \wedge F)]
\end{aligned} \tag{A.11}$$

and demand that these all vanish so that supersymmetry is preserved. Assume that the 3-form field $H^{(3)} = 0$ (this is a strong assumption and can be generalized, for which there has been much recent work, cf. e.g. [112]), we have that upon dimensional reduction $\mathbb{R}^{1,9} \simeq \mathbb{R}^{1,3} \times M$ for some compact (internal) 6-manifold M ,

$$0 = \delta_\epsilon \Psi_{m'=1,\dots,10} = \nabla_{m'} \epsilon = \nabla_{m'} \xi(x^{\mu=1,\dots,4}) \eta(y^{m=1,\dots,6}), \tag{A.12}$$

giving us the Killing spinor equation on M .

Now, the external space, being Minkowski, is flat so that $[\nabla_\mu, \nabla_\nu] \xi(x) = 0$. Thus, the internal space M is also Ricci-flat and admitting not only a spinor (and is thus a spin manifold), but in fact a covariant constant spinor

$$\nabla_m \eta = 0. \tag{A.13}$$

Defining $\eta_+^* = \eta_-$ to split chirality to the original 10-dimensional spinor as $\epsilon(x^{1,\dots,4}, y^{1,\dots,6}) = \xi_+ \otimes \eta_+(y) + \xi_- \otimes \eta_-(y)$, we have the following set of definitions which sequentially specialize M :

- Define $J_m^n = i\eta_+^\dagger \gamma_m^n \eta_+ = -i\eta_-^\dagger \gamma_m^n \eta_-$, one can check that $J_m^n J_n^p = -\delta_m^p$ for Clifford Gamma matrix γ_m^n . Therefore, (M, J) is **almost-complex**;
- However, η covariantly constant $\rightsquigarrow \nabla_m J_n^p = 0 \rightsquigarrow \nabla N_{mn}^p = 0$ so that the Nijenhuis tensor $N_{mn}^p := J_m^q \partial_{[q} J_n^p - (m \leftrightarrow n)$. Therefore, (M, J) is **complex** (in particular, one can choose coordinates (z, \bar{z}) so that $J_m^n = i\delta_m^n$, $J_{\bar{m}}^{\bar{n}} = i\delta_{\bar{m}}^{\bar{n}}$, $J_m^{\bar{n}} = J_{\bar{m}}^n = 0$, rendering the transition functions holomorphic);

be thought of as the natural realm in which to study elementary physics.

- Define $J = \frac{1}{2}J_{mn}dx^m \wedge dx^n$ with $J_{mn} := J_m^k g_{kn}$. One can check that $dJ = (\partial + \bar{\partial})J = 0$, so that (M, J) is **Kähler**.

Now, for a spin 6-manifold, the holonomy group is generically $SO(6) \simeq SU(4)$. The existence of the covariantly constant spinor implies that the holonomy is reduced: in the decomposition $\mathbf{4} \rightarrow \mathbf{3} \oplus \mathbf{1}$ of $SU(4) \rightarrow SU(3)$, this covariantly constant spinor corresponds to the $\mathbf{1}$. Thus, in summary, our internal manifold M is Kähler, $\dim_{\mathbb{C}} = 3$, and with $SU(3)$ holonomy.

A.2 A Lightning Refresher on Toric Varieties

This section, as mentioned in the main text, is not meant to be a review on toric geometry, of which there are many excellent sources in the literature [18, 19, 21–23]. We will use the quadric hypersurface, the “conifold”,

$$\{ab = cd\} \in \mathbb{C}_{(a,b,c,d)}^4, \quad (\text{A.14})$$

to illustrate the 3 equivalent definitions of an affine toric variety. As in the standard case for manifolds, these affine patches, with the appropriate transition functions, can be glued to a compact toric variety.

(i) Combinatorics of Lattice Cones: The most standard definition of an affine toric variety is via

DEFINITION 19 *A convex polyhedral cone is the set $\sigma := \{r_1 v_1 + \dots + r_s v_s \in V : r_i \in \mathbb{R}_{\geq 0}\}$ for $v_i \in V$. Here $V = N_{\mathbb{R}} = N \otimes_{\mathbb{Z}} \mathbb{R}$ is a vector space obtained from a lattice $N \simeq \mathbb{Z}^n$.*

In other words, σ is the cone with tip at the origin and whose edges are rays determined by lattice vectors. The lattice N has its dual lattice $M =$

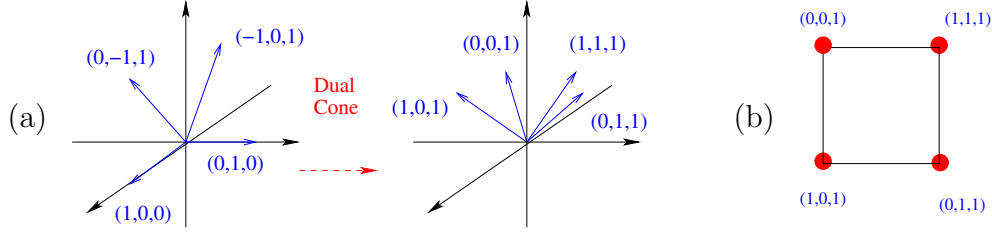


Figure A.1: (a) the cone and dual cone; (b) the toric diagram, for the conifold.

$\text{hom}(N, \mathbb{Z})$ by the inner product $\langle M, N \rangle$, as well as its own associated vector space $M_{\mathbb{R}} = M \otimes_{\mathbb{Z}} \mathbb{R}$.

The **dual cone** σ^{\vee} is the set of vectors in $M_{\mathbb{R}}$ whose inner product with all vectors in σ are non-negative. The affine toric variety U_{σ} for σ is then

$$U_{\sigma} := \text{Spec}(\mathbb{C}[\sigma^{\vee} \cap M]) \quad , \quad \sigma^{\vee} \cap M := \{u \in M : \langle u, v \rangle \geq 0 \quad \forall v \in \sigma\} \quad . \quad (\text{A.15})$$

In the physics literature, the set of end points of the integer vector generators of $\sigma^{\vee} \cap M$ is called the **toric diagram**.

The diagrams in Figure A.1 will reify the above concepts. In part (a), the cone is spanned by the four vectors

$$\{(0, -1, 1), (-1, 0, 1), (0, 1, 0), (1, 0, 0)\} \quad (\text{A.16})$$

in \mathbb{Z}^3 (so the resulting variety is complex dimension 3). One can readily check that the dual cone is spanned by the four vectors

$$\{(0, 0, 1), (1, 1, 1), (0, 1, 1), (1, 0, 1)\} \quad , \quad (\text{A.17})$$

so that all pair-wise inner products of the generators of σ^{\vee} and σ are non-negative. In part (b), the end points of the generators of σ and σ^{\vee} are coplanar, as is in congruence with the fact that our hypersurface is Calabi-Yau. The diagram is a square of unit area and the last coordinate is 1 (of course, any $GL(3; \mathbb{Z})$ transformation on the diagram gives the same variety). In fact, dropping the last coordinate gives the convex polygon, here the square, which

is the diagram used in the main text.

We treat the coordinates of these generators of the dual cone as exponents of 3 complex variables (x, y, z) , giving us

$$S_\sigma = \langle a = z, c = yz, b = xyz, d = xz \rangle . \quad (\text{A.18})$$

Finally, maximal spectrum of the polynomial ring $\mathbb{C}[S_\sigma]$ means we find any basic relations among (a, b, c, d) , which gives the hypersurface (A.14) as desired.

(ii) Kähler Quotients: The second definition is a direct generalization of projective space \mathbb{P}^n , which we recall to be \mathbb{C}^{n+1} (with coordinates $x_{i=0,\dots,n}$ quotiented by a $\lambda \in \mathbb{C}^*$ action $x_i \mapsto \lambda x_i$). Now, consider \mathbb{C}^q with homogeneous (Cox) coordinates $x_{i=0,\dots,q}$ and a $(\mathbb{C}^*)^{q-d}$ action

$$x_i \mapsto \sum_a \lambda_a^{Q_{i=1\dots q}^{a=1\dots q-d}} x_i , \quad \lambda_a \in \mathbb{C}^* , Q_i^a \in \mathbb{Z} , \quad (\text{A.19})$$

where Q is called a charge matrix, the integer kernel of which is given by

$$\sum_{i=1}^d Q_i^a v_i = 0 , \quad (\text{A.20})$$

and the generators v_i is the toric diagram.

For our running example, take $Q = [-1, -1, 1, 1]$, as a \mathbb{C}^* action on \mathbb{C}^4 , so that $\ker(Q) = \begin{pmatrix} 1 & 0 & 0 & 1 \\ 1 & 0 & 1 & 0 \\ 1 & 1 & 1 & 1 \end{pmatrix}$ and the 4 columns are precisely (A.17).

(iii) Computational Definition: This is the simplest definition, the defining equation $ab - cd$ for the conifold is known as a *binomial ideal*, i.e., every defining equation is of the form of “monomial = monomial”. It turns out that [23] every such polynomial ideal defines a toric variety. Interestingly, this condition is crucial to the bipartite interpretation of quiver representa-

tion variety for toric CY3, as in Theorem 10.

A.3 Dramatis Personae

Recall the trichotomy of $g = 0$, $g = 1$ and $g > 1$ from Figure 1.1. As Riemann surfaces/complex manifolds, these are respectively $S^2 \simeq \mathbb{P}^1$ (positive curvature), $CY_1 \simeq T^2$ (zero curvature) and hyperbolic (negative curvature). This trichotomy [13] in complex dimension 1 persists to general Kähler manifolds and are referred to as (1) **Fano**; (2) **Calabi-Yau** and (3) **general type**, the first two falling into some classifiable families whilst the third usually proliferates untamably. More strictly, for a (complete) complex manifold M and consider its anti-canonical sheaf $K_M^\vee := (\wedge^n T_M^\vee)^\vee$, if it is trivial, M is Calabi-Yau and if it is ample, then M is Fano.

In complex dimension two, the Calabi-Yau case consists of T^4 and K3, while the Fano family also enjoys a wealth of structure. Clearly, \mathbb{P}^2 and $\mathbb{P}^1 \times \mathbb{P}^1$ are Fano, the first since $K_{\mathbb{P}^n}^\vee = \mathcal{O}_{\mathbb{P}^n}(n+1)$, and the second, essentially by Künneth. Interestingly, there are 8 more. To introduce these, we need the concept of a **blow-up**.

In brief, a blow-up of a point in an n -fold is to replace the point with a \mathbb{P}^{n-1} . The general definition is rather abstruse (cf. §7, circa Prop 7.11 of [13]) but locally the definition is straight-forward. Consider a codimension k subvariety $Z \subset \mathbb{C}^n$ with affine coordinates $x_{i=1, \dots, n}$, defined, for simplicity, by $x_1 = x_2 = \dots = x_k = 0$. Let y_i be the homogeneous coordinates of \mathbb{P}^{k-1} , then the blow-up $\widetilde{\mathbb{C}^n}$ of \mathbb{C}^n along Z is defined by the equations

$$\{x_i y_j = x_j y_i\}_{i,j=1, \dots, k} \subset \mathbb{C}^n \times \mathbb{P}^{k-1}. \quad (\text{A.21})$$

Thus defined, away from Z , $\widetilde{\mathbb{C}^n}$ is just \mathbb{C}^n as the non-identical-vanishing of x_i fixes y_i to be a single point on \mathbb{P}^{k-1} (i.e., we project back to \mathbb{C}^n), but along Z , where x_i vanish, we have arbitrary y_i , parametrizing \mathbb{P}^{k-1} . Thus, we have “replaced” Z by \mathbb{P}^{k-1} .

del Pezzo Surfaces: We apply the aforementioned to $\mathbb{P}_{[X_0:X_1:X_2]}^2$. Take the point $P = [0 : 0 : 1]$ without loss of generality, and work on the affine patch $X_2 \neq 0$ so that $(x, y) = (X_0/X_2, X_1/X_2) \in \mathbb{C}^2$. We blow the point P up by “replacing” it with a $\mathbb{P}_{[z:w]}^1$. Then the blowup of \mathbb{P}^2 at P is given by

$$\{((x, y); [z : w]) : xz + yw = 0\} \subset \mathbb{C}^2 \times \mathbb{P}^1. \quad (\text{A.22})$$

At points away from P where (x, y) are not simultaneously 0, we can fix a value of $[z : w]$ but at P where $(x, y) = (0, 0)$, $[z : w]$ are arbitrary and parametrizes a full \mathbb{P}^1 . The result is a smooth complex surface, denoted dP_1 , which is \mathbb{P}^2 blown up at a point.

Now, take r generic points² on \mathbb{P}^2 , and perform successive blow-up. We denote the result as dP_r , the r -th del Pezzo surface (with $r = 0$ understood to be \mathbb{P}^2 itself). Letting ℓ be the hyperplane class of \mathbb{P}^1 in \mathbb{P}^2 and $E_{i=1, \dots, r}$ be the **exceptional divisors** corresponding to the various \mathbb{P}^1 blow-ups, the intersection numbers are

$$\ell \cdot \ell = 1, \quad \ell \cdot E_i = 0, \quad E_i \cdot E_j = -\delta_{ij}, \quad (\text{A.23})$$

and the Chern classes are given by

$$c_1(dP_r) = 3\ell - \sum_{i=1}^r E_i, \quad c_2(dP_r) = 3 + r. \quad (\text{A.24})$$

The canonical class K_{dP_r} is $c_1(dP_r)$ and its self-intersection is the **degree**: using (A.23), we see that the degree is $c_1(dP_r)^2 = 9 - r$. For instance, the degree 3 surface in \mathbb{P}^2 , on which there are the famous 27 lines, corresponds to $r = 6$ blowups.

From the degree, we see the $r \leq 8$, thus there are only $8 + 1$ del Pezzo surfaces ($r = 0, \dots, 8$) which are Fano. It is remarkable that they correspond to the exceptional simply-laced series in semi-simple Lie algebras, viz.,

² Generic means that no 3 points are colinear, no 4 points are coplanar, etc., so that the points are in general position, i.e., their projective coordinates can be taken as n random triples $[x_i : y_i : z_i]$.

where “ \rightarrow ” means blow-up by one point. Finally, we remark that of this sequence, $dP_{0,1,2,3}$ and \mathbb{F}_0 are toric varieties but not the others. Incidentally, it was noticed in [83] that this is exactly the structure of M-theory/string theory compactifications on successive circles, a mysterious duality indeed!

Thus, in analogy of the trichotomy of Riemann surfaces/complex curves of Figure 1.1, the situation in complex dimension 2 is

10 Fano surfaces in (A.28)	$CY_2 =$	Surfaces of general type
$dP_{n=0,\dots,8}, \mathbb{P}^1 \times \mathbb{P}^1$	$T^4, K3$	
+ curvature	0 curvature	– curvature

(A.29)

The complex dimension 3 case is, on the other hand, much more complicated and this book is devoted to the middle column of CY3s, of which there already is a superabundance.

Appendix B

Gröbner Bases: The Heart of Computational Algebraic Geometry

As much as almost any problem in linear algebra begins with Gaussian elimination, when encountering a system of polynomials - to which almost any query in algebraic geometry be reduced - one begins with the Gröbner basis. This analogy is actually strict: for a system of polynomials all of degree 1 (i.e., back to a linear system), the Gröbner basis (in elimination ordering) is Gaussian elimination to triangular form.

As promised in the text, we cannot possibly not go into a brief digression into Gröbner bases, which lies at the root of all the algorithms used in this book, the reader is referred to [7] for a marvellous account of the subject of computational geometry. For diehards in **Mathematica**, a package has been written [52] to link it with **Singular** so that much of the algorithms can be performed with a more familiar front-end.

As always, we exclusively work over the polynomial ring $\mathbb{C}[x_i]$, and with $x_i \in \mathbb{C}$, which greatly simplifies things. First, we need to define an ordering of

the monomials, denoted as $\mathbf{x}^\alpha \prec \mathbf{x}^\beta$ where \mathbf{x}^α is the standard vector exponent notation understood to be the monomial $x_1^{\alpha_1} x_2^{\alpha_2} \dots x_n^{\alpha_n}$. This is a *total order* in the sense that if $u \preceq v$ and w is any other monomial, then $uw \preceq vw$ (it is in fact furthermore well-ordered in that $1 \preceq u$ for any u). There are many ways to define such an ordering and indeed the Gröbner basis is dependent on such a choice. The final conclusions in the geometry must, of course, be independent of any ordering choice. The most common choices of ordering are (we will use the four monomials $\{x_1 x_2^2 x_3, x_3^2, x_1^3, x_1^2 x_2^2\}$ to illustrate each case):

lex or Lexicographic ordering, which, like a dictionary, compares the exponent of x_1 , and if equal, proceeds to x_2 , etc., so that the power of $x_{i < j}$ dominates over x_j ; e.g., $x_1^3 \succ x_1^2 x_3^2 \succ x_1 x_2^2 x_3 \succ x_3^2$;

grlex or Graded (or degree)-lexicographic ordering, which compares *total degree* first and in the case of ties, proceeds to lex; e.g., $x_1^2 x_3^2 \succ x_1 x_2^2 x_3 \succ x_1^3 \succ x_3^2$ (tie on highest degree, 4, in the first two, and proceeded to lex so that x_1 dominated);

grevlex or Graded (or degree) reversed lexicographic ordering, which compares total degree first and then uses the reversed order of lex for ties; e.g., $x_1 x_2^2 x_3 \succ x_1^2 x_3^2 \succ x_1^3 \succ x_3^2$;

lexdeg or Elimination (or block) ordering, which divides the variables into ordered blocks, each of which has a chosen ordering, usually grevlex; e.g., suppose we wish to eliminate x_1 , we create two blocks: $\{x_1\}$ and $\{x_2, x_3\}$ so that lex ordering is considered for $\{x_1\}$ before $\{x_2, x_3\}$; e.g., $x_1^3 \succ x_1^2 x_3^2 \succ x_1 x_2^2 x_3 \succ x_3^2$.

With a monomial ordering fixed, we have a definite *leading term* of any polynomial f , denoted $LT(f)$, which is the monomial, together with its coefficients, maximal according to \succ . Suppose we are given $F = \{f_i\}$, a system of multivariate polynomials. The Gröbner basis G of F is obtained by the **Buchberger Algorithm** as follows.

1. Set $G := F$ to initialize;
2. For every pair $f_i, f_j \in G$, find the leading terms $LT(f_i)$ and $LT(f_j)$, as well as their least common multiple¹ $a_{ij} := LCM(LT(f_i), LT(f_j))$;
3. Compute the S-polynomial $S_{ij} := \frac{a_{ij}}{LT(f_i)}f_i - \frac{a_{ij}}{LT(f_j)}f_j$ so that the leading terms cancel by construction;
4. Divide S_{ij} by every element of G to see if there is a remainder, i.e., write $S_{ij} = \sum_{g \in G} p_g g + r$. This is called reduction of S_{ij} over the set G . The remainder r is so that none of its terms divides any of the leading terms from p_g , in analogy to arithmetic division.
5. If there is non-trivial remainder: $r \neq 0$, then add r to G ;
6. Repeat until all pairs are considered in the augmented G (i.e., including the generated remainders included into G as we go along) and until no new remainders are generated.

The final list of polynomials G (which in general will have more elements than F) is the Gröbner basis.

There are many implementation of the Buchberger Algorithm, exemplified by the `GroebnerBasis[]` command in `Mathematica`, the `gb()` command in `Macaulay2`, the `groebner()` command in `Singular`. Let us illustrate with a very simple example, step by step:

1. INPUT: $G = F = \{-12xy + 3y^2, 4x - 6y\}$, with lex ordering $x \succ y$, the leading terms are $LT(F_1) = -12xy$ and $LT(F_2) = 4x$;
2. There is one S-polynomial between the 2 elements of I . First, $a_{12} = LCM(xy, x) = xy$ (where the polynomial LCM is done without the coefficient, but this a mere convention and including the coefficient will

¹ While finding the LCM of two polynomials involves a generalization of the Euclidean division algorithm, since we are only finding the LCM of two monomials, this is easily done by comparing exponents.

just give an overall numerical factor), so $S_{12} = \frac{a_{12}}{LT(F_1)}F_1 - \frac{a_{12}}{LT(F_2)}F_2 = \frac{5y^2}{4}$. Note that here, by design, the leading terms cancelled; Reducing S_{12} by the 2 elements of G gives non-trivial remainder for both, so S_{12} should be kept.

3. At this point G is augmented to $G = \{-12xy + 3y^2, 4x - 6y, \frac{5y^2}{4}\}$, with leading terms $LT(G_{1,2}) = LT(F_{1,2}), LT(G_3) = G_3$. We now have 2 new S-polynomials to compute: $a_{13} = xy^2 \rightsquigarrow G_{13} = -\frac{y^3}{4}$ and $a_{23} = xy^2 \rightsquigarrow G_{23} = -\frac{3y^3}{2}$. Both G_{13} and G_{23} , when reduced on G have zero remainder because $a_{13} = -\frac{1}{5}yG_3$ and $a_{23} = -\frac{6}{5}G_3$. Thus nothing new can be added and G is the final Gröbner basis.

B.0.1 An Elimination Problem

Of the many wonders of the Gröbner basis, let us only illustrate one, viz., elimination, on our favourite quintic from (2.12)

$$Q := \sum_{i=0}^4 z_i^5 - \psi \prod_{i=0}^4 z_i, \quad \psi \in \mathbb{C}. \quad (\text{B.1})$$

Suppose we wish to check the conditions on ψ for which Q is non-singular. To do this, we compute the Jacobian of Q and form an ideal \mathcal{I} together with Q :

$$\mathcal{I} = \left\{ \sum_{i=0}^4 z_i^5 - \psi \prod_{i=0}^4 z_i, \left(5z_j^4 - 5\psi \prod_{k=0, k \neq j}^4 z_k \right)_{j=0, \dots, 4} \right\}. \quad (\text{B.2})$$

We now consider lexdeg ordering by having two blocks: variables $z_{1, \dots, 4}$ and $\{z_0\}$, leaving ψ as a free complex parametre, and establish the Gröbner basis $G(\mathcal{I})$ for the ideal \mathcal{I} , which we then intersect with $\mathbb{C}[z_0]$. That is, we eliminate the variables $z_{0, \dots, 4}$. We find that:

$$G(\mathcal{I}) \cap \mathbb{C}[z_0] = (\psi^5 - 1)z_0^{16}. \quad (\text{B.3})$$

Suppose we are at a generic point $z_0 \neq 0$, this means that if ψ is not a 5-th root of unity, then the above is not zero, meaning that there are no simultaneous solutions to Q and its Jacobian vanishing. In summary then, Q is smooth so long as $\psi^5 \neq 1$.

B.0.2 Hilbert Series

The Hilbert series is an important quantity that characterises an algebraic variety. It is not a topological invariant in that it depends on the embedding under consideration [7, 8]. For a complex variety M in $\mathbb{C}[x_1, \dots, x_k]$, the Hilbert series is the generating function for the dimensions of the graded pieces:

$$H(t; M) = \sum_{i=0}^{\infty} (\dim_{\mathbb{C}} M_i) t^i, \quad (\text{B.4})$$

where M_i , the i -th graded piece of M can be thought of as the number of independent degree i polynomials on the variety M . The coefficients $\dim_{\mathbb{C}} M_i$ (as a function of i) is known as the [Hilbert function](#).

For example, consider the simplest case of $M = \mathbb{C}$, given as the maximal spectrum $\mathbb{C} = \text{Spec}(\mathbb{C}[x])$, i.e., \mathbb{C} being parametrized by a single complex number x . Clearly, at degree i , there is only a single monomial x^i . Thus, $\dim_{\mathbb{C}} M_i = 1$ for all $i \in \mathbb{Z}_{\geq 0}$ so that the Hilbert series becomes $H(t; \mathbb{C}) = (1 - t)^{-1}$. In general, we have that

$$H(t; \mathbb{C}^n) = (1 - t)^{-n}. \quad (\text{B.5})$$

For multi-graded rings with pieces $X_{\vec{i}}$ and grading $\vec{i} = (i_1, \dots, i_k)$, the Hilbert series takes the form $H(t_1, \dots, t_k; M) = \sum_{\vec{i}=0}^{\infty} \dim_{\mathbb{C}}(X_{\vec{i}}) t_1^{i_1} \dots t_k^{i_k}$ and becomes multi-variate. This is sometimes called refinement [228] and one could “un-refine” it to a univariate Hilbert series by, for instance, setting all $t_k = t$.

A useful property of $H(t)$ is that for algebraic varieties it is always rational

function in t and can be written in two ways:

$$H(t; M) = \begin{cases} \frac{Q(t)}{(1-t)^k}, & \text{Hilbert series of the first kind;} \\ \frac{P(t)}{(1-t)^{\dim(\mathcal{M})}}, & \text{Hilbert series of the second kind.} \end{cases} \quad (\text{B.6})$$

Importantly, both $P(t)$ and $Q(t)$ are polynomials with *integer* coefficients. The powers of the denominators are such that the leading pole captures the dimension of the embedding space and the manifold, respectively.

For a Hilbert series in second form,

$$H(t; M) = \frac{P(1)}{(1-t)^{\dim(M)}} + \dots, \quad P(1) = \text{degree}(M). \quad (\text{B.7})$$

In particular, $P(1)$ always equals the degree of the variety. We recall that when an ideal is described by a single polynomial, the degree of the variety is simply the degree of the polynomial. In the case of multiple polynomials, the degree is a generalisation of this notion: it is the number of points at which a generic line intersects the variety.

In the context of §3.3.2 in the text, one of the important expansions of the Hilbert series is a Laurent expansion about 1. When M is a non-compact Calabi-Yau 3-fold, as a cone over a Sasaki-Einstein base Y . The coefficient of the leading pole in the Laurent expansion can be interpreted as the volume of Y . This volume is in turn related to the central charges of supersymmetric gauge theory (*cf.* [142, 183, 186]).

Molien Series: When M is an orbifold (not necessarily Calabi-Yau), of the form \mathbb{C}^n/G for some finite group G acting on the n coordinates, the Hilbert series is just the Molien [149] series for G :

$$H(t; \mathbb{C}^n/G) = \frac{1}{|G|} \sum_{g \in G} \frac{1}{\det(\mathbb{I} - tg)}, \quad (\text{B.8})$$

where all group elements g are $n \times n$ matrices denoting the action on the coordinates. For reference, we tabulate the Hilbert series for the ADE subgroups

of $SU(2)$;

G	$ G $	Generators	Equation	Molien/Hilbert $HS(t; G)$
\hat{A}_{n-1}	n	$\left\langle \begin{pmatrix} \omega_n & 0 \\ 0 & \omega_n^{-1} \end{pmatrix} \right\rangle$	$uv = w^n$	$\frac{(1+t^n)}{(1-t^2)(1-t^n)}$
\hat{D}_{n+2}	$4n$	$\left\langle \begin{pmatrix} \omega_{2n} & 0 \\ 0 & \omega_{2n}^{-1} \end{pmatrix}, \begin{pmatrix} 0 & i \\ i & 0 \end{pmatrix} \right\rangle$	$u^2 + v^2w = w^{n+1}$	$\frac{(1+t^{2n+2})}{(1-t^4)(1-t^{2n})}$
\hat{E}_6	24	$\langle S, T \rangle$	$u^2 + v^3 + w^4 = 0$	$\frac{1-t^4+t^8}{1-t^4-t^6+t^{10}}$
\hat{E}_7	48	$\langle S, U \rangle$	$u^2 + v^3 + vw^3 = 0$	$\frac{1-t^6+t^{12}}{1-t^6-t^8+t^{14}}$
\hat{E}_8	120	$\langle S, T, V \rangle$	$u^2 + v^3 + w^5 = 0$	$\frac{1+t^2-t^6-t^8-t^{10}+t^{14}+t^{16}}{1+t^2-t^6-t^8-t^{10}-t^{12}+t^{16}+t^{18}}$

(B.9)

where $\omega_n := e^{\frac{2\pi i}{n}}$ and

$$\begin{aligned}
 S &:= \frac{1}{2} \begin{pmatrix} -1+i & -1+i \\ 1+i & -1-i \end{pmatrix}, & T &:= \begin{pmatrix} i & 0 \\ 0 & -i \end{pmatrix}, \\
 U &:= \frac{1}{\sqrt{2}} \begin{pmatrix} 1+i & 0 \\ 0 & 1-i \end{pmatrix}, & V &:= \begin{pmatrix} \frac{i}{2} & \frac{1-\sqrt{5}}{4} - i\frac{1+\sqrt{5}}{4} \\ -\frac{1-\sqrt{5}}{4} - i\frac{1+\sqrt{5}}{4} & -\frac{i}{2} \end{pmatrix}.
 \end{aligned}
 \tag{B.10}$$

Toric Hilbert Series: When M is toric Calabi-Yau n -fold as prescribed by a toric diagram which is a convex lattice polyhedron Δ_{n-1} , its Hilbert series is also easy to compute [183]. The fully refined (multi-graded) version is succinctly obtained from the triangulation of Δ_{n-1} as follows

$$H(t_1, \dots, t_n; M(\Delta_{n-1})) = \sum_{i=1}^r \prod_{j=1}^n (1 - \vec{t}^{\vec{u}_{i,j}})^{-1}, \tag{B.11}$$

Here, the index $i = 1, \dots, r$ runs over the $n - 1$ -dimensional simplices in the (fine, regular, stellar) triangulation and $j = 1, \dots, n$ runs over the faces of

each such simplex. Each $\vec{u}_{i,j}$ is an integer n -vector, being the outer normal to the j -th face of the fan associated to i -th simplex. $\vec{t}^{\vec{u}_{i,j}} := \prod_{a=1}^n t_a^{u_{i,j}^{(a)}}$ multiplied over the a -th component of \vec{u} .

General Case: For a general variety, defined by a polynomial ideal, one first finds the Gröbner basis. Then, the Hilbert function $\dim_{\mathbb{C}} M_i$ is the number of monomials of degree i that are not a multiple of any leading monomial in the Gröbner basis.

The Plethystic Programme: As discussed in the very beginning of Chapter 2, there is an intimate relation between the geometry of representation variety of the quiver and the gauge invariants of the quantum field theory. A so-called plethystic programme [228] was established to harness the Hilbert series of $\mathcal{M}(\mathcal{Q})$ which gave some intriguing properties of the Hilbert series of algebraic varieties in general. We will present some key points as observations since a rigorous treatment is yet to be fully administered. We begin with a few definitions:

DEFINITION 20 *Given a smooth function $f(t)$, its plethystic exponential [16] is the formal series*

$$PE[f(t)] = \exp \left(\sum_{n=1}^{\infty} \frac{f(t^n) - f(0)}{n} \right) .$$

One can readily check from this definition by direct manipulation of the series expansions (assuming reasonable regions of convergence), that

PROPOSITION 7 *If $f(t)$ has Taylor series $f(t) = \sum_{n=0}^{\infty} a_n t^n$, then*

- *There is an Euler-type product formula*

$$g(t) = PE[f(t)] = \prod_{n=1}^{\infty} (1 - t^n)^{-a_n} ;$$

- There is explicit inverse (called plethystic logarithm) such that

$$f(t) = PE^{-1}(g(t)) = \sum_{k=1}^{\infty} \frac{\mu(k)}{k} \log(g(t^k))$$

In the above, $\mu(k)$ is the standard Möbius function for $k \in \mathbb{Z}_+$ which is 0 if k has repeated prime factors and is $(-1)^n$ if k factorizes into n distinct primes (also with the convention that $\mu(1) = 1$). From the physical perspective, the plethystic exponential relates single-trace to multi-trace operators in the gauge theory, as mentioned in the dictionary between quiver representation and supersymmetric gauge theory in §3.1.1.

Now, let us apply this formalism to a Hilbert series $H(t; M)$ (whose Taylor coefficients are by definition non-negative integers):

OBSERVATION 1 *Given Hilbert series $H(t; M)$ of an algebraic variety M , the plethystic logarithm is of the form*

$$PE^{-1}[H(t; M)] = b_1 t + b_2 t^2 + b_3 t^3 + \dots$$

where all $b_n \in \mathbb{Z}$ and a positive b_n corresponds to a generator in coordinate ring of M and a negative b_n , a relation. In particular, if M is complete intersection, then $PE^{-1}[H(t; M)]$ is a finite polynomial.

For example, our quadric hypersurface \mathcal{C} in \mathbb{C}^4 from (3.23) has Hilbert series

$$H(t; \mathcal{C}) = (1 - t^2)/(1 - t)^4 = \sum_{n=0}^{\infty} (n + 1)^2 t^n, \quad (\text{B.12})$$

which can be obtained from (B.11) because \mathcal{C} is a toric variety. One checks that

$$PE^{-1}[H(t; \mathcal{C})] = 4t - t^2, \quad (\text{B.13})$$

meaning that there are 4 generators in degree 1 (corresponding to the 4 complex coordinates of \mathbb{C}^4) with 1 relation at degree 2 (meaning that \mathcal{C} is a single quadratic hypersurface, and hence complete intersection, in \mathbb{C}^4). Thus,

one could have retrieve this Hilbert series by simply writing down $4t - t^2$ and taking the plethystic exponential.

On the other hand, for $\text{Cone}(dP_0) = \mathbb{C}^3/(\mathbb{Z}/3\mathbb{Z})$, the Hilbert series is the Molien series

$$H(t; \mathbb{C}^3/(\mathbb{Z}/3\mathbb{Z})) = \frac{1 + 7t + t^2}{(1 - t)^3} = \sum_{n=0}^{\infty} \frac{1}{2}(2 + 9n + 9n^2)t^n, \quad (\text{B.14})$$

and its plethystic logarithm is

$$PE^{-1}[H(t; \mathbb{C}^3/(\mathbb{Z}/3\mathbb{Z}))] = 1 + 10t + 28t^2 + 55t^3 + 91t^4 + 136t^5 + 190t^6 + \dots \quad (\text{B.15})$$

which is non-terminating, in congruence with the fact that the variety, as discussed in §3.3.1, is not complete intersection. While for these examples, it seems PE^{-1} only terminates for complete intersections, but how one might disentangle positive and negative contributions to each b_n is, as far as we are aware, not in general known.

Appendix C

Brane Tilings

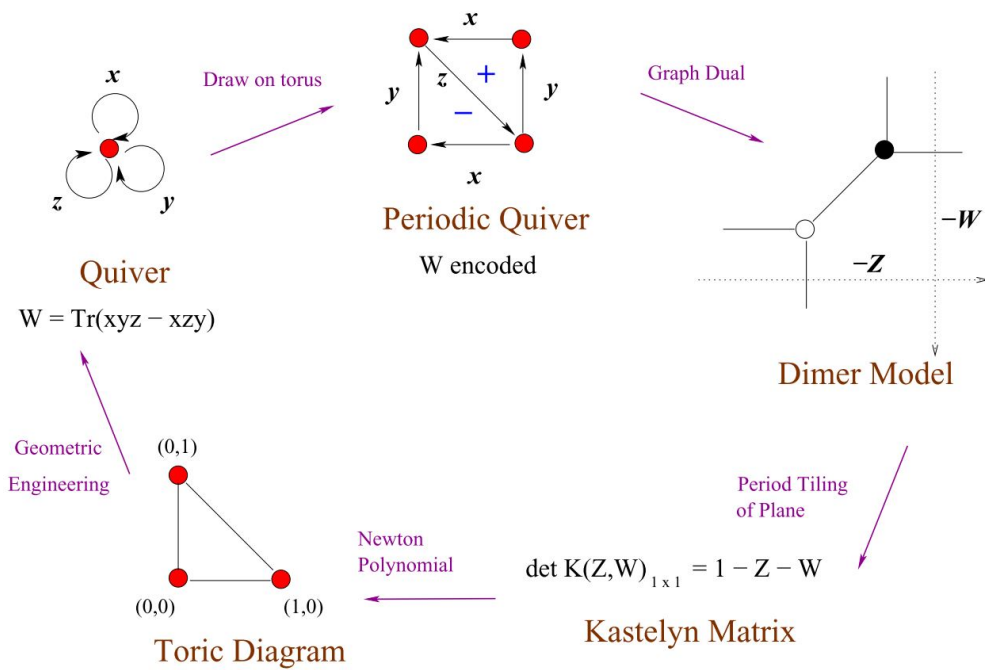


Figure C.1: The web of correspondences of the quiver, bipartite graph and toric Calabi-Yau moduli space for \mathbb{C}^3 .

In this brief appendix, we give a summary diagram of some of the interconnections in the quiver-bipartite tiling-toric Calabi-Yau correspondence.

In Figure C.1, we present the quiver with superpotential for $\mathcal{N} = 4$ super-Yang-Mills theory, whose moduli space of representations trivially the non-compact toric Calabi-Yau 3-fold \mathbb{C}^3 . This can be encoded into a single periodic quiver with the plus/minus term of the superpotential captured by the anti-clockwise/clockwise 3-cycles and identifying the 4 nodes into 1. Subsequently, this can be graph-dualized to a trivalent bipartite graph on T^2 as the dimer model/brane-tiling. The perfect matchings of a dimer model can be found by the Kastyleyn matrix whose determinant, as a bivariate polynomial, is exactly the Newton polynomial for the toric diagram for \mathbb{C}^3 .

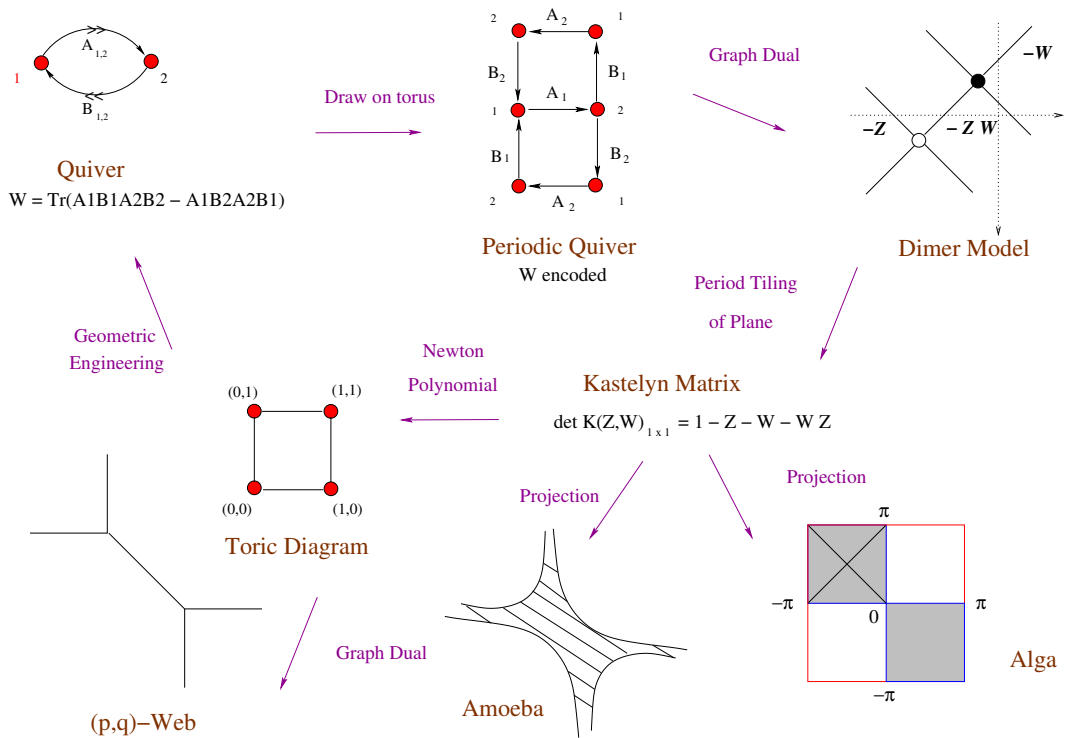


Figure C.2: The web of correspondences of the quiver, bipartite graph and toric Calabi-Yau moduli space for \mathcal{C} .

Likewise in Figure C.2, we present the same for the conifold, the quadric hypersurface in \mathbb{C}^4 , which is also a local toric Calabi-Yau 3-fold. We have also added the two projections of the Newton polynomial, the so-called amoeba and alga (co-amoeba) projections. The reader is referred to the brief lecture [181] as well as the excellent monographs [210, 211] for further details.

Bibliography

- [1] Shing-Tung Yau and Steve Nadis, *Shape of Inner Space: String Theory and the Geometry of the Universe's Hidden Dimension*, Basic Books, Peseus, 2012, ISBN-13: 978-0465028375
- [2] Brian Greene, *The Elegant Universe: Superstrings, Hidden Dimensions, and the Quest for the Ultimate Theory*, Norton & Company, 2003, ISBN 0-393-05858-1
- [3] T. Hubsch, *Calabi-Yau manifolds: A Bestiary for physicists*, World Scientific, 1994, ISBN 9810206623
- [4] Shing-Tung Yau, “A survey of Calabi–Yau manifolds”, *Geometry, analysis, and algebraic geometry: forty years of the Journal of Differential Geometry*, Surveys in Differential Geometry, 13, Somerville, MA, Int. Press, pp. 277–318, (2009).
- [5] M. Gross, D. Huybrechts, and D. Joyce, *Calabi-Yau Manifolds and Related Geometries*, Springer, Universitext 2003, ISBN 978-3-642-19004-9
- [6] R. Laza, M. Schütt, and N. Yui, *Calabi-Yau Varieties: Arithmetic, Geometry and Physics*, Springer 2015, ISBN 978-1-4939-2830-9
- [7] D. Cox, J. Little, D. O’Shea, *Ideals, Varieties, and Algorithms, An Introduction to Computational Algebraic Geometry and Commutative Algebra*, Springer 2007, ISBN 978-0-387-35651-8;
–, *Using Algebraic Geo*, Springer, GTM185 , ISBN 978-0-387-20706-3

- [8] H. Schenck, *Computational algebraic geometry*, CUP, 2003. ISBN: 9780521536509
- [9] Yang-Hui He, Philip Candelas, Amihay Hanany, Andre Lukas, and Burt Ovrut, Ed. *Computational algebraic geometry in string and gauge theory*, Hindawi, Special Vol, 2012, ISBN 1687-7357
- [10] J. Davenport et al., “Machine-Assisted Proofs (ICM 2018 Panel)”, arXiv:1809.08062 [math.HO]
- [11] J. Conlon, “Why String Theory”, CRC, 2015, ISBN 9781482242478
- [12] Miles Reid, “Undergraduate Algebraic Geometry”, LMS Student Texts 12, CUP 1989.
- [13] Robin Hartshorne, “Algebraic Geometry”, GTM, Springer 1997, ISBN 13: 9780387902449.
- [14] Philip Griffiths, Joe Harris, “Principles of Algebraic Geometry”, Wiley, NY, 1978, ISBN 0471327921
- [15] Michael Artin, “Algebra”, Boston: Pearson Education. 2011.
- [16] William Fulton and Joe Harris, *Representation Theory, A First Course*, GTM 129, Springer-Verlag ISBN 978-0-387-97495-8 (1991).
- [17] W. Fulton, *Intersection Theory*, Springer 1998, ISBN 978-1-4612-1700-8.
- [18] W. Fulton, “Introduction to Toric Varieties”, AM-131, PUP 1993, 978-1-4008-8252-6.
- [19] D.A.Cox, H.K.Schenck, J.Little *Toric Varieties*, AMS 2011, ISBN-13: 978-0-8218-4819-7
- [20] P. Candelas, “Lectures On Complex Manifolds,” in *Trieste 1987, proceedings, superstrings '87*, pp1-88.
- [21] V. Bouchard, “Lectures on complex geometry, Calabi-Yau manifolds and toric geometry,” hep-th/0702063 [HEP-TH].

- [22] C. Closset, “Toric geometry and local Calabi-Yau varieties: An Introduction to toric geometry (for physicists),” arXiv:0901.3695 [hep-th].
- [23] G. Ewald, “Combinatorial Convexity and Algebraic Geometry”, Springer, ISBN 978-0-387-94755-6 (1996)
B. Sturmfels, “Gröbner Bases and Convex Polytopes”, AMS, ISBN: 978-0-8218-0487-2 (1996)
- [24] Green, M. B.; Schwarz, J. H.; Witten, E., Superstring Theory. Vol. 1&2, Cambridge Monographs on Mathematical Physics, 1987.
- [25] Burchard de Mont Sion, “Prologus (sive Descriptiones) Terrae Sanctae” (1283); in *Rudimentum Noviciorum*, Brandis, Lübeck, 1475.
- [26] Dean Rickles, “A Brief History of String Theory: From Dual Models to M-Theory”, Springer, 2014, ISBN-13: 978-3642451270.
- [27] Kentaro Hori, Sheldon Katz, Albrecht Klemm, Rahul Pandharipande, Richard Thomas, Cumrun Vafa, Ravi Vakil, Eric Zaslow, *Mirror Symmetry*, AMS 2000, ISBN 0-8218-2955-6.
- [28] Sheldon Katz, *Enumerative Geometry and String Theory*, AMS SML Vol 32, 2006, ISBN: 978-0-8218-3687-3.
- [29] Calabi, Eugenio, “The space of Kähler metrics”, Proc. Internat. Congress Math. Amsterdam, 2, pp. 206 - 207 (1954)
– “On Kähler manifolds with vanishing canonical class”, in Fox, Spencer, Tucker, *Algebraic geometry and topology. A symposium in honor of S. Lefschetz*, Princeton Mathematical Series, 12, PUP, pp. 78 - 89 (1957).
- [30] S.-T. Yau, “Calabi’s conjecture and some new results in algebraic geometry,” Proc. Nat. Acad., USA, 74 (5), pp 1798-9, (1977)
–, “On the Ricci curvature of a compact Kähler manifold and the complex Monge-Ampère equation I”, Comm. Pure and Applied Maths, 31 (3), pp 339-411, (1978).

- [31] Berger, M., “Sur les groupes d’holonomie homogènes des variétés à connexion affines et des variétés riemanniennes”, *Bull. Soc. Math. France*, 83: 279 - 330, (1953)
- [32] D. Grayson, M. Stillman, “Macaulay2, a software system for research in algebraic geometry”, Available at <https://faculty.math.illinois.edu/Macaulay2/>
- [33] Decker, W.; Greuel, G.-M.; Pfister, G.; Schönemann, H.: SINGULAR 4-1-1 — A computer algebra system for polynomial computations. <http://www.singular.uni-kl.de> (2018).
- [34] J. Hauenstein, A. Sommese, C. Wampler, “Bertini: Software for Numerical Algebraic Geometry”, www.nd.edu/~sommese/bertini
- [35] The GAP Group, *GAP – Groups, Algorithms, and Programming, Version 4.9.2*; 2018, <https://www.gap-system.org>
- [36] J. Conway et al., “ATLAS of finite groups”, OUP 2003, ISBN 978-0-19-853199-9.
R. Wilson et al. “ATLAS of finite group representations”, <http://brauer.maths.qmul.ac.uk/Atlas/v3/>
- [37] Magma Comp. Algebra System, <http://magma.maths.usyd.edu.au/>
- [38] SageMath, “the Sage Mathematics Software System”, The Sage Developers, <http://www.sagemath.org>
- [39] Wolfram Research, Inc., *Mathematica*, Champaign, IL (2018). www.wolfram.com
- [40] Y.-H. He and D. Mehta (Organizers), “Applications of Computational and Numerical Algebraic Geometry to Theoretical Physics,” SIAM Conference on Applied Algebraic Geometry, Colorado, 2013;
Y.-H. He, R.-K. Seong, M. Stillman. “Applications of Computational Algebraic Geometry to Theoretical Physics”, SIAM AG, Daejeon, 2015.
- [41] T. W. Dubé, “The Structure of Polynomial Ideals and Gröbner Bases,” *SIAM Journal of Computing*, 19(4):750 – 773, 1990.

- [42] The Graded Ring Database, <http://www.grdb.co.uk/>
The C^3 NG collaboration: <http://geometry.ma.ic.ac.uk/3CinG/index.php/team-members-and-collaborators/> Data at: <http://geometry.ma.ic.ac.uk/3CinG/index.php/data/> <http://coates.ma.ic.ac.uk/fanosearch/>
- [43] The Knots Atlas, http://katlas.org/wiki/Main_Page
- [44] The L-functions & Modular Forms Database, <http://www.lmfdb.org/>
- [45] P. Candelas, A. M. Dale, C. A. Lutken, R. Schimmrigk, “Complete Intersection Calabi-Yau Manifolds,” Nucl. Phys. B **298**, 493 (1988).
- [46] P. Candelas, C. A. Lutken, R. Schimmrigk, “Complete Intersection Calabi-Yau Manifolds. 2. Three Generation Manifolds,” Nucl. Phys. B **306**, 113 (1988).
- [47] M. Gagnon, Q. Ho-Kim, “An Exhaustive list of complete intersection Calabi-Yau manifolds,” Mod. Phys. Lett. A **9** (1994) 2235.
- [48] P. S. Green, T. Hubsch, C. A. Lutken, “All Hodge Numbers of All CICY Manifolds,” Class. Quant. Grav. **6**, 105 (1989).
- [49] L. B. Anderson, Y. H. He and A. Lukas, “Heterotic Compactification, An Algorithmic Approach,” JHEP **0707**, 049 (2007) [hep-th/0702210].
- [50] L. B. Anderson, Y. H. He and A. Lukas, “Monad Bundles in Heterotic String Compactifications,” JHEP **0807**, 104 (2008) [arXiv:0805.2875].
- [51] Links to CICY, Monads, and StringVacua Package: http://www-thphys.physics.ox.ac.uk/people/AndreLukas/Site/Andre_Lukas.html
- [52] J. Gray, Y. H. He, A. Ilderton and A. Lukas, “STRINGVACUA: A Mathematica Package for Studying Vacuum Configurations in String Phenomenology,” Comput. Phys. Commun. **180**, 107 (2009) [arXiv:0801.1508 [hep-th]]. <http://www-thphys.physics.ox.ac.uk/projects/Stringvacua/>

- [53] C. T. C. Wall, “Classification problem in Differential Topology, V: on certain 6-manifolds.” *Invent. Math.* **1** (1966) 355.
- [54] J. W. Milnor, “On simply-connected 4-manifolds ”, *Symposium International de Topologia Algebraica*, Mexico (1958), 122 - 128.
- [55] S.Coughlan, L.Golebiowski, G.Kapustka, M.Kapustka, “Arithmetically Gorenstein Calabi-Yau threefolds in P⁷”, arXiv:1609.01195 [math.AG]
- [56] V. Braun, “On Free Quotients of Complete Intersection Calabi-Yau Manifolds,” *JHEP* **1104**, 005 (2011) [arXiv:1003.3235 [hep-th]].
- [57] B. R. Greene, K. H. Kirklin, P. J. Miron and G. G. Ross, “A Superstring Inspired Standard Model,” *Phys. Lett. B* **180**, 69 (1986).
- [58] C. Schoen, “On fiber products of rational elliptic surfaces with section”, *Math. Z.* **197** (1988) 177-199.
- [59] Victor V. Batyrev, Lev A. Borisov “On Calabi-Yau Complete Intersections in Toric Varieties”, arXiv:alg-geom/9412017
- [60] M. Kreuzer and H. Skarke, “On the classification of reflexive polyhedra,” *Commun. Math. Phys.* **185**, 495 (1997) [hep-th/9512204].
–, “Reflexive polyhedra, weights and toric Calabi-Yau fibrations,” *Rev. Math. Phys.* **14**, 343 (2002) [math/0001106 [math-ag]].
- [61] A. C. Avram, M. Kreuzer, M. Mandelberg and H. Skarke, “The Web of Calabi-Yau hypersurfaces in toric varieties,” *Nucl. Phys. B* **505**, 625 (1997) [hep-th/9703003].
- [62] M. Kreuzer and H. Skarke, “Classification of reflexive polyhedra in three-dimensions,” *Adv. Theor. Math. Phys.* **2**, 853 (1998) [hep-th/9805190].
- [63] M. Kreuzer and H. Skarke, “Complete classification of reflexive polyhedra in four-dimensions,” *Adv. Theor. Math. Phys.* **4**, 1209 (2002) [hep-th/0002240].
- [64] R. Altman, J. Gray, Y. H. He, V. Jejjala and B. D. Nelson, “A Calabi-Yau Database: Threefolds Constructed from the Kreuzer-Skarke List,” *JHEP* **1502**, 158 (2015) [arXiv:1411.1418 [hep-th]].

- [65] J. L. Bourjaily, Y. H. He, A. J. McLeod, M. Von Hippel and M. Wilhelm, “Traintracks Through Calabi-Yaus: Amplitudes Beyond Elliptic Polylogarithms,” arXiv:1805.09326 [hep-th].
- [66] J. L. Bourjaily, A. J. McLeod, M. von Hippel and M. Wilhelm, “A (Bounded) Bestiary of Feynman Integral Calabi-Yau Geometries,” arXiv:1810.07689 [hep-th].
- [67] M. Kreuzer and H. Skarke, “PALP: A Package for analyzing lattice polytopes with applications to toric geometry,” *Comput. Phys. Commun.* **157** (2004) 87 [math/0204356 [math.NA]].
- [68] A. P. Braun, J. Knapp, E. Scheidegger, H. Skarke and N. O. Walliser, “PALP - a User Manual,” arXiv:1205.4147 [math.AG].
- [69] P. Candelas, M. Lynker, R. Schimmrigk, “Calabi-Yau Manifolds in Weighted $P(4)$,” *Nucl. Phys. B* **341**, 383 (1990).
- [70] P. Candelas, X. de la Ossa and S. H. Katz, “Mirror symmetry for Calabi-Yau hypersurfaces in weighted P^{*4} and extensions of Landau-Ginzburg theory,” *Nucl. Phys. B* **450**, 267 (1995) [hep-th/9412117].
- [71] Antonella Grassi, “Minimal Models of Elliptic Threefolds”, (Duke PhD Thesis, 1990), *Math. Ann.* 290 (1991) 287301.
- [72] Mark Gross, “A finiteness theorem for elliptic Calabi-Yau threefolds”, *Duke Math. J.*, 74, 2 (1994), 271 - 299.
- [73] I. Dolgachev, M. Gross, “Elliptic Three-folds I: Ogg-Shafarevich Theory”, arXiv:alg-geom/9210009
- [74] R. Y. Donagi, “Principal bundles on elliptic fibrations,” *Asian J. Math* **1**, 214 (1997) [alg-geom/9702002].
- [75] R. Friedman, J. W. Morgan, E. Witten, “Vector bundles over elliptic fibrations” alg-geom/9709029.
- [76] M. F. Atiyah, “Vector bundles over an elliptic curve,” *Proc. LMS* (3) **7** (1957), 414 - 452.

- [77] D. R. Morrison and C. Vafa, “Compactifications of F theory on Calabi-Yau threefolds. 1 & 2,” Nucl. Phys. B **473**, 74 & **476**, 437 (1996) [hep-th/9602114], [hep-th/9603161].
- [78] R. Friedman, J. Morgan and E. Witten, “Vector bundles and F theory,” Commun. Math. Phys. **187**, 679 (1997) [hep-th/9701162].
- [79] T. Weigand, “TASI Lectures on F-theory,” arXiv:1806.01854 [hep-th].
- [80] L. B. Anderson, X. Gao, J. Gray and S. J. Lee, “Fibrations in CICY Threefolds,” JHEP **1710**, 077 (2017) [arXiv:1708.07907 [hep-th]].
L. B. Anderson, J. Gray and B. Hammack, “Fibrations in Non-simply Connected Calabi-Yau Quotients,” JHEP **1808**, 128 (2018) [arXiv:1805.05497 [hep-th]].
- [81] Y. C. Huang and W. Taylor, “On the prevalence of elliptic and genus one fibrations among toric hypersurface Calabi-Yau threefolds,” arXiv:1809.05160 [hep-th].
–, “Comparing elliptic and toric hypersurface Calabi-Yau threefolds at large Hodge numbers,” arXiv:1805.05907 [hep-th].
W. Taylor and Y. N. Wang, “Non-toric bases for elliptic Calabi-Yau threefolds and 6D F-theory vacua,” Adv. Theor. Math. Phys. **21**, 1063 (2017) [arXiv:1504.07689 [hep-th]].
- [82] A. Grassi, D. R. Morrison, “Group representations and the Euler characteristic of elliptically fibered Calabi-Yau threefolds,” math/0005196 [math-ag].
W. Taylor, “On the Hodge structure of elliptically fibered Calabi-Yau threefolds,” JHEP **1208**, 032 (2012) [arXiv:1205.0952 [hep-th]].
- [83] A. Iqbal, A. Neitzke and C. Vafa, “A Mysterious duality,” Adv. Theor. Math. Phys. **5**, 769 (2002) [hep-th/0111068].
- [84] V. Batyrev, I. Ciocan-Fontanine, B. Kim and D. van Straten, “Conifold transitions and mirror symmetry for Calabi-Yau complete intersections in Grassmannians,” Nucl. Phys. B 514 (1998), no. 3, 640 - 666.
–, “Mirror symmetry and toric degenerations of partial flag manifolds,”

- Acta Math. 184 (2000), no. 1, 1 - 39.”
M. I. Qureshi, B. Szendroi, “Calabi-Yau threefolds in weighted flag varieties” arXiv:1105.4282 [math.AG]
- [85] Charles F. Doran and Ursula A. Whitcher, “From Polygons to String Theory”, Mathematics Magazine Vol. 85, No. 5, pp. 343-359
- [86] B.Nill, “Gorenstein toric Fano varieties”, [math/0405448].
- [87] G.Ewald, “On the classification of toric fano varieties”, Discrete & Computational Geometry 3 (1988) 49-54.
K.Watanabe, M.Watanabe, “The classification of fano 3-folds with torus embeddings”, Tokyo J. of Math. 05 (06, 1982) 37-48.
V.V.Batyrev, “Toroidal fano 3-folds”, Maths of the USSR-Izvestiya 19 (1982) 13.
- [88] V.V.Batyrev and L.A.Borisov, “On Calabi-Yau complete intersections in toric varieties”, alg-geom/9412017.
V. V. Batyrev, “Dual polyhedra and mirror symmetry for Calabi-Yau hypersurfaces in toric varieties”, J. Alg. Geom. 3 (1994) 493 - 545, [alg-geom/9310003].
- [89] B. Poonen, F. Rodriguez-Villegas, “Lattice Polygons and the Number 12”, Amer. Math. Monthly, Vol. 107, No. 3, 2000, pp. 238-250.
- [90] A. P. Braun and N. O. Walliser, “A New offspring of PALP,” arXiv:1106.4529 [math.AG].
A. P. Braun, J. Knapp, E. Scheidegger, H. Skarke and N. O. Walliser, “PALP - a User Manual,” arXiv:1205.4147 [math.AG].
- [91] V.V Batyrev, “Dual polyhedra and mirror symmetry for Calabi-Yau hypersurfaces in toric varieties,” J. Alg. Geom. 3, 493 (1994) [alg-geom/9310003].
- [92] M.Kreuzer and B.Nill, “Classification of toric fano 5-folds”, arXiv:math/0702890.
M. Oebro, “An algorithm for the classification of smooth Fano polytopes”, arXiv:0704.0049.

- T.Bogart, C.Haase, M.Hering, B.Lorenz, B.Nill, A.Paffenholz, G.Rote, F.Santos, H.Schenck, “Few smooth d-polytopes with n lattice points”, Israel J. Math., April 2015, Volume 207, Issue 1, pp 301-329, arXiv:1010.3887
- [93] Andreas Paffenholz, “polyDB: A Database for Polytopes and Related Objects”, arXiv:1711.02936
- [94] Y. H. He, S. J. Lee and A. Lukas, “Heterotic Models from Vector Bundles on Toric Calabi-Yau Manifolds,” JHEP **1005**, 071 (2010) [arXiv:0911.0865 [hep-th]].
- [95] Y. H. He, M. Kreuzer, S. J. Lee and A. Lukas, “Heterotic Bundles on Calabi-Yau Manifolds with Small Picard Number,” JHEP **1112**, 039 (2011) [arXiv:1108.1031 [hep-th]].
- [96] F. Schaller and H. Skarke, “All Weight Systems for Calabi-Yau Fourfolds from Reflexive Polyhedra,” arXiv:1808.02422 [hep-th].
cf. also M. Kreuzer, “On the Statistics of Lattice Polytopes,” Proc. “Information Theory and Statistical Learning”, WORLDCOMP’08, Las Vegas, July 14-15,2008 [arXiv:0809.1188 [math.AG]].
- [97] J. Gray, Y. H. He, V. Jejjala, B. Jurke, B. D. Nelson and J. Simon, “Calabi-Yau Manifolds with Large Volume Vacua,” Phys. Rev. D **86**, 101901 (2012) [arXiv:1207.5801 [hep-th]].
- [98] M. Demirtas, C. Long, L. McAllister and M. Stillman, “The Kreuzer-Skarke Axiverse,” arXiv:1808.01282 [hep-th].
- [99] Y. H. He, “Calabi-Yau Geometries: Algorithms, Databases, & Physics,” Int. J. Mod. Phys. A **28**, 1330032 (2013) [arXiv:1308.0186].
- [100] Y. H. He, V. Jejjala and L. Pontiggia, “Patterns in CalabiYau Distributions,” Commun. Math. Phys. **354**, no. 2, 477 (2017) doi:10.1007/s00220-017-2907-9 [arXiv:1512.01579 [hep-th]].
- [101] S. B. Johnson and W. Taylor, “Calabi-Yau threefolds with large $h^{2,1}$,” JHEP **1410**, 23 (2014) doi:10.1007/JHEP10(2014)023 [arXiv:1406.0514 [hep-th]].

- [102] P. Candelas, A. Constantin and H. Skarke, “An Abundance of K3 Fibrations from Polyhedra with Interchangeable Parts,” *Commun. Math. Phys.* **324**, 937 (2013) [arXiv:1207.4792 [hep-th]].
- [103] P. Candelas, R. Davies, “New Calabi-Yau Manifolds with Small Hodge Numbers,” *Fortsch. Phys.* **58**, 383 (2010) [arXiv:0809.4681 [hep-th]].
V. Braun, P. Candelas and R. Davies, “A Three-Generation Calabi-Yau Manifold with Small Hodge Numbers,” *Fortsch. Phys.* **58**, 467 (2010) [arXiv:0910.5464 [hep-th]].
- [104] P. Candelas, A. Constantin and C. Mishra, “CalabiYau Threefolds with Small Hodge Numbers,” *Fortsch. Phys.* **66**, no. 6, 1800029 (2018) [arXiv:1602.06303 [hep-th]].
- [105] J. Polchinski, “Dirichlet Branes and Ramond-Ramond charges,” *Phys. Rev. Lett.* **75**, 4724 (1995) [hep-th/9510017].
- [106] M. Atiyah and E. Witten, “M theory dynamics on a manifold of G(2) holonomy,” *Adv. Theor. Math. Phys.* **6**, 1 (2003) [hep-th/0107177].
- [107] I. Brunner, M. Lynker and R. Schimmrigk, “Unification of M theory and F theory Calabi-Yau fourfold vacua,” *Nucl. Phys. B* **498**, 156 (1997) [hep-th/9610195].
A. Klemm, B. Lian, S. S. Roan and S. T. Yau, “Calabi-Yau fourfolds for M theory and F theory compactifications,” *Nucl. Phys. B* **518**, 515 (1998) [hep-th/9701023].
- [108] J. M. Maldacena, “The Large N limit of superconformal field theories and supergravity,” *Int. J. Theor. Phys.* **38**, 1113 (1999) [*Adv. Theor. Math. Phys.* **2**, 231 (1998)] [hep-th/9711200].
- [109] L. Randall and R. Sundrum, “An Alternative to compactification,” *Phys. Rev. Lett.* **83**, 4690 (1999) [hep-th/9906064].
- [110] P. Candelas, G. T. Horowitz, A. Strominger and E. Witten, “Vacuum Configurations for Superstrings,” *Nucl. Phys. B* **258**, 46 (1985).

- [111] D. J. Gross, J. A. Harvey, E. J. Martinec and R. Rohm, “The Heterotic String,” *Phys. Rev. Lett.* **54**, 502 (1985).
- [112] X. de la Ossa, M. Larfors and E. E. Svanes, “Exploring $SU(3)$ structure moduli spaces with integrable G_2 structures,” *Adv. Theor. Math. Phys.* **19**, 837 (2015) [arXiv:1409.7539 [hep-th]].
- [113] A. Strominger, “Superstrings with Torsion,” *Nucl. Phys. B* **274**, 253 (1986).
- [114] J. Li and S.-T. Yau, “The Existence of Supersymmetric String Theory with Torsion”, *J. Differential Geom.* Vol 70, Number 1 (2005), 143-181.
- [115] The Particle Data Group, cf. <http://pdg.lbl.gov/>
- [116] P. Candelas, X. de la Ossa, Y. H. He and B. Szendroi, “Triadophilia: A Special Corner in the Landscape,” *Adv. Theor. Math. Phys.* **12**, 429 (2008) [arXiv:0706.3134 [hep-th]].
- [117] Y. H. He, V. Jejjala, C. Matti, B. D. Nelson and M. Stillman, “The Geometry of Generations,” *Commun. Math. Phys.* **339**, no. 1, 149 (2015) [arXiv:1408.6841 [hep-th]].
- [118] R. Donagi, B. A. Ovrut, T. Pantev and D. Waldram, “Standard models from heterotic M theory,” *Adv. Theor. Math. Phys.* **5**, 93 (2002) [hep-th/9912208].
–, “Standard model bundles on nonsimply connected Calabi-Yau threefolds,” *JHEP* **0108**, 053 (2001) [hep-th/0008008].
–, “Standard model bundles,” *Adv. Theor. Math. Phys.* **5**, 563 (2002) [math/0008010 [math-ag]].
E. Buchbinder, R. Donagi and B. A. Ovrut, “Vector bundle moduli and small instanton transitions,” *JHEP* **0206**, 054 (2002) [hep-th/0202084].
R. Donagi, B. A. Ovrut, T. Pantev and R. Reinbacher, “ $SU(4)$ instantons on Calabi-Yau threefolds with $Z(2) \times Z(2)$ fundamental group,” *JHEP* **0401**, 022 (2004) [hep-th/0307273].
- [119] R. Donagi, Y. H. He, B. A. Ovrut, R. Reinbacher, “Particle spectrum of heterotic compactifications,” *JHEP* **0412**, 054 (2004) [hep-th/0405014].

- [120] Y. H. He, “An Algorithmic Approach to Heterotic String Phenomenology,” *Mod. Phys. Lett. A* **25**, 79 (2010) [arXiv:1001.2419 [hep-th]].
- [121] V. Braun, Y. H. He, B. A. Ovrut and T. Pantev, “A Heterotic standard model,” *Phys. Lett. B* **618**, 252 (2005) [hep-th/0501070].
V. Braun, Y. H. He, B. A. Ovrut and T. Pantev, “The Exact MSSM spectrum from string theory,” *JHEP* **0605**, 043 (2006) [hep-th/0512177].
V. Bouchard and R. Donagi, “An SU(5) heterotic standard model,” *Phys. Lett. B* **633**, 783 (2006) [hep-th/0512149].
- [122] M. Gabella, Y. H. He and A. Lukas, “An Abundance of Heterotic Vacua,” *JHEP* **0812**, 027 (2008) [arXiv:0808.2142 [hep-th]].
- [123] V. Braun, P. Candelas and R. Davies, “A Three-Generation Calabi-Yau Manifold with Small Hodge Numbers,” *Fortsch. Phys.* **58**, 467 (2010) [arXiv:0910.5464 [hep-th]].
L. B. Anderson, J. Gray, Y. H. He and A. Lukas, “Exploring Positive Monad Bundles And A New Heterotic Standard Model,” *JHEP* **1002**, 054 (2010) [arXiv:0911.1569 [hep-th]].
V. Braun, P. Candelas, R. Davies and R. Donagi, “The MSSM Spectrum from (0,2)-Deformations of the Heterotic Standard Embedding,” *JHEP* **1205**, 127 (2012) [arXiv:1112.1097 [hep-th]].
- [124] L. B. Anderson, J. Gray, A. Lukas and E. Palti, “Two Hundred Heterotic Standard Models on Smooth Calabi-Yau Threefolds,” *Phys. Rev. D* **84**, 106005 (2011) [arXiv:1106.4804 [hep-th]].
–, “Heterotic Line Bundle Standard Models,” *JHEP* **1206**, 113 (2012) [arXiv:1202.1757 [hep-th]].
–, “Heterotic standard models from smooth Calabi-Yau three-folds,” *PoS CORFU* **2011**, 096 (2011).
A. Constantin and A. Lukas, “Formulae for Line Bundle Cohomology on Calabi-Yau Threefolds,” arXiv:1808.09992 [hep-th].
- [125] F. Gmeiner, R. Blumenhagen, G. Honecker, D. Lust and T. Weigand, “One in a billion: MSSM-like D-brane statistics,” *JHEP* **0601**, 004 (2006) [hep-th/0510170].

- [126] M. R. Douglas, “The Statistics of string / M theory vacua,” JHEP **0305**, 046 (2003) [hep-th/0303194].
K. R. Dienes, M. Lennek, D. Senechal and V. Wasnik, “Supersymmetry versus Gauge Symmetry on the Heterotic Landscape,” Phys. Rev. D **75**, 126005 (2007) [arXiv:0704.1320 [hep-th]].
K. R. Dienes, “Statistics on the heterotic landscape: Gauge groups and cosmological constants of four-dimensional heterotic strings,” Phys. Rev. D **73**, 106010 (2006) [hep-th/0602286].
D. Lust, “The landscape of string theory (orientifolds and their statistics, D-brane instantons, AdS(4) domain walls and black holes),” Fortsch. Phys. **56**, 694 (2008).
J. J. Heckman, “Statistical Inference and String Theory,” Int. J. Mod. Phys. A **30**, no. 26, 1550160 (2015) [arXiv:1305.3621 [hep-th]].
- [127] A. Constantin, Y. H. He and A. Lukas, “Counting String Theory Standard Models,” arXiv:1810.00444 [hep-th].
- [128] S. Kachru, R. Kallosh, A. D. Linde and S. P. Trivedi, “De Sitter vacua in string theory,” Phys. Rev. D **68**, 046005 (2003) [hep-th/0301240].
- [129] J. Halverson, C. Long and B. Sung, “Algorithmic universality in F-theory compactifications,” Phys. Rev. D **96**, no. 12, 126006 (2017) [arXiv:1706.02299 [hep-th]].
J. Carifio, W. J. Cunningham, J. Halverson, D. Krioukov, C. Long and B. D. Nelson, “Vacuum Selection from Cosmology on Networks of String Geometries,” Phys. Rev. Lett. **121**, no. 10, 101602 (2018) [arXiv:1711.06685 [hep-th]].
J. Halverson and F. Ruehle, “Computational Complexity of Vacua and Near-Vacua in Field and String Theory,” arXiv:1809.08279 [hep-th].
- [130] P. Candelas, X. de la Ossa and F. Rodriguez-Villegas, “Calabi-Yau manifolds over finite fields. 1 & 2,” hep-th/0012233; Fields Inst. Commun. **38**, 121 (2013) [hep-th/0402133].
- [131] A. Beauville, “Complex Alg. Surfaces”, LMS. Texts, 34, CUP, 1996.
- [132] Matthias Schuett, “Arithmetic of K3 surfaces”, arXiv:0808.1061.

- [133] P. S. Aspinwall, “K3 surfaces and string duality,” in Yau, S.T. (ed.): *Differential geometry inspired by string theory* pp1-95 [hep-th/9611137].
- [134] A. King, “Moduli of representations of finite-dimensional algebras”, *Quart. J. Math.*, 45 (180): 515 – 530.
- [135] H. Nakajima, “Instantons on ALE spaces, quiver varieties, and Kac-Moody algebras”, *Duke Math. J.* 76 (1994), 365 – 416.
- [136] C. Okonek, A. Teleman, “Master Spaces and the Coupling Principle: From Geometric Invariant Theory to Gauge Theory,” *Commun. Math. Phys.* 205, 437 - 458 (1999).
- [137] A. Belinson, “Coherent sheaves on P^n and problems in linear algebra”, *Funktsional. Anal. i Prilozhen.* 12 (1978), no. 3, 6869.
- [138] B. Huisgen-Zimmermann, “The geometry of uniserial representations of finite dim. algebra. I.”, *J. Pure Appl. Alge.* 127 (1998), no. 1, 3972.
- [139] B. Keller, S. Scherotzke, “Desingularizations of quiver Grassmannians via graded quiver varieties”, arXiv:1305.7502.
- [140] M. Reineke, “Every projective variety is a quiver Grassmannian”, arXiv:1204.5730.
–, “Moduli of representations of quivers”, arXiv:0802.2147
- [141] Lutz Hille, “Moduli of Representations, Quiver Grassmannians, and Hilbert Schemes”, arXiv:1505.06008 [math.RT]
- [142] D. Forcella, A. Hanany, Y. H. He, A. Zaffaroni, “The Master Space of $N=1$ Gauge Theories,” *JHEP* **0808**, 012 (2008) [arXiv:0801.1585].
- [143] F. Buccella, J. P. Derendinger, S. Ferrara, and C. A. Savoy, “Patterns of symmetry breaking in supersymmetric gauge theories,” *Phys. Lett. B* 115 (1982) 375.
R. Gatto and G. Sartori, “Consequences of the complex character of the internal symmetry in supersymmetric theories,” *Commun. Math. Phys.* 109 (1987) 327.

- C. Procesi and G. W. Schwarz, “The geometry of orbit spaces and gauge symmetry breaking in supersymmetric gauge theories,” *Phys. Lett. B* 161 (1985) 117.
- [144] M. A. Luty and W. I. Taylor, “Varieties of vacua in classical supersymmetric gauge theories,” *Phys. Rev. D* 53, 3399 (1996) [hep-th/9506098]
- [145] D. Mehta, Y. H. He and J. D. Hauenstein, “Numerical Algebraic Geometry: A New Perspective on String and Gauge Theories,” *JHEP* **1207**, 018 (2012) [arXiv:1203.4235 [hep-th]].
- [146] I. Satake, “On a generalization of the notion of manifold”, *PNAS* 42: 359 - 363, (1956).
- [147] F. Klein, “Vorlesungen über das Ikosaeder und die Auflösung der Gleichungen vom fünften Grade”, <https://archive.org/details/lecturesonikosa00kleigoog/page/n10>.
- [148] P. Gabriel, “Unzerlegbare Darstellungen. I”, *Manuscripta Mathematica*, 6: 71 - 103 (1972).
- [149] B. Sturmfels, *Algorithms in Invariant Theory*, NY: Springer, 1993, ISBN 0-387-82445-6
- [150] P. du Val, “On isolated singularities of surfaces which do not affect the conditions of adjunction. I,II,III”, *Proc. Cambridge Phil. Soc.*, 30 (4): 453- 459, 460-465, 483-491.
cf. M. Reid, “The Du Val Singularities”, <http://homepages.warwick.ac.uk/~masda/surf/more/DuVal.pdf> for a pedagogical account.
- [151] P. Slodowy, “Platonic Solids, Kleinian singularities, and Lie Groups,” in *Algebraic Geometry*, Proc. Ann Arbor, 1981, Ed. I. Dolgachev.
M. Reid, “McKay Correspondence,” alg-geom/9702016.
M.Reid, “algebraic surfaces”, in *Complex Algebraic Geometry*, IAS/Park City Math. Ser., vol. 3, AMS, 1997, pp. 3-159.
- [152] G. Brown, “A Database of Polarized K3 Surfaces”, *Experimental Math.* Vol 16, 2007, Issue 1

- [153] T.Eguchi, A.Hanson, “Self-dual solutions to euclidean gravity”. *Annals of Physics*. 120 (1): 82-106 (1979);
–, “Gravitational instantons”. *General Relativity and Gravitation*. 11 (5): 315 - 320 (1979).
- [154] P.B.Kronheimer, “The construction of ALE spaces as hyper-Kahler quotients”. *J. Diff. Geom.* 29 (3): 665-683 (1989).
- [155] T.Gannon, “Monstrous moonshine and the classification of CFT”, arXiv:math/9906167 [math.QA].
- [156] P. Cameron, P.-D. Dechant, Y.-H. He, J. McKay, *ADE*, to appear.
- [157] Y. H. He, J. McKay, “Sporadic & Exceptional,” arXiv:1505.06742.
- [158] J. McKay, “Graphs, Singularities, and Finite Groups,” *Proc. Symp. Pure Math.* Vol 37, 183 - 186 (1980).
- [159] E. G. Gimon and J. Polchinski, “Consistency conditions for orientifolds and d manifolds,” *Phys. Rev. D* **54**, 1667 (1996) [hep-th/9601038].
S. Kachru and E. Silverstein, “4D Conformal Field Theories and Strings on Orbifolds,” hep-th/9802183.
W. Lerche, P. Mayr and J. Walcher, “A new kind of McKay correspondence from non-Abelian gauge theories,” hep-th/0103114.
- [160] C. V. Johnson and R. C. Myers, “Aspects of type IIB theory on ALE spaces,” *Phys. Rev. D* **55**, 6382 (1997) [hep-th/9610140].
- [161] M. R. Douglas and G. W. Moore, “D-branes, quivers, and ALE instantons,” hep-th/9603167.
- [162] A. E. Lawrence, N. Nekrasov and C. Vafa, “On conformal field theories in four-dimensions,” *Nucl. Phys. B* **533**, 199 (1998) [hep-th/9803015].
- [163] A. Hanany and Y. H. He, “NonAbelian finite gauge theories,” *JHEP* **9902**, 013 (1999) [hep-th/9811183].
- [164] G. Gonzalez-Sprinberg, J.-L. Verdier, “Construction géométrique de la correspondance de McKay,” *Ann. Sci. ENS* (4) 16 , 3, 409 - 449 (1984).

- L. Dixon, J.A. Harvey, C. Vafa and E. Witten, "Strings on orbifolds", Nuclear Phys. B 261 (1985), no. 4, 678 - 686.
- A. Degeratu, "Flops on Crepant Resolutions", Turk. J. Math., 28, (2004), 23 - 40.
- [165] Y. Ito and M. Reid, "The McKay Correspondence for Finite Subgroups of $SL(3;C)$," alg-geom/9411010.
- S.-S. Roan, "Minimal Resolutions of Gorenstein Orbifolds in Dimension Three," Topology, Vol 35, pp489 - 508, 1996.
- Y. Ito, "Gorenstein quotient singularities of monomial type in dimension three," J. Math. Sci. Univ. Tokyo 2 (1995) 419, alg-geom/9406001.
- [166] H. F. Blichfeldt, "Finite Collineation Groups," U. Chicago Press, 1917.
- [167] A. Hanany and Y. H. He, "A Monograph on the classification of the discrete subgroups of $SU(4)$," JHEP **0102**, 027 (2001) [hep-th/9905212].
- [168] G. Aldazabal, L. E. Ibanez, F. Quevedo and A. M. Uranga, "D-branes at singularities: A Bottom up approach to the string embedding of the standard model," JHEP **0008**, 002 (2000) [hep-th/0005067].
- [169] G. Aldazabal, S. Franco, L. E. Ibanez, R. Rabadan and A. M. Uranga, "Intersecting brane worlds," JHEP **0102**, 047 (2001) [hep-ph/0011132].
- [170] D. Bailin, G. V. Kraniotis and A. Love, "Supersymmetric standard models on D-branes," Phys. Lett. B **502**, 209 (2001) [hep-th/0011289].
- [171] D. Berenstein, V. Jejjala and R. G. Leigh, "The Standard model on a D-brane," Phys. Rev. Lett. **88**, 071602 (2002) [hep-ph/0105042].
- [172] L. F. Alday and G. Aldazabal, "In quest of just the standard model on D-branes at a singularity," JHEP **0205**, 022 (2002) [hep-th/0203129].
- [173] E. Kiritsis, "D-branes in standard model building, gravity and cosmology," Phys. Rept. **421**, 105 (2005) Erratum: [Phys. Rept. **429**, 121 (2006)] [hep-th/0310001].
- [174] H. Verlinde and M. Wijnholt, "Building the standard model on a D3-brane," JHEP **0701**, 106 (2007) [hep-th/0508089].

- [175] A. M. Uranga, “The standard model in string theory from D-branes,” Nucl. Phys. Proc. Suppl. **171**, 119 (2007).
- [176] S. Franco, D. Rodriguez-Gomez and H. Verlinde, “N-ification of Forces: A Holographic Perspective on D-brane Model Building,” JHEP **0906**, 030 (2009) [arXiv:0804.1125 [hep-th]].
- [177] M. Cicoli, S. Krippendorf, C. Mayrhofer, F. Quevedo and R. Valandro, “The Web of D-branes at Singularities in Compact Calabi-Yau Manifolds,” JHEP **1305**, 114 (2013) [arXiv:1304.2771 [hep-th]].
- [178] A. Hanany and A. M. Uranga, “Brane boxes and branes on singularities,” JHEP **9805**, 013 (1998) [hep-th/9805139].
A. Hanany and A. Zaffaroni, “On the realization of chiral four-dimensional gauge theories using branes,” JHEP **9805**, 001 (1998) [hep-th/9801134].
- [179] J. Hauenstein, Y. H. He, D. Mehta, “Numerical elimination & moduli space of vacua,” JHEP **1309**, 083 (2013) [arXiv:1210.6038 [hep-th]].
- [180] P. Candelas and X. C. de la Ossa, “Comments on Conifolds,” Nucl. Phys. B **342**, 246 (1990).
- [181] Y. H. He, “Calabi-Yau Varieties: from Quiver Representations to Dessins d’Enfants,” arXiv:1611.09398 [math.AG].
- [182] A. Futaki, “Complete Ricci-flat Kahler metrics on the canonical bundles of toric Fano manifolds,” arXiv:math/0703138.
A. Futaki, H. Ono and G. Wang, “Transverse Kahler geometry of Sasaki manifolds and toric Sasaki-Einstein manifolds”, arXiv:math.DG/0607586.
A. Futaki, H. Ono and Y. Sano, “Hilbert series and obstructions to asymptotic semistability”, Adv. Math. 226 (2011) 254 - 284, [arXiv:0811.1315].
- [183] D. Martelli, J. Sparks and S. T. Yau, “The Geometric dual of a-maximisation for Toric Sasaki-Einstein manifolds,” Commun. Math. Phys. **268**, 39 (2006) [hep-th/0503183].

- “Sasaki-Einstein manifolds and volume minimisation,” *Commun. Math. Phys.* **280**, 611 (2008) [hep-th/0603021].
- J. P. Gauntlett, D. Martelli, J. Sparks and S. T. Yau, “Obstructions to the existence of Sasaki-Einstein metrics,” *Commun. Math. Phys.* **273**, 803 (2007) [hep-th/0607080].
- [184] A. Butti and A. Zaffaroni, “R-charges from toric diagrams and the equivalence of a-maximization and Z-minimization,” *JHEP* **0511**, 019 (2005) [hep-th/0506232].
- [185] S. S. Gubser, “Einstein manifolds and conformal field theories,” *Phys. Rev. D* **59**, 025006 (1999) [hep-th/9807164].
- K. A. Intriligator and B. Wecht, “The Exact superconformal R symmetry maximizes a,” *Nucl. Phys. B* **667**, 183 (2003) [hep-th/0304128].
- M. Henningson and K. Skenderis, “The Holographic Weyl anomaly,” *JHEP* **9807**, 023 (1998) [hep-th/9806087].
- S. Benvenuti, S. Franco, A. Hanany, D. Martelli and J. Sparks, “An Infinite family of superconformal quiver gauge theories with Sasaki-Einstein duals,” *JHEP* **0506**, 064 (2005) [hep-th/0411264].
- [186] Y.-H. He, R.-K. Seong and S.-T. Yau, “CalabiYau Volumes and Reflexive Polytopes,” *Commun. Math. Phys.* **361**, no. 1, 155 (2018) [arXiv:1704.03462 [hep-th]].
- [187] I. R. Klebanov and E. Witten, “Superconformal field theory on three-branes at a Calabi-Yau singularity,” *Nucl. Phys. B* **536**, 199 (1998) [hep-th/9807080].
- [188] D. R. Morrison and M. R. Plesser, “Nonspherical horizons. 1.,” *Adv. Theor. Math. Phys.* **3**, 1 (1999) [hep-th/9810201].
- A. M. Uranga, “Brane configurations for branes at conifolds,” *JHEP* **9901**, 022 (1999) [hep-th/9811004].
- C. Beasley, B. R. Greene, C. I. Lazaroiu and M. R. Plesser, “D3-branes on partial resolutions of Abelian quotient singularities of Calabi-Yau threefolds,” *Nucl. Phys. B* **566**, 599 (2000) [hep-th/9907186].

- [189] B. Feng, A. Hanany and Y. H. He, “D-brane gauge theories from toric singularities and toric duality,” Nucl. Phys. B **595**, 165 (2001) [hep-th/0003085]
- [190] S. H. Katz, A. Klemm and C. Vafa, “Geometric engineering of quantum field theories,” Nucl. Phys. B **497**, 173 (1997)
- [191] A. Hanany and K. D. Kennaway, “Dimer models and toric diagrams,” hep-th/0503149.
- [192] S. Franco, A. Hanany, K. D. Kennaway, D. Vegh and B. Wecht, “Brane dimers and quiver gauge theories,” JHEP **0601**, 096 (2006) [hep-th/0504110].
S. Franco, A. Hanany, D. Martelli, J. Sparks, D. Vegh and B. Wecht, “Gauge theories from toric geometry and brane tilings,” JHEP **0601**, 128 (2006) doi:10.1088/1126-6708/2006/01/128 [hep-th/0505211].
- [193] A. Hanany and D. Vegh, “Quivers, tilings, branes and rhombi,” JHEP **0710**, 029 (2007) [hep-th/0511063].
- [194] B. Feng, Y. H. He, K. D. Kennaway and C. Vafa, Adv. Theor. Math. Phys. **12**, no. 3, 489 (2008) doi:10.4310/ATMP.2008.v12.n3.a2 [hep-th/0511287].
- [195] A. Hanany, C. P. Herzog and D. Vegh, “Brane tilings and exceptional collections,” JHEP **0607**, 001 (2006) [hep-th/0602041].
- [196] A. Hanany and G. Torri, “Brane tilings and susy gauge theories,” Nucl. Phys. Proc. Suppl. **216**, 270 (2011) [arXiv:1102.3611 [hep-th]].
- [197] A. Hanany and R. K. Seong, “Brane Tilings and Reflexive Polygons,” Fortsch. Phys. **60**, 695 (2012) [arXiv:1201.2614 [hep-th]].
- [198] A. Hanany and R. K. Seong, “Brane Tilings and Specular Duality,” JHEP **1208**, 107 (2012) [arXiv:1206.2386 [hep-th]].
- [199] S. Cremonesi, A. Hanany and R. K. Seong, “Double Handled Brane Tilings,” JHEP **1310**, 001 (2013) [arXiv:1305.3607 [hep-th]].

- [200] A. Hanany, V. Jejjala, S. Ramgoolam and R. K. Seong, “Consistency and Derangements in Brane Tilings,” *J. Phys. A* **49**, no. 35, 355401 (2016) [arXiv:1512.09013 [hep-th]].
- [201] J. Davey, A. Hanany and J. Pasukonis, “On the Classification of Brane Tilings,” *JHEP* **1001**, 078 (2010) [arXiv:0909.2868 [hep-th]].
- [202] S. Franco, Y. H. He, C. Sun and Y. Xiao, “A Comprehensive Survey of Brane Tilings,” *Int. J. Mod. Phys. A* **32**, no. 23n24, 1750142 (2017) [arXiv:1702.03958 [hep-th]].
- [203] S. Franco, “Bipartite Field Theories: from D-Brane Probes to Scattering Amplitudes,” *JHEP* **1211**, 141 (2012) [arXiv:1207.0807 [hep-th]].
- [204] S. Franco and A. Uranga, “Bipartite Field Theories from D-Branes,” *JHEP* **1404**, 161 (2014) [arXiv:1306.6331 [hep-th]].
- [205] S. Franco, D. Galloni and A. Mariotti, “Bipartite Field Theories, Cluster Algebras and the Grassmannian,” *J. Phys. A* **47**, no. 47, 474004 (2014) [arXiv:1404.3752 [hep-th]].
- [206] A. Hanany, Y. H. He, V. Jejjala, J. Pasukonis, S. Ramgoolam and D. Rodriguez-Gomez, “The Beta Ansatz: A Tale of Two Complex Structures,” *JHEP* **1106**, 056 (2011) [arXiv:1104.5490 [hep-th]].
- [207] J. J. Heckman, C. Vafa, D. Xie and M. Yamazaki, “String Theory Origin of Bipartite SCFTs,” *JHEP* **1305**, 148 (2013) [arXiv:1211.4587 [hep-th]].
- [208] Daniel R Gulotta. “Properly ordered dimers, r-charges, and an efficient inverse” algorithm. *JHEP*, 2008(10):014, 2008.
- [209] K. Ueda and M. Yamazaki, “A note on dimer models and McKay quivers”, *Commun.Math.Phys.*301:723-747,2011, arXiv:math/0605780.
- [210] K. D. Kennaway, “Brane Tilings,” *Int. J. Mod. Phys. A* **22**, 2977 (2007) [arXiv:0706.1660 [hep-th]].

- [211] M. Yamazaki, “Brane Tilings and Their Applications,” *Fortsch. Phys.* **56**, 555 (2008) [arXiv:0803.4474 [hep-th]].
- [212] N. Broomhead, “Dimer models and CY Algebras”, arXiv:0901.4662.
- [213] N. Broomhead, S.Franco, Y.-H. He, G. Musiker, *Toric Geometry, Dimers and String Theory*, to appear.
- [214] A. Ishii, K. Ueda. “On moduli spaces of quiver representations associated with dimer models”, arXiv:0710.1898.
- [215] C. Beil, “The geometry of noncommutative singularity resolutions”, arXiv:1102.5741.
- [216] K. Baur, A. King, R. Marsh. “Dimer models and cluster categories of grassmannians”, arXiv:1309.6524.
- [217] R. Bocklandt, A. Craw, A. Quintero-Vélez. “Geometric Reid’s recipe for dimer models”, *Math Annalen*, 361(3-4):689–723, 2015.
- [218] Raf Bocklandt, “Graded Calabi-Yau Algebras of Dimension 3”, *J. pure and app. alg.* 212(1):14–32, 2008.
– “Consistency conditions for dimer models”, *Glasgow Math. J.*, 54(02):429–447, 2012.
– “Generating toric noncommutative crepant resolutions”, *J. Algebra*, 364:119–147, 2012.
- [219] B. Davison, “Consistency conditions for brane tilings” *J. Algebra*, 338(1):1–23, 2011.
- [220] V. Ginzburg, “Calabi-Yau algebras”, arXiv:math/0612139.
- [221] T. Lai, G. Musiker. “Beyond aztec castles: Toric cascades in the dp_3 quiver.” arXiv:1512.00507.
- [222] S. Mozgovoy, M. Reineke, “On the NC Donaldson–Thomas invariants arising from brane tilings”, *Adv. in maths*, 223(5):1521–1544, 2010.
- [223] B. Szendroi, “Non-commutative Donaldson-Thomas theory and the conifold”, *Geom.Topol.*12:1171-1202,2008, arXiv:0705.3419

- [224] R. Vidunas and Y. H. He, “Composite Genus One Belyi Maps,” *Indag. Math.* **29**, 3, (2018) arXiv:1610.08075 [math.AG].
- [225] M. Wijnholt, “Large volume perspective on branes at singularities,” *Adv. Theor. Math. Phys.* **7**, no. 6, 1117 (2003) [hep-th/0212021].
C. P. Herzog and J. Walcher, “Dibaryons from exceptional collections,” *JHEP* **0309**, 060 (2003) [hep-th/0306298].
C. P. Herzog, “Exceptional collections and del Pezzo gauge theories,” *JHEP* **0404**, 069 (2004) [hep-th/0310262].
- [226] E. Calabi, “Métriques Kähleriennes et brés holomorphes”, *Annales Scientifiques de ENS*, 12 (1979), 268 - 294.
- [227] R.P.Stanley, “Hilbert functions of graded algebras,” *Advances in Mathematics* **28** (1978) 57 - 83.
- [228] S. Benvenuti, B. Feng, A. Hanany and Y. H. He, “Counting BPS Operators in Gauge Theories: Quivers, Syzygies and Plethystics,” *JHEP* **0711**, 050 (2007) [hep-th/0608050].
B. Feng, A. Hanany and Y. H. He, “Counting gauge invariants: The Plethystic program,” *JHEP* **0703**, 090 (2007) [hep-th/0701063].
- [229] Y. H. He, “Deep-Learning the Landscape,” arXiv:1706.02714 [hep-th].
- [230] Y. H. He, “Machine-learning the string landscape,” *Phys. Lett. B* **774**, 564 (2017).
- [231] T. Rudelius, “Learning to Inflate,” arXiv:1810.05159 [hep-th].
- [232] J. Halverson and F. Ruehle, “Computational Complexity of Vacua and Near-Vacua in Field and String Theory,” arXiv:1809.08279 [hep-th].
- [233] D. Klaewer and L. Schlechter, “Machine Learning Line Bundle Cohomologies of Hypersurfaces in Toric Varieties,” arXiv:1809.02547 [hep-th].
- [234] Y. H. He, V. Jejjala, B. D. Nelson, “hep-th,” arXiv:1807.00735 [cs.CL].
- [235] R. Jinno, “Machine learning for bounce calculation,” arXiv:1805.12153 [hep-th].

- [236] W. J. Cunningham, “High Performance Algorithms for Quantum Gravity and Cosmology,” arXiv:1805.04463 [gr-qc].
- [237] Y. N. Wang and Z. Zhang, “Learning non-Higgsable gauge groups in 4D F-theory,” JHEP **1808**, 009 (2018) [arXiv:1804.07296 [hep-th]].
- [238] G. K. Demir, N. Snmez and H. Dogan, “Deep-Learning in Search of Light Charged Higgs,” arXiv:1803.01550 [hep-ph].
- [239] K. Hashimoto, S. Sugishita, A. Tanaka and A. Tomiya, “Deep learning and the AdS/CFT correspondence,” Phys. Rev. D **98**, no. 4, 046019 (2018) [arXiv:1802.08313 [hep-th]].
- [240] J. Halverson, P. Langacker, “TASI Lectures on Remnants from the String Landscape,” PoS TASI **2017**, 019 (2018) [arXiv:1801.03503].
- [241] J. Carifio, W. J. Cunningham, J. Halverson, D. Krioukov, C. Long and B. D. Nelson, “Vacuum Selection from Cosmology on Networks of String Geometries,” Phys. Rev. Lett. **121**, no. 10, 101602 (2018) [arXiv:1711.06685 [hep-th]].
- [242] J. Liu, “Artificial Neural Network in Cosmic Landscape,” JHEP **1712**, 149 (2017) [arXiv:1707.02800 [hep-th]].
- [243] J. Carifio, J. Halverson, D. Krioukov and B. D. Nelson, “Machine Learning in the String Landscape,” JHEP **1709**, 157 (2017) [arXiv:1707.00655 [hep-th]].
- [244] T. Cohen, M. Freytsis and B. Ostdiek, “(Machine) Learning to Do More with Less,” JHEP **1802**, 034 (2018) [arXiv:1706.09451 [hep-ph]].
- [245] F. Ruehle, “Evolving neural networks with genetic algorithms to study the String Landscape,” JHEP **1708**, 038 (2017) [arXiv:1706.07024].
- [246] D. Krefl and R. K. Seong, “Machine Learning of Calabi-Yau Volumes,” Phys. Rev. D **96**, no. 6, 066014 (2017) [arXiv:1706.03346 [hep-th]].
- [247] A. Mtter, E. Parr and P. K. S. Vaudrevange, “Deep learning in the heterotic orbifold landscape,” arXiv:1811.05993 [hep-th].

- [248] R. Altman, J. Carifio, J. Halverson and B. D. Nelson, “Estimating Calabi-Yau Hypersurface and Triangulation Counts with Equation Learners,” arXiv:1811.06490 [hep-th].
- [249] K. Bull, Y. H. He, V. Jejjala and C. Mishra, “Machine Learning CICY Threefolds,” Phys. Lett. B **785**, 65 (2018) [arXiv:1806.03121 [hep-th]].
- [250] J. P. Conlon, F. Quevedo and K. Suruliz, “Large-volume flux compactifications: Moduli spectrum and D3/D7 soft supersymmetry breaking,” JHEP **0508**, 007 (2005) [hep-th/0505076].
- [251] J. Gray, Y. H. He, V. Jejjala, B. Jurke, B. D. Nelson and J. Simon, “Calabi-Yau Manifolds with Large Volume Vacua,” Phys. Rev. D **86**, 101901 (2012) [arXiv:1207.5801 [hep-th]].
- [252] Python Software Foundation. Python Language Reference, <http://www.python.org>
G. van Rossum, Python tutorial, Technical Report CS-R9526, Centrum voor Wiskunde en Informatica (CWI), Amsterdam, May 1995.
- [253] Jupyter Dev. Team, “Jupyter Notebooks a publishing format for reproducible computational workflows”, 10.3233/978-1-61499-649-1-87.
- [254] The MNIST database of handwritten digits, <http://yann.lecun.com/exdb/mnist/>
- [255] F. Rosenblatt, “The Perceptron—a perceiving and recognizing automaton”. Report 85-460-1, Cornell Aeronautical Laboratory (1957).
- [256] K. J. C. Leney [ATLAS Collaboration], “A Neural-Network Clustering Algorithm for the ATLAS Silicon Pixel Detector,” J. Phys. Conf. Ser. 523, 012023 (2014).
C. P. Novaes, A. Bernui, I. S. Ferreira and C. A. Wuensche, “A Neural-Network based estimator to search for primordial non-Gaussianity in Planck CMB maps,” JCAP 1509, no. 09, 064 (2015) [arXiv:1409.3876 [astro-ph.CO]].
A. J. Ballard, R. Das, S. Martiniani, D. Mehta, L. Sagun, J. Stevenson, D. Wales, “Perspective: Energy Landscapes for Machine Learning”,

arXiv:1703.07915.

W. C. Gan and F. W. Shu, “Holography as deep-learning,” arXiv:1705.05750 [gr-qc].

Deep-Learning and Physics Conference: http://kabuto.phys.sci.osaka-u.ac.jp/~koji/workshop/tsrp/Deep_Learning.html

- [257] J. Herz, A. Krough, R. G. Palmer, “Introduction to the Theory of Neural Computation”, Addison-Wesley, 1991.
M. H. Hassoun, “Fundamentals of Artificial Neural Networks”, MIT Press, 1995.
S. Haykin, “Neural Networks: A Comprehensive Foundation”, 2nd ed, Macmillan, New York, 1999.
C. Bishop, “Pattern Recognition and Machine Learning”. Springer 2006.
- [258] N. Srivastava, G. Hinton, A. Krizhevsky, I. Sutskever, and R. Salakhutdinov, “Dropout: A simple way to prevent neural networks from overfitting”, *J. Machine Learning Research* 15 (2014) 1929 - 1958.
- [259] A. J. Smola and B. Scholkopf, “A tutorial on support vector regression”, Tech. Rep., Statistics and Computing, 2003.
- [260] K.-M. Ting, “Encyclopedia of machine learning”, Springer 2011. ISBN 978-0-387-30164-8.
- [261] B. Matthews, “Comparison of the predicted and observed secondary structure of T4 phage lysozyme”. *Biochimica et Biophysica Acta (BBA) - Protein Structure*. 405 (2): 442 - 451 (1975).
J. Gorodkin, “Comparing two K-category assignments by a K-category correlation coefficient”, *Comp. Biology and Chemistry*. Elsevier. 28 (5): 367 - 374 (2004).
- [262] C. Van Rijsbergen, *Information Retrieval* (2nd ed.). Butterworth-Heinemann (1979).
D. Powers, “Evaluation: From Precision, Recall and F-Measure to ROC, Informedness, Markedness & Correlation”, *J. Machine Learning Technologies*. 2 (1): 37 - 63 (2011).